Targeting mLST8 in mTORC2-dependent cancers

By

Laura Chonghae Kim

Dissertation

Submitted to the Faculty of the

Graduate School of Vanderbilt University

in partial fulfillment of the requirements

for the degree of

DOCTOR OF PHILOSOPHY

in

Cancer Biology

June 30th, 2020

Nashville, Tennessee

Approved:

Albert B. Reynolds, Ph.D. (chair)

Mark R. Boothby, M.D., Ph.D.

Christine M. Lovly, M.D. Ph.D.

William P. Tansey, Ph.D.

Jin Chen, M.D., Ph.D. (adviser)

DEDICATION

This dissertation is dedicated to all cancer patients and their loved ones for their strength and courage in the fight against this disease.

This is also dedicated to my family (Kalhee and Jenny Kim, Stephanie Kim) for their unwavering love and support.

ACKNOWLEDGEMENTS

Completion of this work would have been impossible without the support of many, and I would like to express my sincere gratitude here.

First and foremost, I must thank my mentor, Jin Chen. Her support, mentorship, and high-fives have been invaluable in my development as a scientist, and I plan to continue seeking her guidance even when I am many years beyond graduate school. I would also like to acknowledge my committee members Al Reynolds, Bill Tansey, Mark Boothby, Rebecca Cook, and Christine Lovly, who continuously challenged me and provided scientific guidance. Much of this work stems from their insightful questions, and I am extremely appreciative of the time they put into thinking about my projects.

I would also like to thank the past and present members of the Chen Lab: Shan Wang, Deanna Edwards, Wenqiang Song, Dana Brantley-Sieders, Katherine Hastings, Victoria Youngblood, Tammy Sobolik, Yoonha Hwang, Eileen Shiuan, Kalin Wilson, Verra Ngwa, Ashwin Inala, and Chris Rhee. I am tremendously grateful for their training, scientific brilliance, and most importantly their friendship throughout this journey. In particular, I would like to highlight Deanna, Shan, Wenqiang, and Eileen, who were always willing to lend an ear to my questions and musings for the last five years. I am going to miss our morning coffee runs, breakroom lunches, and even the long weekends in lab!

I also need to thank those who supported me financially throughout my graduate career, specifically Dr. Jin Chen for supporting me through the Microenvironmental Influences in Cancer Training Grant and the National Cancer Institute for the Predoctoral Ruth L. Kirschstein National Research Service Award (F31). I would also like to thank all the members of the Program in Cancer Biology for day-to-day logistical support.

Last, I must thank my friends and family. Meeting such wonderful people around Nashville and in graduate school at Vanderbilt has made this process infinitely easier. I am incredibly grateful for the wonderful memories and enduring friendship. I also feel immensely lucky to have friends from back home in North Carolina that always supported me from afar. From weekend trips to incessant messages, they all put in an incredible amount of energy into staying connected despite the distance. I cannot thank them enough for this effort. Finally, I must thank my parents, Kalhee and Jenny Kim, and sister, Stephanie, for their unconditional love and trust. Their support gave me the confidence to persevere against every hurdle, and I feel extraordinarily privileged to have them in my corner.

TABLE OF CONTENTS

DEDICATION ..... **ii**

ACKNOWLEDGEMENTS ..... **iii**

LIST OF TABLES ..... **viii**

LIST OF FIGURES ..... **ix**

LIST OF ABBREVIATIONS ..... **xi**

CHAPTERS

I. Introduction **1**

Overview 1
Lung Cancer 2
Targeted Therapy 3
Immunotherapy 7
The mTOR Complexes 9
mTORC1 Signaling 14
mTORC1 in Cancer 16
mTORC2 signaling 19
mTORC2 in Cancer 21
mTOR Inhibitors for Cancer Therapy 21
mTOR in Vasculature 26
mTOR in Tumor Immunity 38
Summary and Thesis Projects 30

II. Disruption of the scaffolding function of mLST8 selectively inhibits mTORC2 assembly and function and suppresses mTORC2-dependent tumor growth in vivo **33**

Abstract 33
Significance 33
Introduction 34
Materials and Methods 34
Cell Lines and cell culture 34
Generation of the mTOR E2285A knock-in cell line by CRISPR-Cas9 technology 35
Xenograft Assay 35
Plasmids 36
Lentivirus production and transduction 36
Western Blot and Co-immunoprecipitation 36
In Vitro Kinase Assay 37
Results 39

mLST8 is required for mTORC2, but not mTORC1, integrity and function 39
mLST8 mutations that uncouple binding to LBE domain of mTOR disrupt mTORC2 complex formation and signaling 42
mLST8 serves as a molecular bridge between mTOR and SIN1 46
mLST8 point mutations that block mLST8-mTOR interactions impair mTORC2 signaling and tumor growth *in vivo* 50
Discussion 54

III. Rictor promotes NSCLC cell proliferation through formation and activation of mTORC2 at the expense of mTORC1 56

Abstract 56
Introduction 57
Results 58
RICTOR is amplified and overexpressed in non-small cell lung cancer 58
Alterations in Rictor expression lead to corresponding changes in mTORC2 and mTORC1 64
Rictor promotes proliferation of NSCLC cells 67
Increased Rictor expression promotes NSCLC tumor growth *in vivo* 68
Targeting mTORC2 for loss-of-function inhibits tumor growth of *RICTOR*-amplified NSCLC 70
Discussion 73
Materials and Methods 75
Cell lines and cell culture 75
Plasmids and sgRNA Sequences 76
Lentivirus Production and Transduction 76
Xenograft Assay 76
Western Blot and Co-immunoprecipitation (Co-IP) 77
Proximity Ligation Assay 77
Cell Growth Assays 77
3D Cultures 78
Immunohistochemistry Staining 78
TCGA Data Analysis 79

IV. Conclusions and Future Directions 81

Conclusions 81
Future Directions 82
How do other oncogenic alterations or co-amplified genes interact with *RICTOR* to promote tumorigenesis? 82
How does *RICTOR* amplification alter tumor metabolism? 89
How is mTORC2 regulated and how does mTORC2 regulation impact cancer? 92
What are the feasible strategies for development of mTORC2-specific inhibitors? 94
Concluding Remarks 96

REFERENCES **97**

APPENDIX **134**

A. Phosphorylation of PLCγ1 by EphA2 receptor tyrosine kinase promotes tumor growth in lung cancer **134**

Abstract 134
Implications 134
Introduction 134
Results 136
EphA2 interacts with PLCγ 136
EphA2 kinase activity is required for PLCγ1 phosphorylation 139
EphA2 activates PLCγ in human lung cancer cells 140
Loss of PLCγ1 blocks cell growth of human lung cancer cells 143
PLCγ1 deficiency decrease tumor growth in a mouse KPL lung tumor model 145
Discussion 148
Materials and Methods 149
Cell lines, plasmids, and reagents 149
Building a human protein-protein interactome 150
Cell growth assays 151
Yeast-two-hybrid screen 151
Proximity Ligation Assay 151
Immunoblots, immunoprecipitation, and immunohistochemistry 152
Animal Studies 152
Statistical Analysis 153

LIST OF TABLES

Table		Page
1.1	mTOR inhibitors approved by the FDA for cancer treatment	22
1.2	mTOR inhibitors currently in clinical trials	25
1.3	Function of mTORC1 and mTORC2 in tumor and endothelial cells	27
2.1	DNA oligonucleotide sequences used in Chapter II	38
3.1	sgRNA sequences and plasmids used in Chapter III	79
3.2	List of antibodies used in Chapter III	80
4.1	Significantly co-amplified genes with RICTOR in TCGA Lung Adenocarcinoma samples	85

LIST OF FIGURES

Figure		Page
1.1	Most common NSCLC mutations	5
1.2	Schematic Representation of mTOR complexes	11
1.3	Overview of the mTOR signaling pathway	13
1.4	Downstream Cellular Processes	19
2.1	mLST8 is required for assembly and activity of mTORC2	40
2.2	Supplemental figure related to Figure 2.1	41
2.3	Mutations disrupting mTOR-mLST8 interface affect mTORC2 assembly and function	44
2.4	Supplemental figure related to Figure 2.3	45
2.5	SIN1 NH_2-terminal domain binds to mLST8	48
2.6	Supplemental figure related to Figure 2.5	49
2.7	mLST8-mTOR uncoupling mutations inhibit *PTEN*-null prostate cancer growth	52
2.8	Supplemental figure related to Figure 2.7	53
3.1	CRISPR Synergistic Activation Mediator (SAM) system can be used to model *RICTOR* amplification in NSCLC	61
3.2	Copy number analysis of TCGA NSCLC samples with RICTOR-amplification	63
3.3	Rictor alterations promote corresponding changes in mTORC2 and mTORC1	66
3.4	Rictor promotes NSCLC proliferation and tumor growth	69
3.5	mLST8 loss-of-function inhibits growth of *RICTOR*-amplified tumors *in vivo*	72
4.1	Common co-altered genes in RICTOR-amplified NSCLC	83
4.2	Loss of mLST8 inhibits phosphorylation of ACLY	91
4.3	mRNA expression levels of mTOR complex components are unchanged in Rictor overexpressing NSCLC cells	93
4.4	Reduction in Sin1 expression occurs 24hrs after reduction in Rictor expression	94

5.1 EphA2 interacts with PLCγ 138
5.2 EphA2 kinase activity is required for phosphorylation of PLCγ1 141
5.3 PLCγ1 is activated by EphA2 in human lung cancer cell lines 142
5.4 PLCγ1 loss inhibits human KRAS-mutant lung cancer cell growth 144
5.5 PLCγ1 deficiency hinders mouse KPL lung tumor growth.....147

LIST OF ABBREVIATIONS

4EBP1 – eIF4E Binding Protein 1

AAV – Adeno-associated Virus

ACLY – ATP Citrate Lyase

ALW – ALW-II-42-27

AMPK – AMP Kinase

ANOVA – Analysis of Variance

ATP – Adenosine Triphosphate

CRISPR – Clustered Regularly Interspaced Short Palindromic Repeats

DAG - Diacylglycerol

EGFR – Epidermal Growth Factor Receptor

EIF – Elongation Initiation Factor

EPHA2 – Ephrin Type-A Receptor 2

FBS – Fetal Bovine Serum

GAP – GTPase Activating Protein

GDP – Guanosine Diphosphate

GEF- Guanine Nucleotide Exchange Factor

GFP – Green Fluorescent Protein

GPCR – G-Protein Coupled Receptor

GTP – Guanosine Triphosphate

HCC – Hepatocellular Carcinoma

HEK – Human Embryonic Kidney

HIF – Hypoxia Inducible Factor

ICB – Immune Checkpoint Blockade

IRS – Insulin Receptor Substrate

IP – Immunoprecipitation

IP3 – Inositol Triphosphate

KO – Knockout

KRAS – Kirsten Rat Sarcoma

KPL – KRAS-p53-LKB1

LOF – Loss-of-function

mTOR – Mechanistic Target of Rapamycin

mTORC1 – mTOR Complex 1

mTORC2 – mTOR Complex 2

MTT- 3-(4,5-Dimethylthiazol-2-yl)-2,5-Diphenyltetrazolium Bromide

NSCLC – Non-Small Cell Lung Cancer

PH – Pleckstrin Homology

PI3K – Phosphatidylinositol 3-kinase

PIP2 – Phosphatidylinositol 4,5-bisphosphate

PIP3 – Phosphatidylinositol (3,4,5)-triphosphate

PKC – Protein Kinase C

PLA – Proximity Ligation Assay

PLCG – Phospholipase C Gamma

PTEN – Phosphatase and Tensin Homolog

PPI – Protein-Protein Interaction

RTK – Receptor Tyrosine Kinase

S6K1 – Ribosomal protein S6 kinase beta-1

S6RP – S6 Ribosomal Protein

SAM – Synergistic Activation Mediator

SCLC – Small Cell Lung Cancer

SD – Standard Deviation

SEM – Standard Error of the Mean

SGK – Serum/glucocorticoid-regulated kinase

sgRNA – Small Guide RNA

shRNA – Short Hairpin RNA

siRNA – Small Interfering RNA

ssODN – Single Stranded Oligodeoxy-nucleotide

T-ALL – T-cell Acute Lymphoblastic Leukemia

TAM – Tumor-associated Macrophage

TKI – Tyrosine Kinase Inhibitor

TME – Tumor Microenvironment

Treg – Regulatory T Cells

TSC – Tuberous Sclerosis Complex

TUNEL – Terminal Deoxynucleotidyl Transferase dUTP Nick End Labeling

VEGF – Vascular Endothelial Growth Factor

WDR – WD40 Repeat

WT – Wild-type

Y2H – Yeast-two-hybrid

Chapter I

Introduction

Work presented in this section is published in *Oncogene*.

Overview

Cancer is a disease characterized by its hallmarks (1), including uncontrolled cell proliferation, increased cell survival, evasion of anti-tumor immunity, aberrant angiogenesis, and acquisition of metabolic events unique to cancers. Importantly, activation of Mechanistic Target of Rapamycin (mTOR) signaling is associated with each of these oncogenic cellular processes, making the mTOR signaling node a promising target for treating multiple hallmarks of the cancer phenotype. mTOR is a serine/threonine kinase that was discovered in the early 1990s as the target of the anti-fungal drug rapamycin (2,3). mTOR acts in two distinct complexes (mTORC1 and mTORC2) and both nodes integrate a variety of environmental and intracellular cues to coordinate downstream cellular processes. Efforts to sequence and identify targetable oncogenic alterations, led to the discovery several mutations that activate mTORC2, such as loss of PTEN, activation of PIK3CA, and amplification of RICTOR. While the importance of mTORC2 as a mediator of tumor progression is well-known, an mTORC2-specific inhibitor does not yet exist. Herein, we describe the requirement of mLST8, a shared mTOR co-factor, for mTORC2 integrity and function alone by acting as a molecular bridge between the mTOR kinase and regulatory co-factor Sin1 in mTORC2, but not in mTORC1. Using CRISPR-Cas9 technology, we provide evidence that loss of mLST8 in mTORC2-dependent cancers can inhibit mTORC2 signaling and tumor cell proliferation in both in vitro cell culture and mouse xenograft models. These results suggest targeting mLST8 or the mLST8-mTOR interface could effectively block mTORC2 signaling and could be used for targeted therapy in mTORC2-dependent cancers. We also report herein, a mechanism for *RICTOR*-amplification mediated mTORC2

activation and lung tumor growth. We use the CRISPR Synergistic Activation Mediator (SAM) system to overexpress Rictor and show increased formation and activity of mTORC2 at the expense of mTORC1. Overexpression of Rictor leads to increased mTORC2 downstream signaling, tumor cell proliferation, and ultimately tumor xenograft growth. We also show that tumor growth of *RICTOR*-amplified tumors can be inhibited by targeting mLST8 to specifically inhibit mTORC2.

Lung Cancer

Lung cancer is the leading cause of cancer-related deaths world-wide, causing approximately 1.6 million deaths each year. In 2020, an estimated 228,820 new cases of lung cancer will be diagnosed in the United States and 135,720 patients are expected to succumb to the disease(4). Despite significant advances in therapies, the five-year survival rate for lung cancer remains low, at approximately 19%(4). Lung cancer is defined by its histological subtype: non-small cell lung cancer (NSCLC), which accounts for 80-85% of cases, and small cell lung cancer (SCLC) which accounts for 10-15% of cases. Other subtypes such as lung carcinoid tumors also exist, but account for less than 5% of cases. NSCLC is further defined by its cell of origin into three categories: adenocarcinoma, occurring in the mucus-secreting cells at the periphery of the lung; squamous cell carcinoma, which occurs in the squamous cell lining the airways of the lungs; and large cell carcinoma, which occurs throughout the lung and can originate from neuroendocrine cells. Tobacco smoking, a well-known cause of lung cancer, is most commonly associated with SCLC and squamous cell carcinoma, while never smokers tend to present with adenocarcinoma histology. The course of treatment for lung cancer patients is determined by the stage, or extent of disease, at diagnosis. Early stage cancers are often treated through surgical resection which can be followed by adjuvant chemotherapy and/or radiotherapy. Later stage and metastatic lung cancer are often treated with the surgery/chemotherapy/radiation therapy with additional targeted therapies or immunotherapy.

The advent of genomic screening technologies has led to further classification of lung cancer by molecular subtype, identifying unique genetic alterations that promote tumor growth. The most common NSCLC mutations are displayed in **Figure 1.1**. Despite knowledge of multiple subtypes of NSCLC, treatment options for all patients remained similar with a combination of chemotherapy, radiotherapy, and/or surgical resection until the late 1990s to early 2000s(5).

Targeted Therapy

Treatment strategies for NSCLC underwent a dramatic paradigm shift with the discovery of distinct driver alterations in individual tumors, even within the same histological subtype. The "addiction" of tumors to these oncogenic signaling pathways revealed unique vulnerabilities that could be targeted for therapeutic intervention.

The best example of targeted therapy developed for treatment of NSCLC is the EGFR tyrosine kinase inhibitor (TKI). EGFR, or epidermal growth factor receptor, is a receptor tyrosine kinase upstream of several signaling cascades including the MAPK and PI3K/mTOR pathways. Exon 19 deletion and L858R at exon 21 were identified as the most common EGFR mutations and occur near the ATP-binding pocket leading to constitutive activation and ligand independence(6). These mutations have been targeted with first-generation EGFR inhibitors which act through reversible ATP binding competition(7,8) on EGFR or second-generation inhibitors that irreversibly bind to the ATP binding pocket of EGFR, HER2, and HER4. Despite significant initial responses and higher progression free survival, patients treated with these inhibitors inevitably develop resistance. Sequencing of resistant tumors revealed a T790M mutation in EGFR resulting in steric hindrance of the inhibitor or increased ATP affinity to the receptor(9). Third-generation inhibitors designed to combat these resistance mutations have been developed, this time covalently binding to the cysteine at 797 and reducing the increased ATP binding affinity caused by the T790M mutation(10). Interestingly, the third-generation TKI

displayed superior performance to the first-generation inhibitors in untreated patients, leading to its use as a first-line therapy(11). However, as is with almost all targeted therapies, resistance to the third-generation inhibitor is eventually conferred with the development of a C797S mutation(12,13). Multiple strategies are being used to develop fourth-generation TKIs including allosteric inhibition of the receptor and combined therapies with EGFR antibodies(14,15).

It is also important to note that other mechanisms can confer resistance to EGFR TKIs, most often through increased reliance on bypass signaling pathways to maintain rapid cell proliferation and increased cell survival(16,17). Some of these mechanisms include amplification of HER2, mutations in MET, BRAF and PIK3CA, and overexpression of EPHA2(16,18). Co-occurring mutations in KRAS can also facilitate resistance to EGFR TKIs(19).

After the discovery of precision medicine for EGFR mutations, other oncogenic alterations, including the ALK tyrosine kinase, have been targeted for cancer therapies. Unlike the mutations within the EGFR locus that lead to constitutive activation, oncogenic ALK is activated through gene rearrangements. Typically, an intact tyrosine kinase domain is fused to an N-terminal partner with a promoter that is constitutively expressed and has an oligomerization domain leading to constitutive transactivation of the ALK kinase(20). Some common ALK fusion partners in NSCLC include EML4, TFG, and KIF5B. Crizotinib was the first ALK TKI shown to be successful in treating ALK-positive NSCLC(21). As with other TKIs, resistance either through mutations within the ALK kinase or through bypass signaling pathways(22), has led to development of second and third-generation ALK TKIs that continue to be used in the clinic(23).

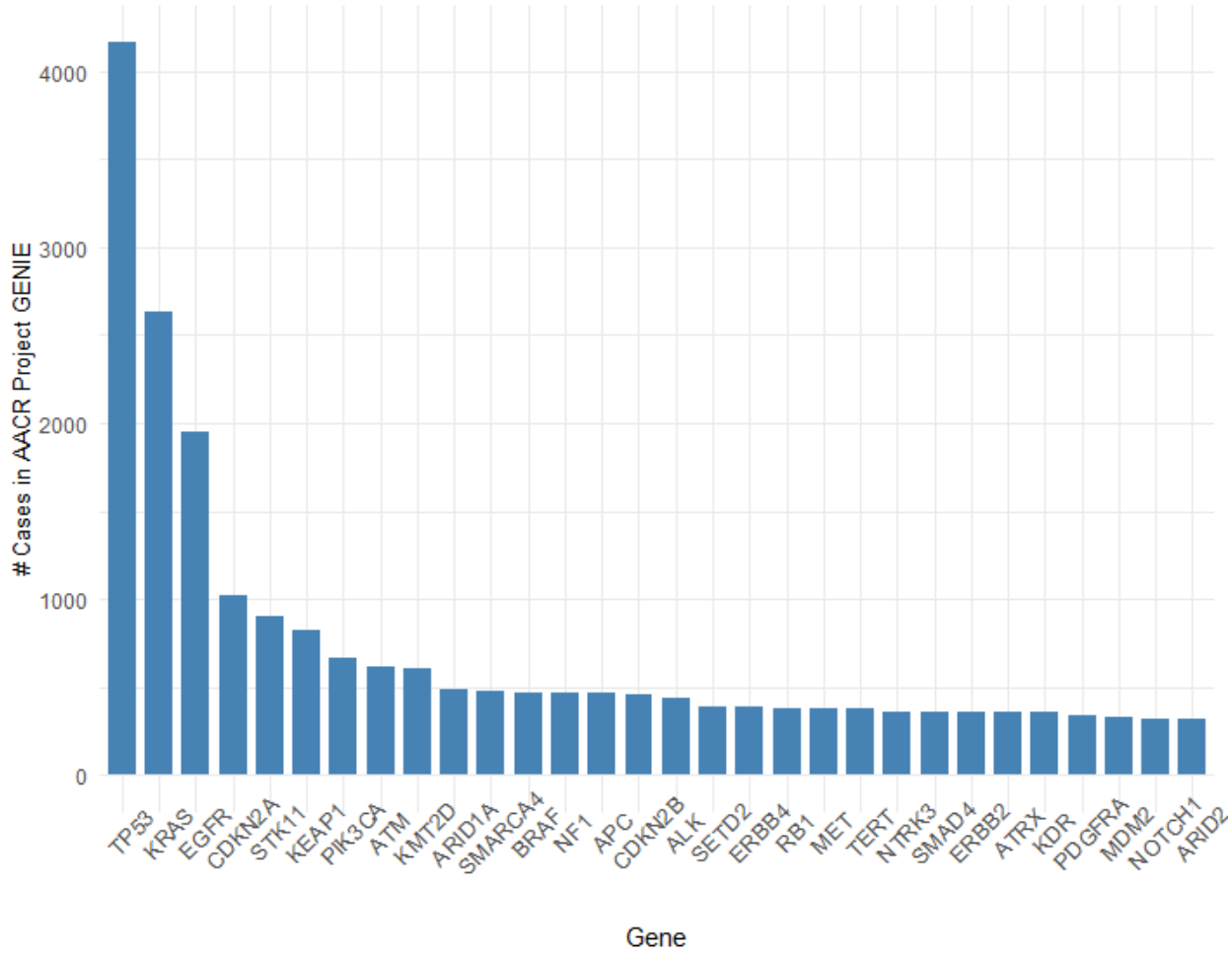

Figure 1.1 Most common mutations in NSCLC adapted from mycancergenome.org(24,25)

Unlike mutations in EGFR and ALK tyrosine kinases, KRAS mutations, which occur in more than 20% of NSCLC cases, have been considered undruggable due to the extremely high affinity for its co-factor, GTP(26). KRAS is one of 3 isoforms of RAS, a GTPase that when bound to GTP, can activate a variety of downstream signaling pathways. Oncogenic RAS mutations are thought to inhibit GTP hydrolysis, locking RAS in its active form and resulting in constitutive downstream signaling. In NSCLC, KRAS missense mutations are most often occur at codon 12, although mutations can also occur at codon 13 and 61(27). The success of targeted therapies led many to hypothesize that, hyperactivated signaling pathways downstream of KRAS, such as the MAPK pathway, could be targeted to inhibit tumor growth. Trametinib and Selumetinib, both MEK inhibitors, saw some success in clinical trials, but neither have been approved for use in treating KRAS-mutant NSCLC(28). Other strategies to target KRAS mutations have included activating the KRAS GEF, SOS1, to inhibit GTP exchange or blocking proper KRAS subcellular localization through inhibition of membrane-association(29).

In the last decade, a significant breakthrough occurred with the development of a $KRAS^{G12C}$ inhibitor. $KRAS^{G12C}$ mutations comprise more than 40% of the KRAS mutations NSCLC, making it the most common KRAS mutation(27). The novel inhibitor covalently interacts with the cysteine at codon 12 in the GDP bound form, sterically hindering the binding of GTP and inhibiting KRAS activation(30,31). The discovery of this molecule also suggests that nucleotide signaling does indeed occur with mutant forms of KRAS, bringing into question the original model of oncogenic KRAS thought to be locked into its active state. Additionally, the specificity of this inhibitor to $KRAS^{G12C}$ suggests that individual mutations may need to be targeted with distinct inhibitors and a pan-KRAS inhibitor may not be feasible. $KRAS^{G12C}$ inhibitors have since been optimized for *in vivo* and clinical use and have shown efficacy in pre-clinical NSCLC mouse models(32,33). Clinical trials with these inhibitors in NSCLC are currently ongoing and preliminary results are promising, with two patients having a partial response and

two patients presenting with stable disease(33). While there is great hope that KRAS inhibitors will be successful as a first-line therapy, a study has already demonstrated that resistance to the targeted therapy is inevitable(34,35).

Immunotherapy

Resistance to targeted therapy and continued low survival rates for NSCLC have stimulated research into other treatment strategies. A recent resurgence of interest in immunotherapy has dramatically altered cancer treatment and several studies have been published suggesting this strategy will be very beneficial to NSCLC patients. Cancer cells often increase the expression of immune checkpoints which suppress the host immune response, allowing the tumor to grow unchecked by the host immune system. Immune checkpoint blockade (ICB) blocks the activity of these checkpoint molecules, releasing the brakes on the immune system and restoring anti-tumor immunity. ICBs have proven remarkably successful in the clinic, often extending progression-free survival by several months and in many cases, eliminating disease and extending survival long-term. NSCLC might be particularly sensitive to ICB due to its high mutational burden, which aids in the creation of neoantigens that can be recognized by an activated immune system killed through increased cytotoxic T-cells(36).

The first ICB approved for cancer therapy was ipilumumab, an anti-CTLA-4 monoclonal antibody(37,38). Since, ICBs targeting the PD-1/PD-L1 axis have been developed including nivolumab and pembrolizumab, antibodies against PD-1, and atezolizumab, durvalumab, and avelumab, antibodies against PD-L1(5,39–41).

Pembrolizumab has been approved as a single agent first-line treatment for patients with stage III NSCLC who are not candidates for surgical resection or chemoradiation, or metastatic NSCLC whose tumors express PD-L1 (Tumor Proportion Score >= 1%) with no EGFR or ALK mutation(42). Pembrolizumab can also be used in combination with pemetrexed and platinum

chemotherapy as a first-line treatment for patients with non-squamous NSCLC, with no EGFR or ALK mutations(43). For patients with metastatic squamous NSCLC, pembrolizumab can be used in combination with carboplatin and paclitaxel as a first-line treatment(44).

For progressive disease after chemotherapy or targeted therapies, nivolumab, atezolizumab, and durvalumab are FDA approved depending on PD-L1 expression and type of initial chemotherapy(45). Additionally, ongoing clinical trials are testing PD-1 or PD-L1 therapy in combination with CTLA-4 therapy or chemotherapy both as a first-line treatment or for progressive disease.

Many factors impact the efficacy of ICB therapy including the expression of immune checkpoints, effective presentation of neoantigens, and sufficient infiltration of active anti-tumor immune cell populations. Without proper characteristics, tumors are considered “cold” and are unlikely to respond to ICBs. Currently, expression of targeted immune checkpoints is required before receiving ICB therapy. However, many other aspects of the tumor microenvironment can affect neoantigen presentation and immune infiltration. Chemotherapy, for example, is hypothesized to increase the mutational burden of tumors, potentially increasing the number of neoantigens and the efficacy of ICBs(46). Chemotherapy may also increase the ratio of infiltrating immune cells to tumor cells, leading to an increase in both the overall number of T-cells and the availability of metabolites required for T-cell activity which could potentiate a stronger immune response when chemotherapy is used in combination with ICBs(46,47). The vascularization of tumors affects the amount and types of immune cells capable of infiltrating a tumor. Tumor angiogenesis has been shown to increase the number of immunosuppressive cells, so strategies combining anti-angiogenic or vessel-normalizing drugs with ICBs are being explored(48). Recent evidence also suggests the epigenetic state of immune cells is important for maintaining their activity, suggesting epigenetic therapy in combination with ICB will also be an important frontier to explore(49).

While not yet FDA approved for treatment of NSCLC, other strategies to reactivate the immune system as a method of cancer therapy are currently being explored. Adoptive cell transfer (ACT) of T-cell receptor (TCR)-modified or chimeric antigen receptor (CAR) T-cells utilize genetically re-engineered autologous T-cells to target tumor antigens presented by MHC molecules or on the cell surface, respectively. The ability to design an immunotherapy specifically targeting a tumor antigen is a major benefit of ACT. CAR T-cell therapies targeting CD-19 have already been FDA-approved for treating patients with lymphoma or leukemia, but NSCLC-specific antigens need to be discovered before these therapies can be approved for NSCLC. In addition to ACT, cancer vaccines are also under development. Therapeutic cancer vaccines typically deliver immunogenic tumor antigens that mount a T-cell response directed at the tumor(50). Clinical trials for a cancer vaccine in NSCLC are currently underway, although the approach for this vaccine is different. Delivery of the CIMAvax-EGF vaccine leads to an antibody response against self EGF, thus preventing the engagement of EGFR on tumor cells and blocking tumor growth(51).

As with other molecularly targeted therapy, many patients develop resistance to immunotherapy. Thus far, mechanisms of acquired resistance to include loss of HLA, loss of tumor antigen expression, and escape mutations in IFNγ signaling(52). Better understanding of inherent and acquired resistance to immunotherapy will be necessary to expand the number of patients that will benefit from this promising treatment option.

The mTOR Complexes

Although rapamycin was originally defined as an anti-fungal agent, it was soon realized that rapamycin possesses broad anti-proliferative, cytostatic effects in a wide variety of cells, including cancer cells. Subsequent molecular analyses revealed that rapamycin binds to FKBP12, and in doing so, blocks some (but not all) mTOR activity. In searching for the

molecular underpinnings of why rapamycin produced only partial mTOR inhibition, it was discovered that mTOR acts in two functionally distinct complexes (53,54), one that is relatively sensitive to rapamycin (mTOR complex 1, or mTORC1), and one that is relatively rapamycin resistant (mTORC2) (55). Both mTORC1 and mTORC2 harbor several common components: the mTOR kinase, which acts as the central catalytic component, the scaffolding protein mLST8, mTOR regulatory subunit DEPTOR, and the Tti1/Tel2 complex, which is important for mTOR complex assembly and stability. Additionally, each complex harbors distinct subunits (**Figure 1.2**) that contribute to substrate specificity, subcellular localization, and complex specific regulation. mTORC1 is defined by its association with Raptor, a scaffolding protein important for mTORC1 assembly, stability, substrate specificity, and regulation, and PRAS40, a factor that blocks mTORC1 activity until growth factor receptor signaling relieves PRAS40-mediated mTORC1 inhibition. The recently solved structure of mTORC1 shows that it acts as a lozenge shaped dimer with the kinase domains coming in close proximity to one another in the center of the structure and Raptor and mLST8 binding on the periphery (56,57).

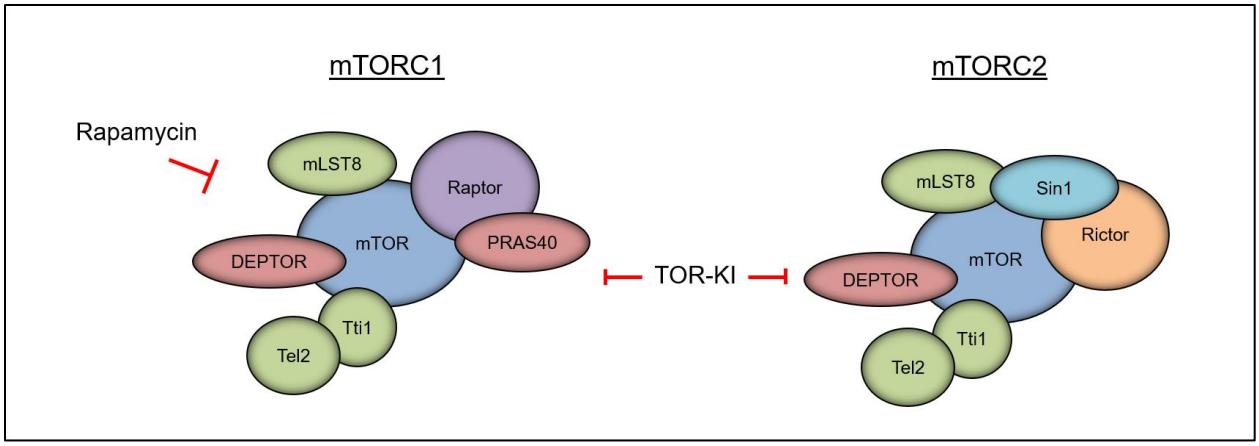

Figure 1.1 Schematic representation of mTOR complexes. mTORC1 consists of the mTOR kinase, mLST8, DEPTOR, Tti/Tel2, Raptor and PRAS40. mTORC2 also shares the mTOR kinase, mLST8, Tti/Tel2 and DEPTOR, but contains unique components Rictor and Sin1. Rapamycin is a known allosteric inhibitor of mTORC1, whereas TOR kinase inhibitors (TOR-KIs) inhibit the activities of both complexes.

Rictor and Sin1 are subunits specific to mTORC2. Genetic engineering of cells deficient for Rictor demonstrate that Rictor is required for mTORC2 assembly, stability, substrate identification, and subcellular localization of mTORC2 to the appropriate sites of action (53). Sin1 is also required for subcellular localization of mTORC2 to the plasma membrane (58). Importantly, Sin1 is a key negative regulator of mTORC2 kinase activity, until growth factor receptor-derived signaling through the phosphatidylinositol-3-kinase (PI3K) recruits Sin1/mTORC2 to the plasma membrane, where Sin1-mediated mTORC2 inhibition is relieved. Although the structure of mammalian mTORC2 has yet to be resolved, cross-linking mass spectrometry and electron microscopy have been used to determine the architecture of TORC2 in yeast (59). The structure of TORC2 looks similar to that of TORC1, although TORC2 specific components bind to different locations along the TOR kinase. Since yeast has separate TOR kinases for each complex, solving the structure of mammalian mTORC2 is still an important goal that will lead to further understanding of mTORC2 function.

The differing components and structures of mTORC1 and mTORC2 allow for independent regulation through subcellular localization. For example, active mTORC2 associates closely with the plasma membrane, and has been detected in association with ribosomal membranes (60), where it can interact with its key substrates, the AGC kinases including AKT1-3, serum glucose kinase (SGK) isoforms, and protein kinase C (PKC) family members. In contrast, mTORC1 appears to be affiliated with endosomal and lysosomal membranes, where it interacts with its effectors 4EBP1 and S6K1 (**Figure 1.3**). The unique composition of each complex followed by distinct downstream effectors allows each complex to regulate a variety of different downstream cellular processes (**Figure 1.4**).

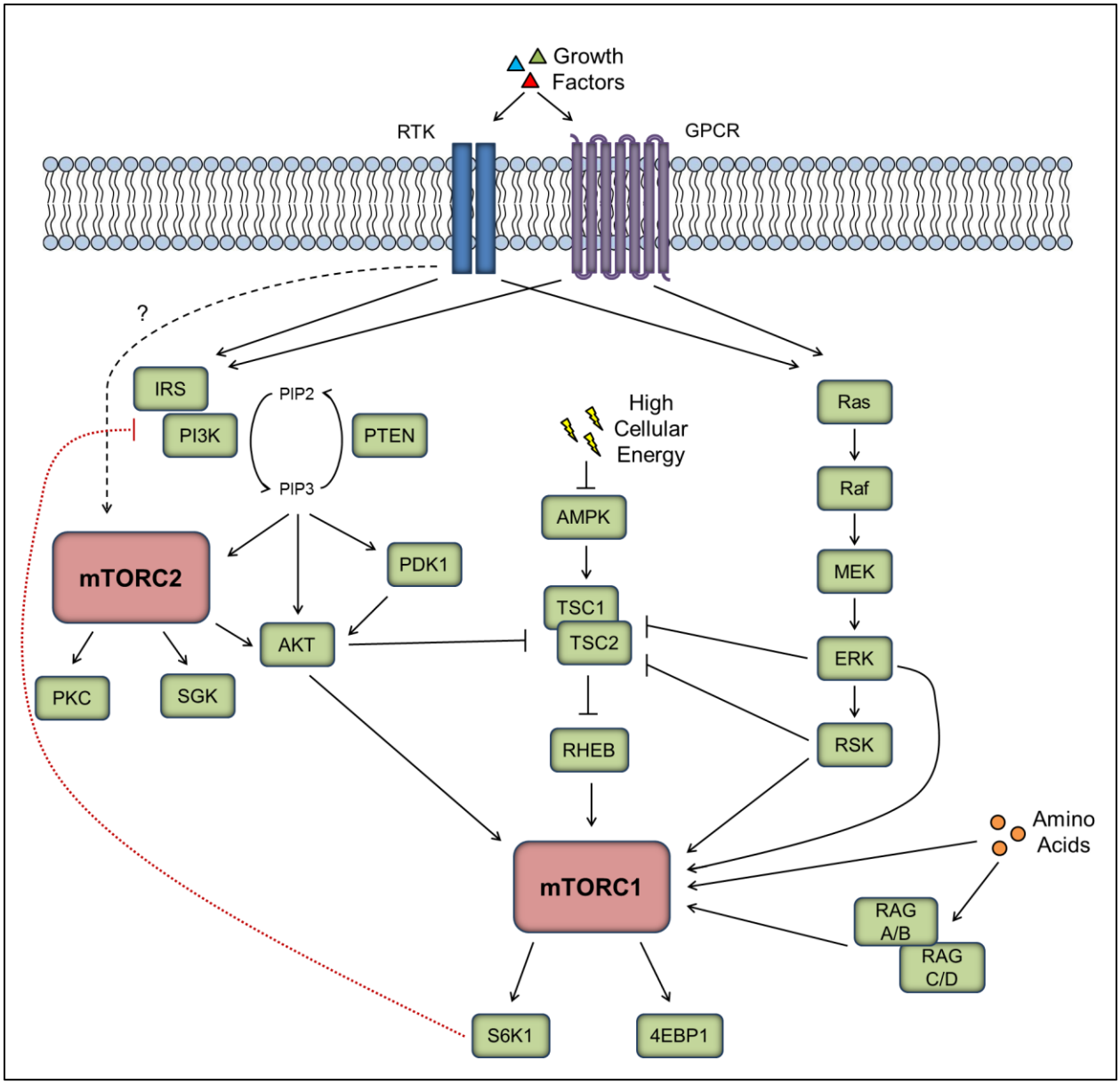

Figure 1.2 Overview of the mTOR signaling pathway. mTOR signaling is activated by a variety of environmental cues including growth factors, high cellular energy and amino acids. Growth factors activate both mTORC1 and mTORC2, through binding of receptor tyrosine kinases (RTKs) or G-protein coupled receptors (GPCRs) and activation of PI3K or Ras-MAPK signaling cascades. PI3K phosphorylates PIP2 to increase the amount of PIP3 in the membrane, allowing colocalization of AKT, PDK1, and mTORC2. PDK1 phosphorylates AKT at T308, while mTORC2 phosphorylates AKT at S473 for complete activation. AKT in turn activates mTORC1 by inhibiting TSC2, a GAP for RHEB, an activator of mTORC1. AKT phosphorylation of PRAS40 promotes its dissociation from mTORC1 for full activation. ERK and RSK, both part of the Ras-MAPK signaling pathway, can also inhibit TSC2 to activate mTORC1 or activate mTORC1 directly through phosphorylation of PRAS40. High ATP levels in the cell inhibit AMPK, an

activator of TSC2, thereby increasing the activities of RHEB and mTORC1. Intralysosomal arginine and cytoplasmic leucine stimulate Rag-dependent localization of mTORC1 to the lysosome where RHEB can activate mTORC1. Cytoplasmic glutamine triggers lysosomal localization of mTORC1 through a Rag-independent mechanism. Downstream targets of mTORC1 include S6K1 and 4EBP1, while downstream targets of mTORC2 include AKT, PKC and SGK. S6K1 inhibits PI3K, completing a negative feedback loop on AKT signaling.

mTORC1 Signaling

The PI3K pathway is frequently activated in response to oncogenic growth factor receptor signaling. PIK3CA activating mutations, RAS mutations, or PTEN loss result in increased production of the second messenger phosphatidylinositol (3,4,5)-triphosphate (PIP3) (61). Although PIP3 directly recruits and activates mTORC2, PI3K signaling also indirectly activates mTORC1, primarily through AKT. Activation of AKT occurs through phosphorylation at Ser473 mediated by mTORC2, and at T308 mediated by PDK1, another serine-threonine kinase recruited to the plasma membrane by PIP3. Once activated, AKT phosphorylates tuberous sclerosis complex 2 (TSC2), blocking its association with TSC1 (62–64). Since TSC1/2 is a negative regulator of the mTORC1 activator RHEB, AKT-mediated TSC2 phosphorylation allows GTP-loaded RHEB to bind and activate mTORC1 (65,66). AKT also phosphorylates the mTORC1 inhibitor PRAS40, causing PRAS40 to dissociate from Raptor, permitting mTORC1 activation (67–70).

In addition to the PI3K pathway, the Ras-MAPK signaling cascade can activate mTORC1. Similar to AKT-mediated phosphorylation of TSC2, ERK and RSK also phosphorylate TSC2 (71,72), albeit at different residues, to inhibit the TSC1/2 complex and trigger RHEB-mediated activation of mTORC1. Similarly, RSK can also phosphorylate PRAS40 (73), leading to dissociation from Raptor and promoting mTORC1 activation.

Although growth factor signaling through the PI3K/AKT and Ras-MAPK cascades is a key trigger for cellular proliferation, it is important that cells do not proceed with proliferation if the necessary nutrients, energy, and macromolecules are not available to support the high demands of cellular replication. Consistent with this notion, mTORC1 is highly responsive to intracellular ATP, glucose, and certain amino acids, including leucine, arginine and glutamine. Low ATP/high AMP levels activate AMP kinase (AMPK), an indirect mTORC1 inhibitor which functions by promoting TSC1/2 complex formation (74). Thus, AMP accumulation would override growth factor signals and block cellular proliferation in the absence of a sufficient energy supply. Similarly, a lack of amino acids would prevent localization of mTORC1 to lysosomal surfaces where RHEB activates mTORC1, overriding growth factor receptor-derived proliferation signals (75,76), and blocking mTORC1-dependent proliferation in the absence of the needed supply of amino acids. Interestingly, the intracellular location and type of amino acid can be sensed by the cell to determine the mechanism by which mTORC1 lysosomal localization is regulated (77). For example, intralysosomal arginine (78) or cytoplasmic leucine (79–81) activates RAG-GTPases which associate with Raptor directly to localize mTORC1 to lysosomal membranes (82). Meanwhile, cytoplasmic glutamine regulates mTORC1 localization through RAG-independent mechanisms (83,84).

Once activated, mTORC1 phosphorylates substrates, including elongation initiation factor (EIF)-4E binding protein 1 (4EBP1) and ribosomal protein S6 kinase 1 (S6K1), two proteins that are key regulators of both cap-dependent and cap-independent translation. Interestingly, increased cap-dependent translation caused by aberrant mTORC1 activation results in increases in cell size (85) and proliferation (86), two common traits of cancer. 4EBP1 and S6K1 bind to eIF-4E and eIF-3, respectively, inhibiting formation of the translation initiating complex. mTORC1-mediated phosphorylation of 4EBP1 and S6K1 liberates their respective binding partners, facilitating preinitiation complex formation (87). S6K1 phosphorylates eIF-4B

and S6 ribosomal protein (S6RP), initiating translation (88). S6K1 also plays a key role in translational elongation, phosphorylating eukaryotic elongation factor 2 kinase (eEF2K), allowing eEF2 to continue translational elongation (89). Interestingly, mTORC1 does not affect all transcripts equally. For instance, prostate cancer studies showed that the most common targets of increased translation were those involved in invasion, metastasis, and protein synthesis, highlighting the role of mTORC1 in oncogenic translation (90). Increased translation of protein synthesis genes, consisting mostly of genes involved in ribosomal biogenesis (91–93), is a well-known phenomenon related to mTORC1 hyper-activation. This is a logical target for mTORC1-mediated oncogenic translation since sufficient ribosome levels are required to maintain the increased translation of other genes important for transformation.

mTORC1 in Cancer

Direct evidence for mTORC1 activity in tumorigenesis comes from Tuberous Sclerosis, a disease caused by loss of TSC1 or TSC2, consequently hyper-activating mTORC1, and resulting in widespread but benign tumor formation. The limited progression of these tumors may be due to mTORC1-mediated negative feedback on insulin receptor substrate (IRS)-1, potently downregulating PI3K signaling downstream of most receptor tyrosine kinases (RTKs) (94–96). Also, mTORC1 directly phosphorylates Grb10, an adaptor that directly binds RTKs (97,98), although Grb10 phosphorylation is reported to have the capacity to stimulate and block PI3K activation, perhaps in isoform-specific fashions. Regardless, tuberous sclerosis patients demonstrate that mTORC1 signaling as a single molecular aberration is a potent driver of cellular proliferation. In the context of added genetic and molecular alterations, mTORC1 signaling potentiates the severity of tumor progression through numerous molecular mechanisms.

Transformed cells display metabolic reprogramming, a requirement that may enable cancer to surmount the demands of rapid proliferation. For example, many tumors display aerobic glycolysis, in which glycolysis occurs in the presence of oxygen, perhaps not as a main source of ATP, but rather as a generator of building blocks that can be shunted to alternative anabolic pathways to generate molecules needed for proliferation, including lipids, amino acids, and nucleotides. There is evidence that mTORC1 regulates aerobic glycolysis through increased translation of hypoxia inducible factor (HIF)-1α (99), a transcription factor that drives expression of several glycolytic enzymes (100). mTORC1 upregulates the synthesis of lipids from glycolysis-derived intermediates through phosphorylation of Lipin1 and S6K1, thus activating the transcription factor sterol regulatory element binding factor (SREBP)-1, driving transcription of genes involved in lipogenesis (101,102). Loss of mTORC1-mediated activation of SREBP1 in breast cancer cells blocked lipogenesis, interfering with cellular proliferation and tumor growth (103). Shunting of glycolytic intermediates into nucleotide synthesis is also controlled in part by mTORC1. mTORC1-mediated phosphorylation of S6K1 stimulates both purine and pyrimidine synthesis, which is necessary for cancer cells to rapidly duplicate their DNA (104–106).

These studies would suggest that targeted inhibition of glycolysis would be a feasible approach to blocking cell growth, despite mTORC1 activation. However, phase I clinical trials of the glycolysis inhibitor 2DG yielded disappointing results, with disease progression in the majority of cases, although a few showed stable disease or partial responses (107). Ovarian cancer cells cultured in 2DG to select for glycolysis resistance had upregulated mTORC1 activity as well as increased lipogenesis and nucleotide synthesis (108). These findings suggest that mTORC1-mediated glycolysis may support cancer cells, but that in the absence of glycolysis, other mTORC1-mediated anabolic pathways still support cell proliferation. However,

how these tumor cells are supplied with the necessary intermediates for shunting into alternative metabolic pathways, but in the absence of glycolysis, is a question that remains.

Answers may be found in the ability of cells to upregulate macropinocytosis, the process used by cells to obtain macro-nutrients from the extracellular environment. mTORC1 negatively regulates lysosomal degradation of extracellular protein taken up by macropinocytosis. Experiments in which tumor cells were starved of amino acids in culture and in tumors that were poorly vascularized in vivo, demonstrated that mTORC1 inhibition provided a growth advantage, through upregulation of macropinocytosis and catabolism of engulfed proteins (109). The dual roles of mTORC1 in tumor metabolism and growth will need further consideration, particularly in patients treated with mTOR inhibitors.

Aside from regulating cell growth and metabolism, mTORC1 also controls autophagy, an intracellular process that allows orderly degradation and recycling of cellular components. mTORC1 negatively regulates autophagy by phosphorylation of ULK to block initiation of autophagy, VPS34 to block autophagosome formation (110). Autophagy is sometimes considered a tumor suppressor (111), since blockade of autophagy, through deletion of Beclin1 for example, promotes tumor formation (112,113). However, there is abundant evidence to support that autophagy can be harnessed by tumor cells to drive survival under conditions of metabolic duress (114). In this scenario, inhibition of mTORC1 might enhance autophagy, and in doing so, may allow cells to generate nutrients and molecular building blocks to support tumor cell survival to a greater extent than if mTORC1 signaling was left intact.

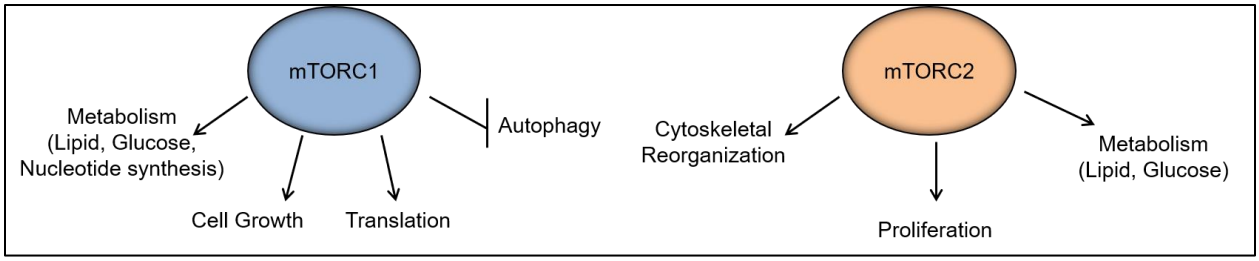

Figure 1.4 Downstream cellular processes for mTORC1 and mTORC2. Each mTOR complex regulates distinct downstream cellular processes including metabolism, cell growth, translation, and autophagy for mTORC1, and cytoskeletal reorganization, proliferation, and metabolism for mTORC2.

mTORC2 Signaling

Unlike mTORC1, the upstream regulation of mTORC2 is not well defined, although growth factor stimulation and ribosome association are both known mTORC2 activators (60,115). Importantly, mTORC2 localization at the cell membrane through the Sin1 subunit places mTORC2 in close proximity to its substrates AKT, SGK, and PKC. Thus localization at the plasma membrane is a key aspect of mTORC2 regulation (58). An oncogenic mutation in the PH domain of Sin1 that blocks Sin1-mediated mTOR inhibition leading to constitutive mTORC2-AKT signaling has been identified in an ovarian cancer patient (58). Direct phosphorylation of Sin1 at T86 by AKT may also regulate mTORC2, leading to a positive feedback loop that sustains mTORC2-AKT signaling, while Sin1 phosphorylation by S6K1 at this same site may inhibit mTORC2 activity as a feedback mechanism downstream of mTORC1 (116–118). Recent studies have identified another function for Sin1 in mTORC2 regulation. The PH domain of Sin1 can also bind to phosphorylated cytoplasmic Rb through to inhibit mTORC2 complex formation and reduce AKT signaling (119). Regulation of mTORC2 by Sin1 may be cell-type and/or context dependent. Clarification of these feedback mechanisms will be important for complete understanding of mTORC2 activation and signaling in cancer.

AKT, a key substrate of mTORC2, is among the most commonly hyper-activated proteins in cancer. AKT integrates signals from PI3K/mTORC2 and from PI3K/PDK1 to promote cell growth and survival. Like mTORC2, AKT localization to the plasma membrane is regulated by PIP3. In PTEN null prostate cancer, loss of mTORC2 activity inhibits tumorigenesis, illustrating the importance of mTORC2 signaling downstream of PIP3 (120). Interestingly, PTEN null glioma patients exhibit mTORC2-mediated chemotherapy resistance in an AKT independent manner (121), suggesting that inhibition of mTORC2 may be useful in treatment of patients with PTEN or PI3K mutations. mTORC2 also regulates cancer cells' preferential use of glycolysis for energy production through the AKT-independent acetylation of FoxO1/3 (122), demonstrating a mTORC2-mediated role in cancer metabolism. In addition to its activation by mTORC2, AKT activates mTORC1 signaling (62,70), adding another layer of complexity to this signaling pathway.

mTORC2 also phosphorylates SGK and PKC family members. Activation of SGK3 is implicated in cancer particularly because of its ability to reinforce PI3K signaling through INPP4B (123). Importantly, SGK1 promotes resistance to chemotherapy (124) and AKT inhibitors (125). Substrates of SGK include both NDRG1 and FoxO family transcription factors, two factors that are not growth promoting under oxygen and/or nutrient replete conditions, but which can promote survival in response to oxygen or nutrient deprivation, or in response to PI3K inhibition (124,126). NDRG1 is a potent suppressor of tumor cell invasion and metastasis and is degraded in response to SGK-mediated phosphorylation.

PKC, which exists in several isoforms, is also known to be involved in tumorigenesis, although the exact role of each isoform has yet to be defined. Studies have shown that each isoform may work in a cell-type specific manner. In the mouse mammary gland, genetic disruption of Rictor blocked mTORC2-dependent ductal branching, and reduced motility, invasion, and survival of mammary epithelial cells. Importantly this was rescued upon

reactivation of PKCα and its downstream effector, Rac1 (127). Although studied in the developmental setting, all of these phenotypes are known to be important in breast cancer metastasis, suggesting a role for the mTORC2/PKCα signaling axis in breast cancer as well.

mTORC2 in Cancer

While mTORC1 is extensively studied in cancer, recent reports also demonstrate a distinct role for mTORC2 in prostate, breast, and lung cancer, glioblastoma, and T-cell acute lymphoblastic leukemia (T-ALL) (120,128). Amplification of *RICTOR* was observed in non-small cell lung cancer patients (129), breast cancer (130), and in residual disease of triple-negative breast cancers treated with neoadjuvant chemotherapy (131), reinforcing the importance of mTORC2 signaling in cancer and as a potential target for inhibition. Rictor overexpression was also previously noted in gliomas, in which about 70% of patients have increased AKT activity (132). In HER2-positive breast cancer, enriched Rictor expression leads to hyper-activation of AKT and tumor progression. Knockdown of Rictor (but not Raptor) or treatment with mTORC1/2 dual kinase inhibitors (but not mTORC1-specific rapalogs) decreased AKT-mediated tumor cell survival and increased therapeutic tumor cell killing in cells treated with the HER2/EGFR tyrosine kinase inhibitor, lapatinib (130). Collectively, these data suggest a distinct role for mTORC2 in cancer.

mTOR Inhibitors for Cancer Therapy

Rapamycin was the original mTOR inhibitor, which allosterically inhibits mTORC1 (**Figure 1.1**), but not mTORC2. The yeast structure of TORC2 suggests the Rictor analog Avo3 may block FKBP12-rapamycin complex binding to the mTOR kinase, granting rapamycin insensitivity, although the lack of mammalian mTORC2 structure prevents confirmation of this mechanism in humans (59). Interestingly, prolonged treatment with rapamycin inhibits mTORC2 in certain cell types, suggesting a cell-type specific mechanism of regulation of mTORC2 (133).

Rapamycin analogs (“rapalogs”) have been developed (**Table 1.1**) with enhanced pharmacokinetic properties for more effective treatment of patients (134). The first rapalog, temsirolimus, was approved by the FDA in 2007 after it was shown to be effective in treating advanced renal cell carcinoma (135). Since then, everolimus, another rapalog, has been approved for treatment of several other cancers including breast, pancreatic, lung, and subependymal giant cell astrocytoma. Rapalogs most often cause disease stabilization rather than regression, consistent with the idea that mTORC1 is a driver of cellular proliferation, but not cell survival.

Drug	**Date of approval**	**Cancer Type**	**Therapeutic Condition**	**Marketed By**
Rapamycin/Sirolimus (Rapamune)	5.29.2015	Lymphangioleiomyomatosis	Monotherapy	Pfizer (Wyeth)
Temsirolimus (Torisel)	5.30.2007	Renal Cell Carcinoma	Monotherapy	Pfizer (Wyeth)
Everolimus (Afinitor)	5.30.2009	Advanced Renal Cell Carcinoma	Monotherapy	Novartis
	10.29.2010	Subependymal Giant Cell Astrocytoma (SEGA) associated with Tuberous Sclerosis Complex (TSC)	Monotherapy	
	5.5.2011	Progressive Neuroendocrine Tumors of Pancreatic Origin	Monotherapy	
	7.20.2012	Hormone Receptor Positive, HER2 Negative Breast Cancer	In combination with Exemestane	
	8.29.2012	Pediatric and Adult SEGA associated with TSC	Monotherapy	
	2.26.2016	Neuroendocrine Tumors of Gastrointestinal or Lung Origin	Monotherapy	
	4.10.2018	TSC-associated partial-onset seizures	Monotherapy	

Table 1.1 mTOR inhibitors approved by the FDA for cancer treatment

There are several potential reasons for the limited efficacy of rapalogs in treating cancer. First, inhibition of mTORC1 action on its substrates is incomplete. Inhibition of mTORC1 by rapamycin completely blocks the phosphorylation of S6K1, but phosphorylation of 4EBP1 is often only modestly inhibited (136). Since 4EBP1 regulates cap-dependent translation, it is possible that 4EBP1 is still able to translate proteins important in tumorigenesis. Additionally, inhibition of mTORC1 will release mTORC1-mediated restraints on PI3K/mTORC2/AKT signaling, resulting in resurgent AKT signaling, increased growth, and heightened cell survival (137,138). mTORC1 inhibition may also cause increased cell proliferation within vascularly compromised tumor regions due to elevated micropinocytosis (109) of extracellular proteins or increased cell survival through enhanced autophagy (114).

Recent advances have been realized in ATP-competitive mTOR kinase inhibitors (TOR-KIs), which block mTOR catalytic activity, whether embedded within mTORC1 or mTORC2 (**Figure 1.1**) (136). Preclinical testing of these inhibitors has shown complete 4EBP1 inhibition, with sustained repression of mTORC2-mediated AKT phosphorylation, resulting in superior tumor cell killing and growth inhibition as compared to rapalogs (89). mTOR kinase inhibitors are currently in Phase II clinical trials, after promising results in Phase I trials (**Table 1.2**) (140,141). While partial responses and stable disease have been reported, toxicity and adverse side effects are still a concern.

Pre-clinical studies have identified mutations in both the kinase domain and FRB domain of mTOR that prevent binding of either rapalogs or ATP-competitive mTOR kinase inhibitors, leading to loss of efficacy and eventual resistance. Most recently, a third generation mTOR inhibitor has been developed to overcome resistance to currently available inhibitors. This third-generation inhibitor has a bivalent structure consisting of a rapamycin-FRB binding element linked to a TOR-KI (142), so that when at least one half the ligand binds, the other half is in close proximity to the second binding site, overcoming point mutations that prevent binding of

either drug alone. Even with development of third generation mTOR inhibitors, concerns about toxicity remain. Additionally, mTORC1 inhibition, even within the context of mTORC2 inhibition, may promote tumor cell proliferation under nutrient-stressed conditions, as evidenced by the mutant KRAS pancreatic ductal carcinoma tumor model (109). Therefore, it will be important to investigate the impact of TOR-KIs on macropinocytosis and autophagy in distinct tumor types under both nutrient replete and deprived conditions.

Small molecular weight kinase inhibitors capable of simultaneous blockade of mTOR and PI3K have also been developed (**Table 1.2**). As expected, these inhibitors overcome the limitations of rapalogs and inhibit mTORC2-independent activation of AKT, while providing superior blockade of resurgent PI3K activity. Unfortunately, Phase I clinical trials using PI3K/mTOR dual kinase inhibitors revealed significant dose-limiting on-target toxicities (143,144), consistent with the important roles these enzymes fulfill in homeostasis of healthy tissues and systemic metabolism.

There is significant interest in developing mTORC2 specific inhibitors that will leave the activities of mTORC1 intact. Selectively targeting the mTORC2 branch may avoid feedback loop inhibition caused by rapalogs and may be particularly effective in vascularly compromised tumors under metabolic stress. As an added and important benefit, toxicities related to mTORC1 inhibition, including lesions within the oral mucosa, rash, and immune suppression, may also be reduced. Notably, genomic aberrations in Rictor and Sin1 have been identified in several tumor types (58,129,130,132) and patients with these genetic alterations may benefit from an mTORC2 specific inhibitor.

Drug Target	Drug Name	Published Clinical Trial	Cancer Type	References	Active Clinical Trials	Combination Therapy
mTOR kinase inhibitor	OSI-027	Phase I	Advanced solid tumors	(145)		
	AZD2014	Phase I/II	Advanced solid tumors, clear cell renal cancer	(141,146)	18	-Paclitaxel -AZD5363 -Selumetinib -Palbociclib -fulvestrant -rituximab -anastrozole -olaparib
	AZD8055	Phase I	Advanced solid tumors, lymphoma	(140)		
	CC223	Phase I	Advanced solid tumors, multiple myeloma	(147)	2	-CC122 or CC292 +/- Rituxumab
	MLN0128	None available			10	-Paclitaxel -Bevacizumab -MLN1117 -Alisertib or Paclitaxel or Cetuximab or Irenotecan -Exemestane or Fulvestrant
PI3K/mTOR dual inhibitor	BEZ235	Phase I/II	Advanced solid tumors, transitional cell carcinoma, pancreatic neuroendocrine tumors	(148–150)	1	
	XL765/SAR254409	Phase I	Advanced solid tumors, high-grade glioma, lymphoma	(144,151–153)		
	GDC0980	Phase I/II	Advanced solid tumors, metastatic renal cell carcinoma	(154,155)	2	-Fulvestrant -Abiraterone Acetate
	PKI587	Phase I	Advanced solid tumors	(156)	3	-Carboplatin and paclitaxel -Docetaxel or Cisplatin or Dacomitinib -Palbociclib and Faslodex

	GSK2126458	Phase I	Advanced solid tumors	(157)		
	PF04691502	Phase I/II	Advanced solid tumors, endometrial cancer	(143,158)		
	SF1126	Phase I	Advanced solid tumors, B-cell malignancies	(159)	1	
	BGT226	Phase I	Advanced solid tumors	(160)		

Table 1.2 mTOR inhibitors in clinical trials as of July 2015

mTOR in Vasculature

In addition to its essential role in tumor cells, mTOR signaling is critical in the tumor microenvironment (TME) (**Table 1.3**). For example, mTOR is key for tumor angiogenesis (161,162), a well-studied hallmark of cancer. In response to oxygen and/or nutrient deprivation, tumor cells secrete factors that recruit new vessel formation to support the growing tumor. Blockade of tumor angiogenesis would effectively limit tumor growth. Additionally, tumor vessels provide a route for tumor cells to disseminate to distant sites; as such, blockade of tumor angiogenesis could be harnessed to prevent tumor metastasis.

Hypoxia in the tumor stimulates angiogenesis via HIF transcription factors. In some cases, oncogenic mTOR signaling can actively promote cap-dependent translation of HIF-1α (163,164). HIF-1α activates expression of proangiogenic factors that are secreted by the tumor cell, including vascular endothelial growth factor (VEGF). VEGF binds to the VEGF receptors on the surface of vascular endothelial cells, to promote angiogenesis. Interestingly, loss of the mTORC1 negative regulator TSC1 from vascular endothelial cells drives proliferative lesions resembling lymphangiosarcoma, suggesting that mTORC1 is a dominant driver of endothelial cell proliferation(165), although evidence suggests mTORC2 could also play a role in endothelial cell proliferation through downstream effector PKCα (166). TSC1-deficient

lymphangiosarcoma formation was suppressed not only by rapamycin, but also was by inhibitors of VEGF, defining a mTORC1-VEGF feed-forward loop in the angiogenic process that drives endothelial cell proliferation, survival, and vascular assembly (165). Rapalogs have been successful in treating highly vascularized tumors like Kaposi's sarcoma and renal cancer.

Tumor Cell		**Endothelial Cell**	
mTORC1			
Cell Size and Proliferation	Refs. 36,37	Autocrine VEGF signaling through HIF-1α translation	Refs. 100,109,110
Metabolic Reprogramming: glycolysis, glutaminolysis, nucleotide synthesis, lipogenesis	Refs. 50-57, 59	Vessel Permeability	Ref. 101
Stimulation of Angiogenesis	Refs. 97-99, 126-128	Cell Proliferation	Ref. 96,100
mTORC2			
Cell Survival	Ref.71	Vessel Morphology and Permeability	Refs. 101,105
Metabolic reprogramming: glycolysis, hypoxic response	Refs. 73,77	Cell Proliferation and Vascular Assembly	Ref. 101
Chemotherapy Resistance	Refs. 75	Metabolic Activity	Ref.106-108

Table 1.3 Function of mTORC1 and mTORC2 in tumor and endothelial cells

Interest in mTORC2 activity in the tumor vasculature was initiated with the observation that mTORC2 loss from endothelial cells causes deficiencies in physiological vascular development (173). Importantly, mTORC2 signaling has been implicated in sprouting angiogenesis stimulated by VEGF (174) and CXCL12 (175), both factors secreted by tumor cells to promote a more favorable microenvironment. Downstream of mTORC2, aberrant AKT signaling within the vascular endothelium promotes the tortuous and leaky vascular structures often associated with tumors (172). AKT has also been shown to primarily regulate vascular endothelial cell assembly (166). FoxO1, a substrate of the mTORC2 effectors AKT and SGK, has also been implicated in endothelial cell viability (176), growth (177), and metabolism (178). Since AKT can also activate mTORC1, it is possible that mTORC2 may have regulatory functions in the autocrine VEGF signaling within the vascular endothelium (165,167,168).

The use of mTOR inhibitors in treating cancers has provided insight into the effects of these inhibitors on the tumor vasculature. Everolimus, like VEGF inhibitors, decreased the tumor vasculature associated with a variety of solid tumor cell lines. While VEGF inhibitors were more potent at blocking formation of new vessels, everolimus was effective at reducing the viability of existing vessels (179). Consistent with the ability of everolimus to impair the integrity of existing tumor vasculature, radiation therapy caused excess damage to vascular endothelial cells upon mTOR kinase inhibition (180,181).

mTOR in Tumor Immunity

Along with the tumor vasculature, the immune system is another facet of the TME that supports tumor initiation, progression, and metastasis, as tumor cells must actively evade immune surveillance to prevent eradication by the host. Tumors often express immunosuppressive ‘checkpoint’ markers such as CTLA-4 and PD-L1/PD-L2, that anergize CD8+ T-cells that would otherwise mount a cytotoxic attack (182). Inhibiting these immune

checkpoints allows cytotoxic CD8+ T-cell activation and anti-tumor immune responses. Anti-PD-1/PD-L1 therapy has been extraordinarily successful in the treatment of melanoma patients and is currently in clinical trials for many other types of cancer.

A recent study in non-small cell lung cancer cells demonstrated that hyperactivated AKT-mTOR signaling directly increases PD-L1 expression (183). Interestingly, melanoma tumors grown in immunocompromised mice still respond to anti-PD1 therapy, suggesting a tumor intrinsic role for these immune checkpoint molecules (184). Further investigation showed that PD-1/PD-L1 interaction on tumor cells signals through mTORC1 to promote tumor cell proliferation. Together, these data suggest combination of checkpoint inhibitors and mTOR inhibition may be more efficacious than either therapy alone.

mTOR signaling within the immune cells themselves also deserves scrutiny, since rapamycin was first used in the clinic as an immune suppressant in organ transplant patients. The role of mTOR signaling in determining the fates of helper T cells has been relatively well defined. mTORC1 activity is predominately associated with Th1 differentiation and anti-tumor immunity (185). Inhibition of mTORC1 using rapalogs or rapamycin encourages engraftment in organ transplant patients through inhibition of cytotoxic immunity, particularly through expansion of CD4+regulatory T cells (T_{reg}) (186). In contrast to mTORC1, mTORC2 activity is often associated with immune suppressive Th2 phenotypes (185,187). This is regulated by mTORC2 downstream effector, SGK, which when depleted, limits differentiation of Th2 CD4+ T-cells (188).

In addition to CD4+ T-cells, mTOR signaling also regulates CD8+ T-cell effector function and differentiation, both important processes for mounting an immune response towards tumor cells. The role of mTORC1 as a regulator of CD8+ T-cell effector function has been well-defined by genetic deletion of the mTORC1 suppressor TSC2 in T-lymphocytes which resulted in

mTORC1 upregulation and profound CD8+ T-cell effector function (189). Conversely, the role of mTOR signaling in establishing CD8+ memory T-cells has yet to be clearly defined. Rapamycin treatment reduced mTORC1 activity and increased CD8+ memory T-cell formation (190). Contrarily, other reports suggest that memory T-cell formation is predominately regulated by the mTORC2 pathway, as demonstrated by an increase in memory T-cell formation upon genetic deletion of Rictor in T-lymphocytes (189,191). This discrepancy may be explained by the ability for rapamycin to inhibit mTORC2 in certain cell types, which would confirm the role of mTORC2 as the predominant regulator of memory T-cell differentiation.

While the role of T-cells is currently most well-studied in terms of mTOR signaling and tumor immunity, there is also evidence that mTOR signaling plays a role in other immune cells that could be important in the tumor microenvironment. TSC2 deletion in myeloid lineages increased mTORC1 signaling and blocked differentiation of macrophages towards an M2 phenotype, the phenotype most closely correlating to pro-malignant and immune suppressive tumor-associated macrophages (TAMs) (192). Although the roles played by B cells in tumor immunity is less understood, it is known B-cells can promote inflammation and carcinogenesis, as well as regulate anti-tumor T-cell responses. mTOR signaling is implicated in physiological B cell maturation, survival and proliferation, suggesting a possible role for mTOR in antibody-mediated regulation of tumor immunity (193).

Summary and Thesis Projects

Increasing investigations of mTOR signaling in cancer cells and throughout the complex TME has provided the platforms from which new studies will reveal a more refined understanding of mTOR within each tumor compartment, the distinct and intertwining roles of mTORC1 and mTORC2, and how this knowledge can be applied towards novel therapeutic strategies that will safely and effectively eradicate cancers. The following three chapters of this

dissertation aim to answer some of these questions. The first chapter examines the role of mLST8, a shared mTOR co-factor, as a molecular scaffold required for integrity and function of mTORC2, but not mTORC1. We knocked out mLST8 using CRISPR-Cas9 genome editing technology in a panel of cancer and “normal” cell lines and showed that mLST8 was only required for mTORC2, not mTORC1, integrity and downstream signaling as judged by co-immunoprecipitation of the mTOR complex components and immunoblotting for phosphorylation of downstream targets. This was phenocopied by mLST8 mutants lacking the ability to bind to mTOR. We also expressed a series of Sin1 truncation mutants and determined that the N-terminal domain of Sin1 interacts with mLST8 in mTORC2. These data suggest the mechanism for the mTORC2-specific requirement of mLST8 comes from its role as a scaffold bridging the mTOR kinase and mTORC2-specific component Sin1. Mutation of the mTOR-binding interface on mLST8 in PTEN-null prostate cancer cells inhibited tumor growth in mouse xenograft models. This demonstrated that mLST8 is a novel target for mTORC2-specific inhibition, and this strategy may be useful in targeting mTORC2-dependent cancers. The second chapter examines the mechanism by which *RICTOR* amplification can drive mTORC2 activity and promote lung tumor growth. We used both traditional CRISPR-Cas9 and CRISPR Synergistic Activation Mediator techniques to knockout or overexpress Rictor in NSCLC cells, respectively. When Rictor expression levels were altered in either direction, we saw corresponding changes in levels in mTORC2 through both proximity ligation assays and co-immunoprecipitation experiments. However, mTORC1 levels were always inversely correlated suggesting a competitive relationship between mTORC1 and mTORC2 for shared co-factors. We also demonstrate the overexpression of Rictor can promote NSCLC proliferation in vitro and in vivo. Taking from the observations in Chapter II, we knocked mLST8 to inhibit mTORC2 in RICTOR-amplified NSCLC in vivo, and showed that tumor size and proliferation were reduced, again demonstrating mLST8 can be targeted to inhibit mTORC2 and be used as a therapeutic in mTORC2-dependent cancers. Finally, the third chapter of this dissertation summarizes our

findings and discusses remaining questions regarding mTOR signaling in the tumor and surrounding tumor microenvironment.

Chapter II

Disruption of the scaffolding function of mLST8 selectively inhibits mTORC2 assembly and function and suppresses mTORC2-dependent tumor growth in vivo

The work presented in this section is published in Cancer Research.

Abstract

Mechanistic target of rapamycin (mTOR) is a serine/threonine kinase that acts in two distinct complexes, mTORC1 and mTORC2, and is dysregulated in many diseases including cancer. mLST8 is a shared component of both mTORC1 and mTORC2, yet little is known regarding how mLST8 contributes to assembly and activity of the mTOR complexes. Here we assessed mLST8 loss in a panel of normal and cancer cells and observed little to no impact on assembly or activity of mTORC1. However, mLST8 loss blocked mTOR association with mTORC2 cofactors RICTOR and SIN1, thus abrogating mTORC2 activity. Similarly, a single pair of mutations on mLST8 with a corresponding mutation on mTOR interfered with mTORC2 assembly and activity without affecting mTORC1. We also discovered a direct interaction between mLST8 and the NH_2-terminal domain of the mTORC2 co-factor SIN1. In *PTEN*-null prostate cancer xenografts, mLST8 mutations disrupting the mTOR interaction motif inhibited AKT S473 phosphorylation and decreased tumor cell proliferation and tumor growth *in vivo*. Together these data suggest that the scaffolding function of mLST8 is critical for assembly and activity of mTORC2, but not mTORC1, an observation which could enable therapeutic mTORC2-selective inhibition as a therapeutic strategy.

Significance

Findings show that mLST8 functions as a scaffold to maintain mTORC2 integrity and kinase activity, unveiling a new avenue for development of mTORC2-specific inhibitors.

Introduction

Mechanistic target of rapamycin (mTOR) is a serine/threonine kinase controlling multiple cellular processes including cell growth, survival, metabolism, and cytoskeletal reorganization (194,195). mTOR functions in two distinct complexes, mTORC1 and mTORC2, both of which share the mTOR kinase and mLST8, but also contain components unique to each complex (Raptor for mTORC1; Rictor and SIN1 for mTORC2). While tremendous progress has been made in understanding the regulation and function of mTORC1/2, the specific role of mLST8 in each complex is less well defined. Although originally identified as an mTORC1 subunit (196), increasing evidence suggests that mLST8 is dispensable for mTORC1, but indispensable for mTORC2 activity (173,197). However, the molecular mechanisms underlying the requirement for mLST8 in mTORC2 activation remain unclear.

In this report, we identify interaction points between mLST8 and mTOR, which when disrupted, specifically impair mTORC2 assembly and activity without affecting mTORC1. Furthermore, we found a direct interaction between mLST8 and SIN1 and further identified the region of the SIN1 NH_2-terminal domain that interacts with mLST8. We found that prostate cancer xenografts expressing the mLST8 mutant incapable of mTOR interaction displayed impaired mTORC2 signaling *in vivo* and reduced tumor growth, suggesting that targeted disruption of mLST8-mTOR interactions could be employed as a therapeutic strategy to selectively target mTORC2, while sparing the activity of mTORC1.

Materials and Methods

Cell lines and cell culture

Human embryonic kidney 293T (HEK293T) cells, BT-549, DU159, and PC3 cells were obtained from ATCC and maintained in Dulbecco's Modified Eagle's Medium (DMEM) containing 10 % fetal bovine serum (FBS). HEK293FT were obtained from Thermo Scientific and maintained in DMEM containing 10% FBS. Primary and immortalized human bronchial epithelial cells BEAS 2B cells were maintained in RPMI media containing 10% FBS. Normal human dermal fibroblast (NHDF) were obtained from Lonza. NHDF cells were cultured according to the manufacturer's protocol using the FGM-2 Bullet kit. All cells were cultured in a humidified incubator with 5% CO_2 at 37°C. Cell lines were used between passages 1 and 50 after thaw. Cell lines from ATCC were authenticated using short tandem repeat profiling. Mycoplasma testing was performed every 6 months, most recently in January 2019, using the PlasmoTest kit from Invivogen.

Generation of the mTOR E2285A knock-in cell line by CRISPR–Cas9 technology

The mTOR E2285A knock-in under *MLST8* knockout background cell line was generated using the CRISPR/Cas9 technology. The sgRNA targeting the genomic sequence close to the codon of the 2285 glutamate residue on mTOR was designed using the CRISPR design tool (http://crispr.mit.edu) and cloned into pSpCas9(BB)-2A-GFP vector. Single-stranded oligodeoxynucleotides (ssODNs) were used as the template for the E2285A mutation and a synonymous change to the PAM site. For ease of genotyping, a *Sph*I site near the target was mutated synonymously. The Cas9/sgRNA construct and the ssODNs were co-transfected into *MLST8* KO HEK293T cells. 48 hours post-transfection, transfected cells were seeded into a 96-well plate by limited dilution. The genomic DNA of individual clones was extracted to amplify the DNA fragment containing the E2285 site. PCR products were digested by *Sph*I-HF to screen for correct clones. Knock-in mutations were verified by the Sanger sequencing of cloned genomic PCR. sgRNA oligos, primers for genomic PCR and ssODN are listed in **Table 2.1**.

Xenograft Assay

5 x 10^6 cells suspended in 100 uL of Matrigel and PBS (1:1) were injected into the hind flanks of 6-week old athymic nude mice (Foxn1^{nu}; Envigo). Tumor measurements were started 10 days after injection and were monitored for 3 weeks. Tumors were measured every 2-3 days with digital calipers and tumor volume calculated according to the formula (V=4/3π(l/2)(h/2)(w/2)). Data are presented as mean ± SEM (n=10). Two-way ANOVA with Bonferroni's Correction was used for statistical analysis. Experiments with mice were pre-approved by the Vanderbilt Institutional Animal Care and Use Committee and followed all state and federal rules and regulations.

Plasmids

CRISPR-Cas9 backbone vectors were obtained from Addgene and guide RNA sequences were cloned into the vector according to depositor's instructions. Guide RNA primers are listed in **Table 2.1**. Guide RNA resistant wild-type and mutant mLST8 ORF were synthesized and cloned into lentiviral expression vector plentiCMV-Blast using the Gibson assembly kit. Full-length mTOR expression vector was obtained from Addgene and mutated by Q5 site-directed mutagenesis kit. Full-length SIN1 ORF was cloned into TagGFP2 vector from Evrogene and deletion mutants were mutated using the Q5 site-directed mutagenesis kit. All constructs are available at Addgene.

Lentivirus production and transduction

CRISPR-Cas9 knock-out and stable expression cell lines were established using the lentiviral delivery system. Briefly, lentiviruses were packaged in HEK293FT cells by transfecting cells with CRISPR or expression plasmids together with psPAX2 (lentiviral packaging) and pCMV-VSV-G (envelope) plasmids at 1:1:1 molar ratio using the Lipofectamine 2000 Reagent. Media was changed after 6 hrs of transfection and virus was collected after 48~72 hrs. Indicated cells were infected with virus in the presence of 8 μg/ml Polybrene for 24 hr and selected with 1~2 μg/ml

Puromycin or 20~40 μg/ml Blasticidin for about one week to establish stable cell lines before being used for experiments.

Western Blot and Co-immunoprecipitation (Co-IP)

Cultured cells or tumor tissue were lysed with CHAPS lysis buffer (40 mM Tris, pH 7.5, 120 mM NaCl, 1 mM EDTA, 0.3% CHAPS) and RIPA buffer, respectively supplemented with protease inhibitors and phosphatase inhibitors (Complete Mini and PhosStop inhibitor cocktail, Roche). Protein concentration of each sample was determined by Pierce BCA Protein Assay kit. Equal amounts of protein extracts were mixed with 4x Laemmli sample buffer and separated by electrophoresis on 10% or 4%–20% SDS-PAGE Gel, and then transferred onto nitrocellulose membranes. Membranes were blocked with 5% skim milk in TBS/T buffer and incubated with corresponding primary antibodies and IRdye-conjugated secondary antibodies. Immunoreactivity was detected using the Odyssey scanner (Li-cor Biosciences). To perform immunoprecipitation, equal amounts of input lysates (2~4 mg) were incubated with the primary antibodies (1~2 μg) for 2 hrs to overnight at 4°C. Protein G Dynabeads were added and lysates were incubated for 1 hr and washed four times with CHAPS lysis buffer. For western blot analysis, 2~5% of input lysate or immunoprecipitate was separated by SDS–PAGE and probed with indicated antibodies.

***In Vitro* Kinase Assay**

Cells were lysed as described above using CHAPS lysis buffer and lysates were subjected to IP using anti-mTOR for mTORC2 kinase assay and anti-Raptor for mTORC1 kinase assay at 4°C overnight. Immunoprecipitated mTOR complexes were washed once with kinase reaction buffer (25 mM HEPES pH 7.4, 50 mM KCl, 10 mM $MgCl_2$). Kinase assays were carried out by incubating immunoprecipitated mTOR complexes, recombinant AKT1 or S6K1 in 20 μl of kinase reaction buffer together with 50 μM cold ATP and 10 μCi [γ-^{32}P] ATP for 30 min at 30°C. GST-S6K1 was purified from HA-GST PreScission-p70S6K1 (Addgene #15511) transfected

HEK293FT cells with GSTrap FF glutathione column and eluent was desalted and adjusted to 0.2 μg/μl. Reactions were terminated by adding 4x Laemmli sample buffer, separated by SDS-PAGE and transferred onto nitrocellulose membranes. Radioactivity was determined by autoradiography on X-ray film and complex components and substrate proteins were probed with indicated antibodies.

Names	Sequence (5'→3')	Remark/Reference
sgRNA oligos for cloning (guide RNA sequences are capitalized)		
sgMLST8 #1	caccgCTGCAGGCTACGACCACACC	(198,199)
	aaacGGTGTGGTCGTAGCCTGCAGc	
sgMLST8 #2	caccgCTGGATGTACACGGGCGGCG	
	aaacCGCCGCCCGTGTACATCCAGc	
sgMLST8 #3	caccgCAACAAGAACATCGCGTCTG	
	aaacCAGACGCGATGTTCTTGTTGc	
sgMLST8 #4	caccgGCTATGTCTGGAATCTGACG	
	aaacCGTCAGATTCCAGACATAGCc	
sgMLST8 #1-Mm	caccgTGGAGTTGAGATCATACATG	This study
	aaacCATGTATGATCTCAACTCCAc	
sgMLST8 #2-Mm	caccgTATGTCTGGAACCTGACAGG	
	aaacCCTGTCAGGTTCCAGACATAc	
sgMTOR_exon 49	caccgGACTCTGATGCAGAAGGTGG	
	aaacCCACCTTCTGCATCAGAGTCc	
sgMAPKAP1 (SIN1) #1	caccgTGACACGGGAATGTGTGAGA	
	aaacTCTCACACATTCCCGTGTCAc	
sgMAPKAP1 #2	caccgTGAGGTAATATCGACTGACT	
	aaacAGTCAGTCGATATTACCTCAc	
sgMAPKAP1 #3	caccgTGCTGGCAGTATACAAGCGA	
	aaacTCGCTTGTATACTGCCAGCAc	
Genomic PCR Primers		
MLST8 Ex7-F	ggcatccttccctgtgtctc	153 bp
MLST8 Ex7-R	cgtgtgggcagggatcttag	
SIN1 Ex2-F	gaccagtgatgacacgggaa	531 bp
SIN1 Ex2-R	ccattcgcagtcgcagagat	
MTOR Ex49-F	ctctcatctgcacagaaggcct	485 bp
MTOR Ex49-R	cgctgtgtgcacatgaacagat	
ssODN		
mTOR E2285A donor	cagtggcctacctcggagctggggcttttcagccacagcagcttgg ccaggtcgtccccagctgtattattgacggcatgTtcaaacacAG ccaccttctgcatcagagtcaagtggtcatagtccggagc	This study

Table 2.1. DNA oligonucleotide sequences used in Chapter II.

Results

mLST8 is required for mTORC2, but not mTORC1, integrity and function

We generated 293T cells carrying loss of function indel mutations in the *MLST8* gene by CRISPR/Cas9-mediated genome editing, using multiple sgRNAs targeting human *MLST8* exon 2, 4, or 7 (**Figure 2.2A**) and confirmed loss of mLST8 protein expression (**Figure 2.1A**). mLST8 loss impaired co-precipitation of mTOR with the mTORC2 cofactors RICTOR and SIN1, without affecting the mTORC1 cofactor, RAPTOR. Consistent with the idea that mLST8 loss impairs mTORC2, mLST8-deficient cells displayed decreased pAKT^{Ser473}, the mTORC2 phosphorylation site, under steady-state growth conditions (**Figure 2.1A**), or in response to amino acid or serum induction (**Figure 2.1B**). Phosphorylation of other mTORC2 downstream effectors such as PKC and NDRG1 were also reduced (**Figure 2.1A**) with no impact on phosphorylation of the mTORC1 substrate S6K1^{Thr389} or mTORC1 effector S6RP. *In vitro* kinase assays performed using mTOR immunoprecipitates (IPs) from 293T cells lacking mLST8 showed strongly diminished phosphorylation of 6His-Akt (**Figure 2.1C**). In contrast, RAPTOR IPs from cells lacking mLST8 phosphorylated GST-S6K1 *in vitro* at similar levels to those from control cells expressing mLST8 (**Figure 2.2B**). These findings agree with recent data demonstrating that mLST8 is important for mTORC2 activity, but is dispensable for mTORC1 signaling, despite being a component of the mTORC1 holoenzyme. Importantly, restoration of mLST8 expression in several individually selected mLST8-deficient 293T cell clones (293T-sgMLST8) rescued co-precipitation of RICTOR and SIN1 with mTOR, as well as pAKT^{Ser473} (**Figure 2.1D**). We confirmed our findings in a panel of human and murine cell lines. (**Figure 2.2C&D**).

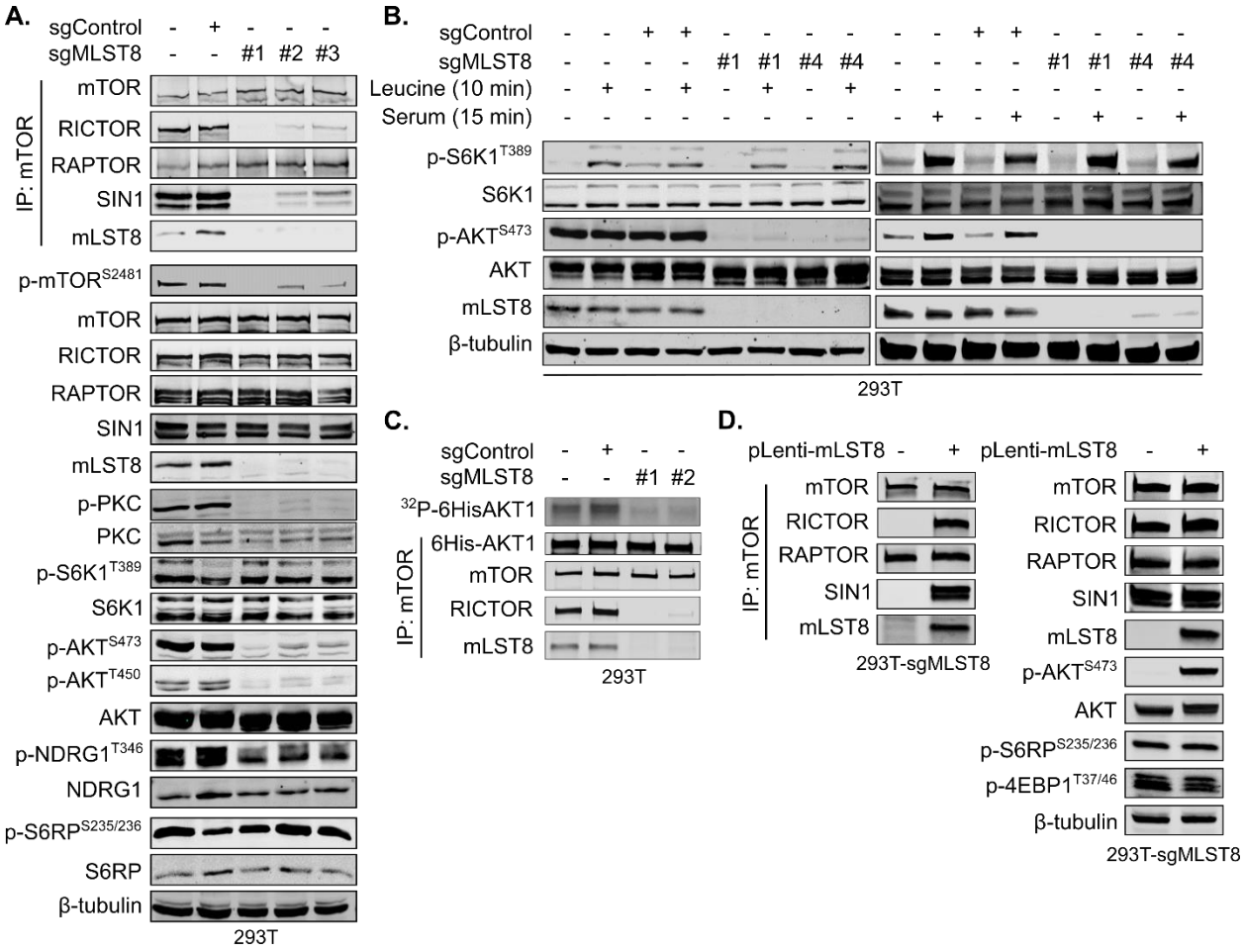

Figure 2.1. mLST8 is required for assembly and activity of mTORC2. (A) mTOR IPs or cell lysates from sgControl or sgMLST8 293T cells were assessed by western analysis. (B) sgControl or sgMLST8 293T cells were leucine or serum starved overnight, pulsed with L-leucine or 10% serum, and cell lysates were assessed by western analysis. (C) Immunoprecipitated mTOR complexes were incubated with purified 6His-AKT1 and ^{32}P-γ labeled ATP. Kinase activity was detected by autoradiography. (D) Wildtype mLST8 was re-expressed in a 293T-mLST8 knockout cell clone (sgRNA #4). mTOR IPs or cell lysates were assessed by western analysis.

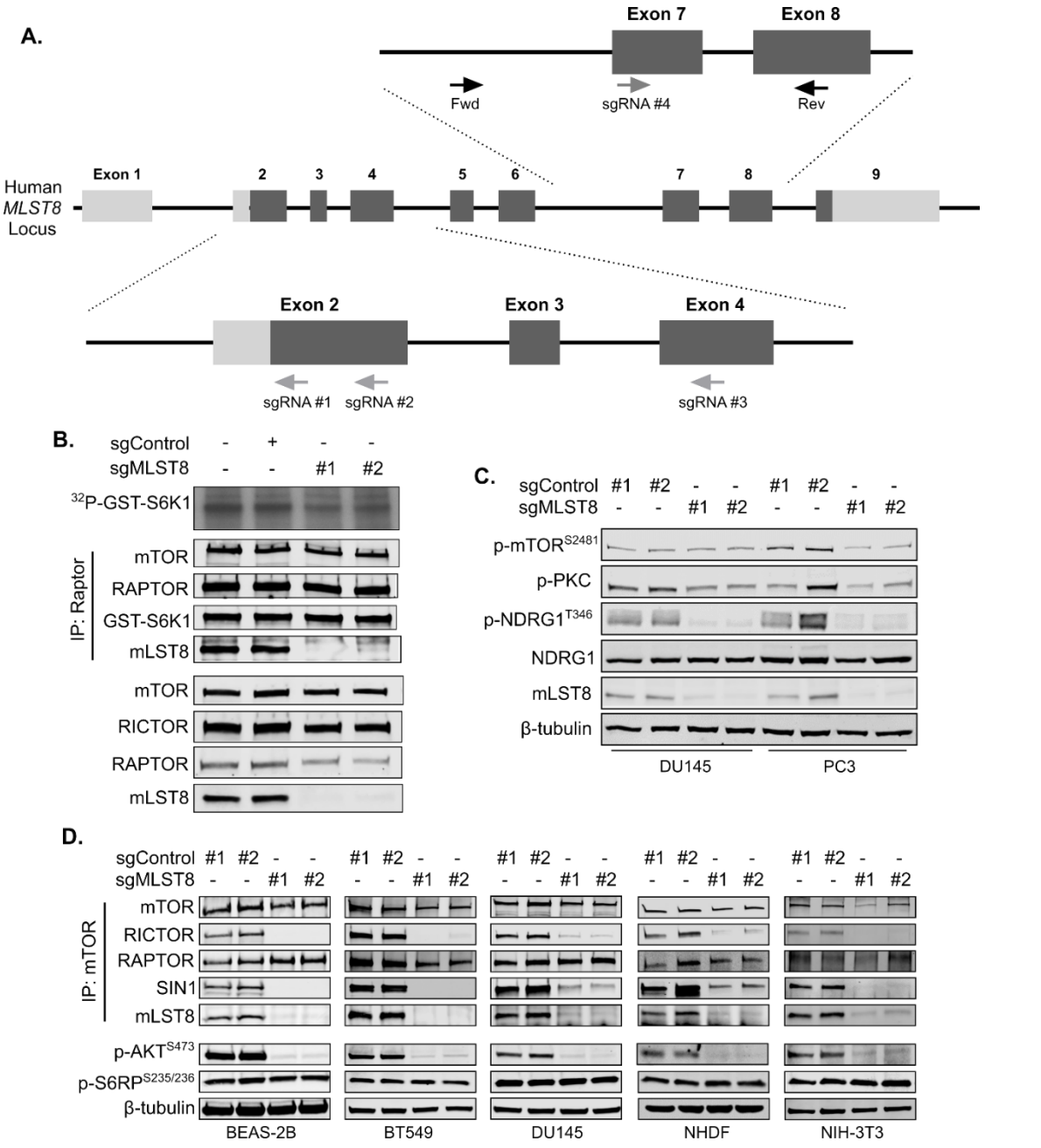

Figure 2.2. Supplemental figure related to Figure 2.1 (A) Schematic Representation of the human MLST8 locus with guideRNAs and genotyping primer locations. (B) Cell lysates from 293T cells expressing Cas9 with either sgControl or sgMLST8 were immunoprecipitated for Raptor and incubated with purified GST-S6K1 and 32P-γ labeled ATP. Kinase activity was detected by autoradiography and IP and whole cell lysates were assessed using the indicated antibodies. (C&D) Whole cell lysates from DU145, PC3, BEAS-2B, BT549, NHDF, and NIH-3T3 cells expressing Cas9 and either sgControl or sgMLST8 were assessed by western analysis using indicated antibodies.

mLST8 mutations that uncouple binding to LBE domain of mTOR disrupt mTORC2 complex formation and signaling

Previous analyses of the mLST8-mTOR kinase crystal structure identified structural areas of mTOR and mLST8 that might interact through formation of hydrogen bonds(56). In mLST8, the interaction points may occur across six of seven WD40 repeat domains that cooperate to form a beta-propeller structure(56). We introduced mLST8 point mutations at evolutionarily conserved residues predicted to be involved in hydrogen bonds, where important interactions with mTOR would most likely occur (**Figure 2.4A**). These mutations included mLST8-Q44E/N46L (mLST8^{Mut1}), and mLST8-W272F/W274F (mLST8^{Mut2}, **Figure 2.3A** and **Figure 2.4A**). mLST8^{WT}, mLST8^{Mut1}, and mLST8^{Mut2} were expressed in an mLST8-deficient 293T-sgMLST8 cell clone, as was mLST8$^{Mut1/2}$, harboring Q44E, N46L, W272F, and W274F mutations. Expression of each mLST8 species was confirmed by western analysis (**Figure 2.3B**). Co-precipitation of mTOR with RICTOR and SIN1 was seen in cells expressing mLST8^{WT}, mLST8^{Mut1}, and mLST8^{Mut2}, but not in cells expressing mLST8$^{Mut1/2}$. RAPTOR co-precipitation with mTOR was not affected by any mutation in mLST8 (**Figure 2.3B**), consistent with the idea that mLST8 is not necessary for mTORC1 assembly. Notably, cells expressing mLST8$^{Mut1/2}$ exhibited far less pAKT^{Ser473} as compared to cells expressing mLST8^{WT}, mLST8^{Mut1} or mLST8^{Mut2} (**Figure 2.3B**). This was confirmed by *in vitro* kinase assays (**Figure 2.4B**).
A reciprocal approach was used to confirm these results, by introducing mutations into mTOR at the predicted site of its interaction with mLST8 amino acids 272/274 (**Figure 2.3A**), and thus was expected to mimic the effects of mLST8^{Mut2}. Transfection of 293T cells with mTOR expression constructs confirmed that mTOR^{E2285A} produced a functional mTOR protein capable of co-precipitation with mTORC2 components, including wild-type mLST8 (**Figure 2.3C**). The mTOR^{E2285A} mutation was knocked-in to the endogenous mTOR gene in a 293T-sgMLST8 cell clone, which was confirmed by sequencing of genomic DNA (**Figure 2.4C**). Expression of

mTOR^{E2285A} with wild-type mLST8 was permissive for mTORC2 assembly, as assessed by co-precipitation of RICTOR with mTOR (**Figure 2.3D**). However, a combination of mTOR^{E2285A} knock-in with mLST8^{Mut1} expression completely abolished mTORC2 assembly, and blocked pAKT^{Ser473}. These data indicate that compromised mTORC2 integrity with mLST8$^{Mut1/2}$ were not due to disruption of overall conformation of mLST8 by introducing the mutations but caused by elimination of the interaction with mTOR.

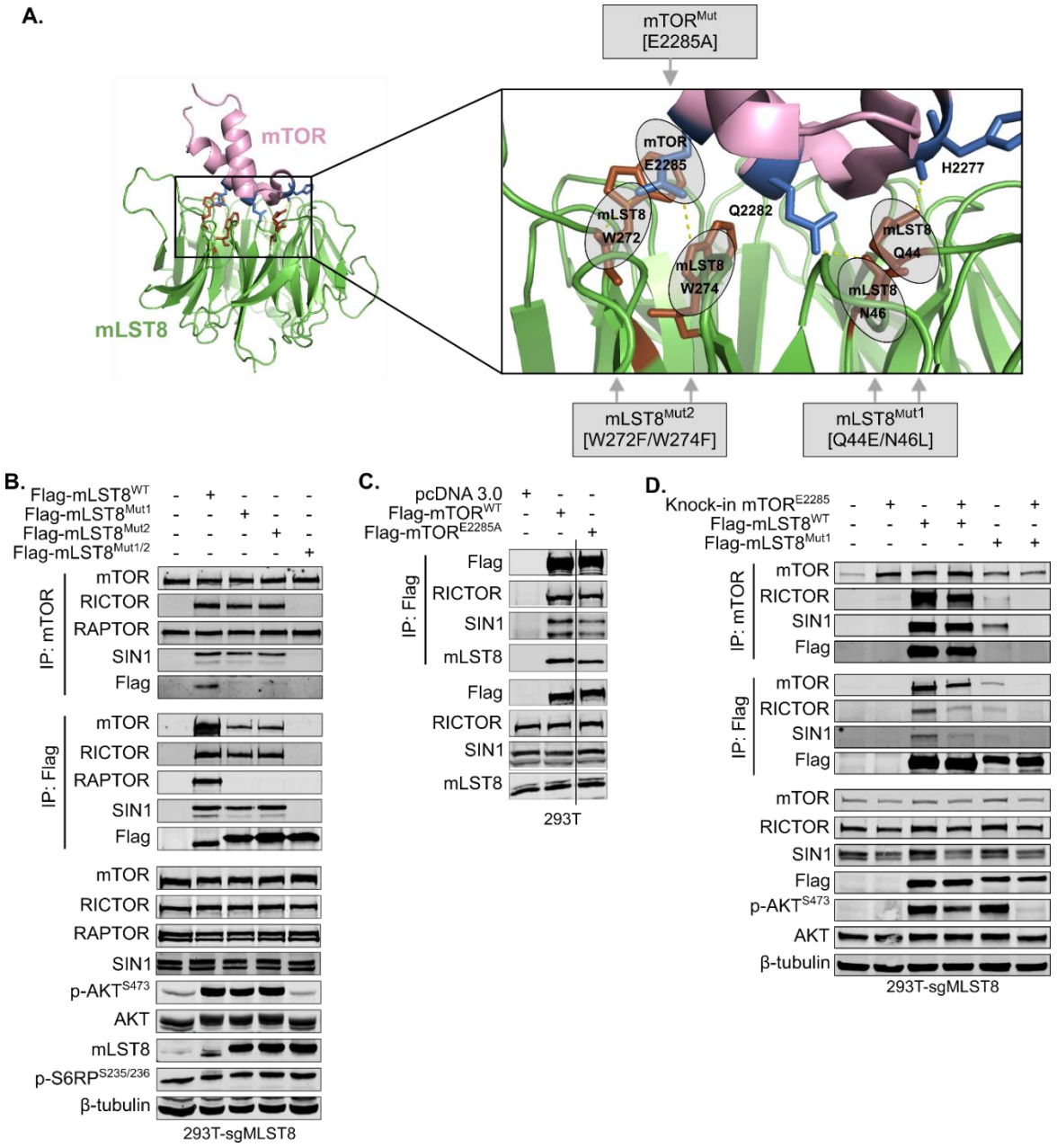

Figure 2.3. Mutations disrupting mTOR-mLST8 interface affect mTORC2 assembly and function. (A) The structure of the mTOR-mLST8 interface generated from the mTOR$^{\Delta N}$-mLST8 crystal structure (PDB ID: 4JSN; Yang et al., 2013) using PyMol software. Conserved residues proposed as hydrogen bonding sites between mTOR (blue) and mLST8 (brown) are shown. (B) mTOR IPs, Flag IPs, and cell lysates from 293T-sgMLST8 cells (sgRNA #4) expressing wild-type or mutant mLST8 were assessed by western analysis. (C) Western analysis of Flag IPs and cell lysates from 293T cells expressing mTOR^{WT} or mTOR^{E2285A}. (D) Western analysis of mTOR IPs, Flag IPs, and cell lysates from 293T-sgMLST8 cells, with or without the mTOR^{E2285A} knock in, expressing wild-type or mutant mLST8.

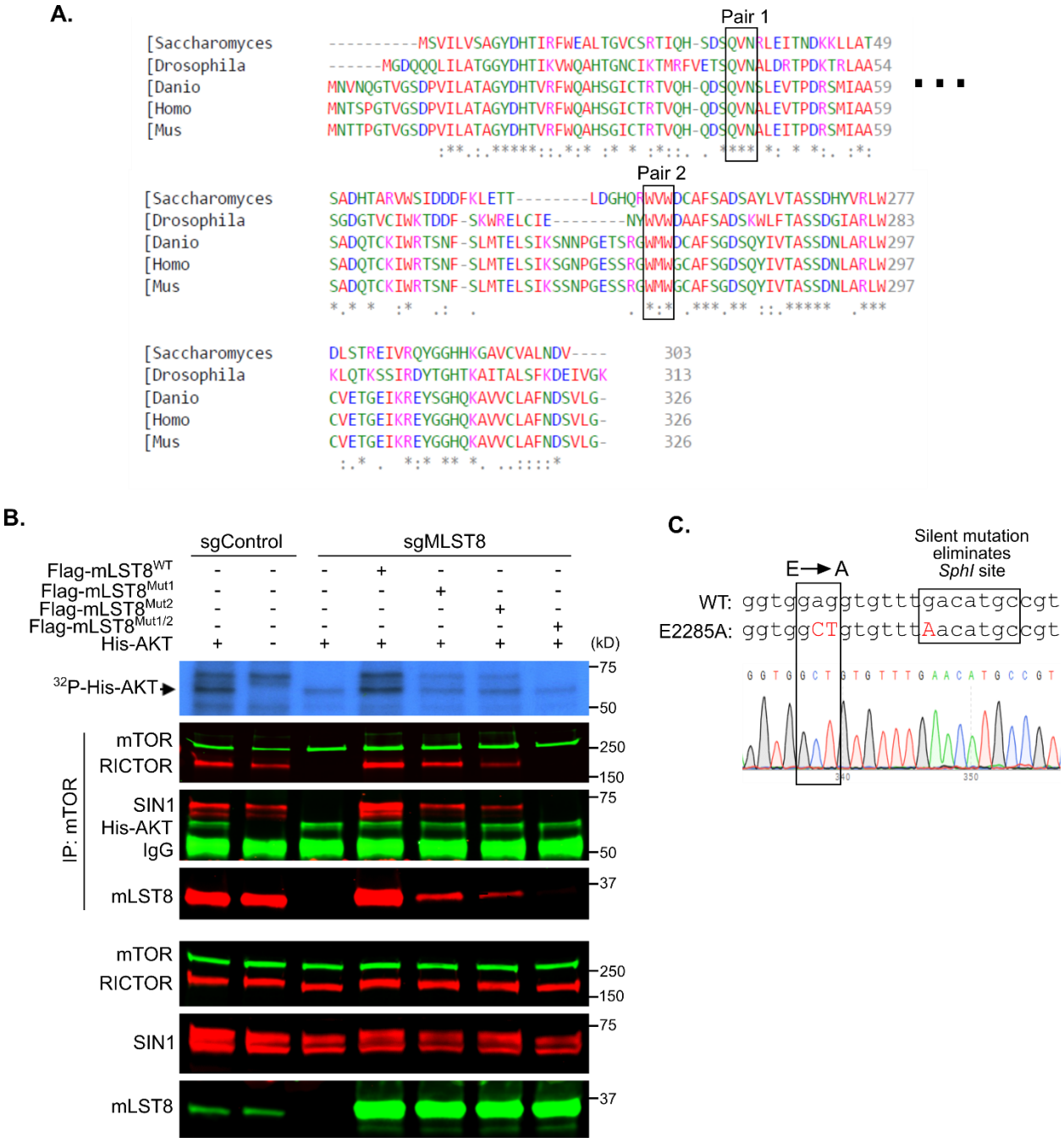

Figure 2.4. Supplemental figure related to Figure 2.3. (A) Aligned sequences of MLST8 from several species. Evolutionarily conserved residues important for hydrogen bonding were chosen for site-specific mutation, as indicated by boxes. (B) Cell lysates from 293T-sgControl or 293T-sgMLST8 (sgRNA #4) cells expressing WT or mutant Flag-mLST8 were immunoprecipitated for mTOR and incubated with purified 6His-AKT1 and 32P-γ labeled ATP. Kinase activity was detected by autoradiography and IP and whole cell lysates were assessed using the indicated antibodies. (C) An mTORE2285A mutation was knocked into 293T-sgMLST8 cells using CRISPR/Cas9, and confirmed by sequencing.

mLST8 serves as a molecular bridge between mTOR and SIN1

Recent Cryo-EM structural analyses of yeast TORC2 revealed that LST8 is sandwiched between Avo1 (the yeast SIN1 homologue) and TOR kinase(59,200). In contrast, cryo-EM studies of human mTORC1 show that mLST8 is not sandwiched or embedded within mTORC1, but rather protrudes from the structure core, leaving mLST8 highly exposed(56). This does not rule out a potential role of mLST8 in mTORC1 regulation but may explain why mLST8 is critical for assembly and function distinctly of mTORC2. We directly tested this hypothesis by mutational analysis of SIN1 and co-immunoprecipitation of mTORC2 components.

To determine if mLST8 is a molecular bridge between mTOR and SIN1 in human mTORC2, we first assessed mLST8-SIN1 interactions by co-IP. 293T cell clones deficient for SIN1 (293T-sgSIN1) were generated by CRISPR/Cas9 gene editing of the SIN1-encoding gene, *MAPKAP1* (**Figure 2.6A**). Phosphorylation of AKT^{Ser473} was completely abolished in SIN1-deficient cells (**Figure 2.6B**). Next, SIN1 expression was reconstituted in 293T-sgSIN1 cells using expression of a SIN1-green fluorescent protein (GFP) fusion construct bearing wild-type SIN1 ($SIN1^{WT}$), or a SIN1 mutant bearing deletions of the NH_2-terminal 136 amino acids ($SIN1^{\Delta 1-136}$), conserved CRIM region ($SIN1^{\Delta CRIM}$) or the PH domain ($SIN1^{\Delta PH}$) (**Figure 2.6C**). mTOR and RICTOR each co-precipitated with GFP in cells expressing $SIN1^{WT}$, $SIN1^{\Delta CRIM}$, and $SIN1^{\Delta PH}$, but not in cells expressing $SIN1^{\Delta 1-136}$ (**Figure 2.5A**), suggesting that the SIN1 NH_2-terminal domain is key for interaction with mTORC2 co-factors. Further, cells expressing $SIN1^{\Delta CRIM}$ or $SIN1^{\Delta 1-136}$ showed decreased $pAKT^{Ser473}$, consistent with decreased mTORC2 signaling. Notably, the CRIM domain of SIN1 has a known interaction site with AKT and other AGC kinases(201), explaining the reduced pAKT in these cells (**Figure 2.5A**).

Examination of the SIN1 NH_2-terminus revealed that expression of a SIN1 fragment comprised solely of aa1-136 was sufficient for co-precipitation of mTOR with SIN1 in cells

otherwise deficient for SIN1, presumably through a direct interaction between SIN1 and mLST8 (**Figure 2.5B**). Further characterization of the NH_2 terminal domain by expression of sequential deletion mutants (**Figure 2.6C**) in 293T cell clones lacking SIN1 expression identified aa97-127, as the required region for mLST8 binding (**Figure 2.5C**). Importantly, cells expressing $mLST8^{Mut1/2}$ retain a level of co-precipitation with SIN1 (**Figure 2.5D**), despite the fact that $mLST8^{Mut1/2}$ does not support complex formation between mTOR and SIN1. Interestingly, SIN1 co-precipitation of RICTOR was not affected by disruption of mTOR-mLST8 binding (**Figure 2.5D**), suggesting mLST8 brings SIN1 and RICTOR together with mTOR to build the mTORC2 complex. These data are in agreement with previous studies in yeast describing potential sites of interaction between Avo1 and LST8 within the aa98-136 region of LST8 (**Figure 2.6D**)(59). Collectively, these data support the hypothesis that mLST8 is the key molecular bridge between mTOR and the mTORC2-specific component, SIN1.

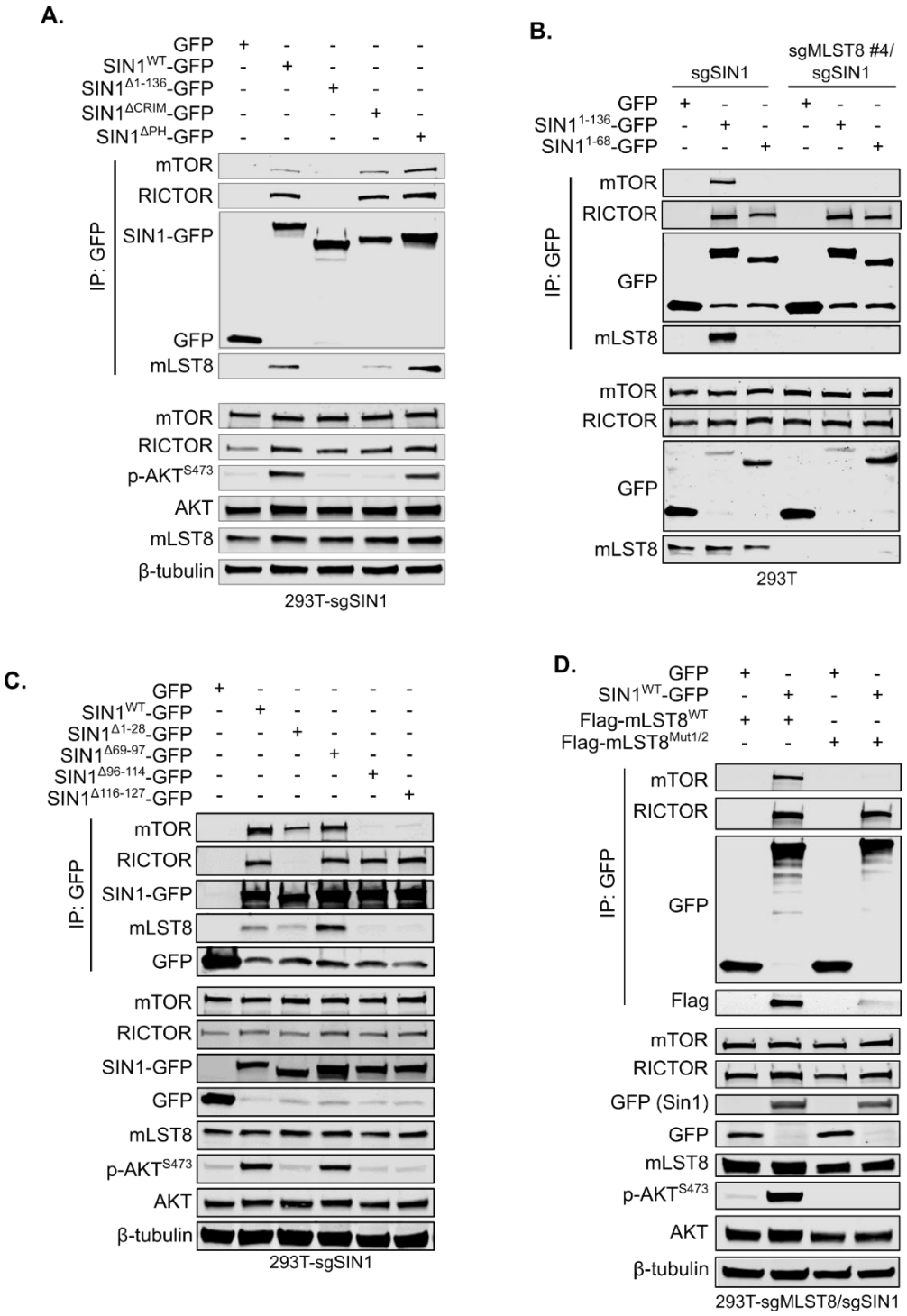

Figure 2.5. SIN1 NH_2-terminal domain binds to mLST8. (A-D) 293T-sgSIN1 cells (Sin1 KO), and 293T-sgMLST8/sgSIN1 cells (Sin1 and mLST8 duel KO), were generated by CRISPR/Cas9-mediated gene editing (sgRNA #4) and reconstituted with GFP-SIN1 (A-D) and/or Flag-tagged mLST8 (D). GFP IPs or whole cell lysates were assessed by western analysis.

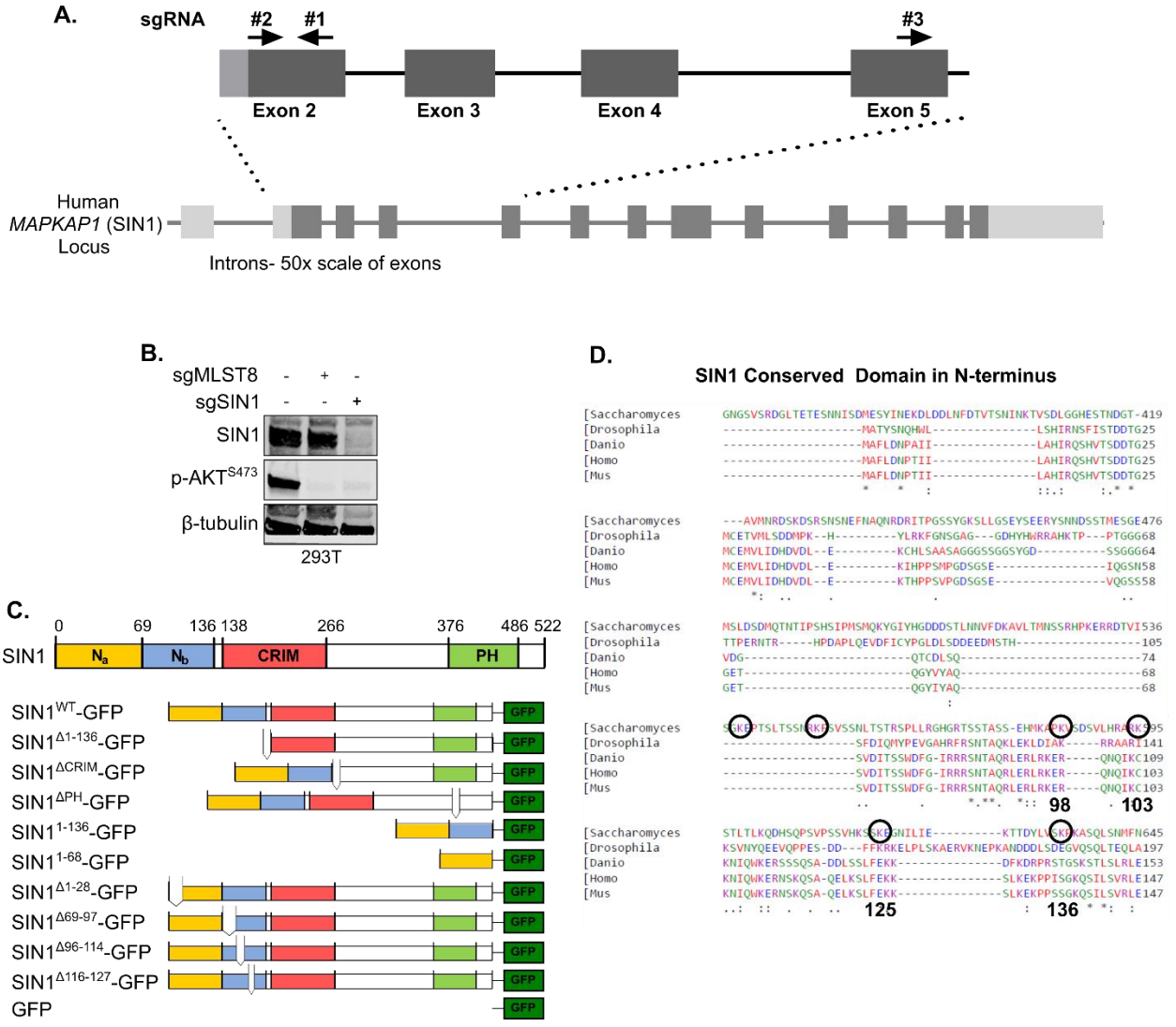

Figure 2.6. Supplemental figure related to Figure 2.5. (A) Schematic representation of the human MAPKAP1 locus (encoding SIN1) with guide RNA locations. (B) Western blot analysis by indicated antibodies of 293T cells expressing Cas9 with either sgMLST8 or sgSIN1. (C) Diagram of the functional domains of SIN1. Deletion mutants of GFP-SIN1 fusion proteins were generated and used for analysis in 293T cells. (D) Sequence alignment for the SIN1 conserved domain in the N-terminus. Circles indicate crosslinked lysine residues identified by Gaubitz et al., 2015. Numbers indicate amino acid coordinates corresponding to human SIN1.

mLST8 point mutations that block mLST8-mTOR interactions impair mTORC2 signaling and tumor growth *in vivo*.

Given that mLST8 is required for mTORC2 signaling yet remains dispensable for mTORC1 signaling, it is possible that therapeutic approaches aimed at targeted disruption of mLST8-mTOR interactions might be used for selective targeting of mTORC2 in the setting of cancer. Notably, *PTEN*-null PC3 human prostate tumor cells require PI3K-mTORC2 signaling for cell survival(120), making these an ideal model in which to test this potential strategy for selective mTORC2 inhibition.

We generated mLST8-deficient PC3 cell clones (PC3-sgMLST8), which were confirmed by western analysis to lack mLST8 expression, mTORC2 assembly, and pAKT^{Ser473} (**Figure 2.7A**). A PC3-sgMLST8 cell clone was reconstituted with mLST8^{WT} or with mLST8$^{Mut1/2}$, the mLST8 mutant lacking specific mTOR-interaction points (**Figure 2.3**). Ectopic mLST8^{WT}, but not mLST8$^{Mut1/2}$, co-precipitated with mTOR in PC3-sgMLST8 cells, and rescued pAKT^{Ser473} (**Figure 2.7A**), confirming that this approach successfully blocked mTORC2 signaling within the setting of increased PI3K activity driven by *PTEN*-loss. Compared to parental PC3 cells, PC3-sgMLST8 cells grew at a markedly reduced rate (**Figure 2.7B**). Although expression of mLST8^{WT} restored the growth rate of PC3-sgMLST8 cells, mLST8$^{Mut1/2}$ did not. The reduction in cell growth caused by loss of mLST8 was mimicked by loss of SIN1, suggesting that mLST8 is an mTORC2-specific regulatory cofactor (**Figures 2.8A&B**). Further, PC3-sgMLST8 cells reconstituted with mLST8$^{Mut1/2}$ generated tumors that were nearly 5 times smaller in volume and with a 2.5-fold decrease in final tumor weight (**Figure 2.7C**). pAKT^{Ser473} was markedly diminished in PC3-sgMLST8 tumors expressing mLST8$^{Mut1/2}$, consistent with inhibition of mTORC2 signaling *in vivo*, although pS6K1 was similar in both (**Figure 2.7D**). Tumor cell proliferation, measured by Ki-67 staining, was significantly decreased in tumors expressing mLST8$^{Mut1/2}$, while tumor cell death, as measured by cleaved Caspase-3 staining, was modestly elevated (**Figure 2.8C**). Collectively,

these results show that disruption of the mLST8-mTOR interaction can be used for selective inhibition of mTORC2 in cancer.

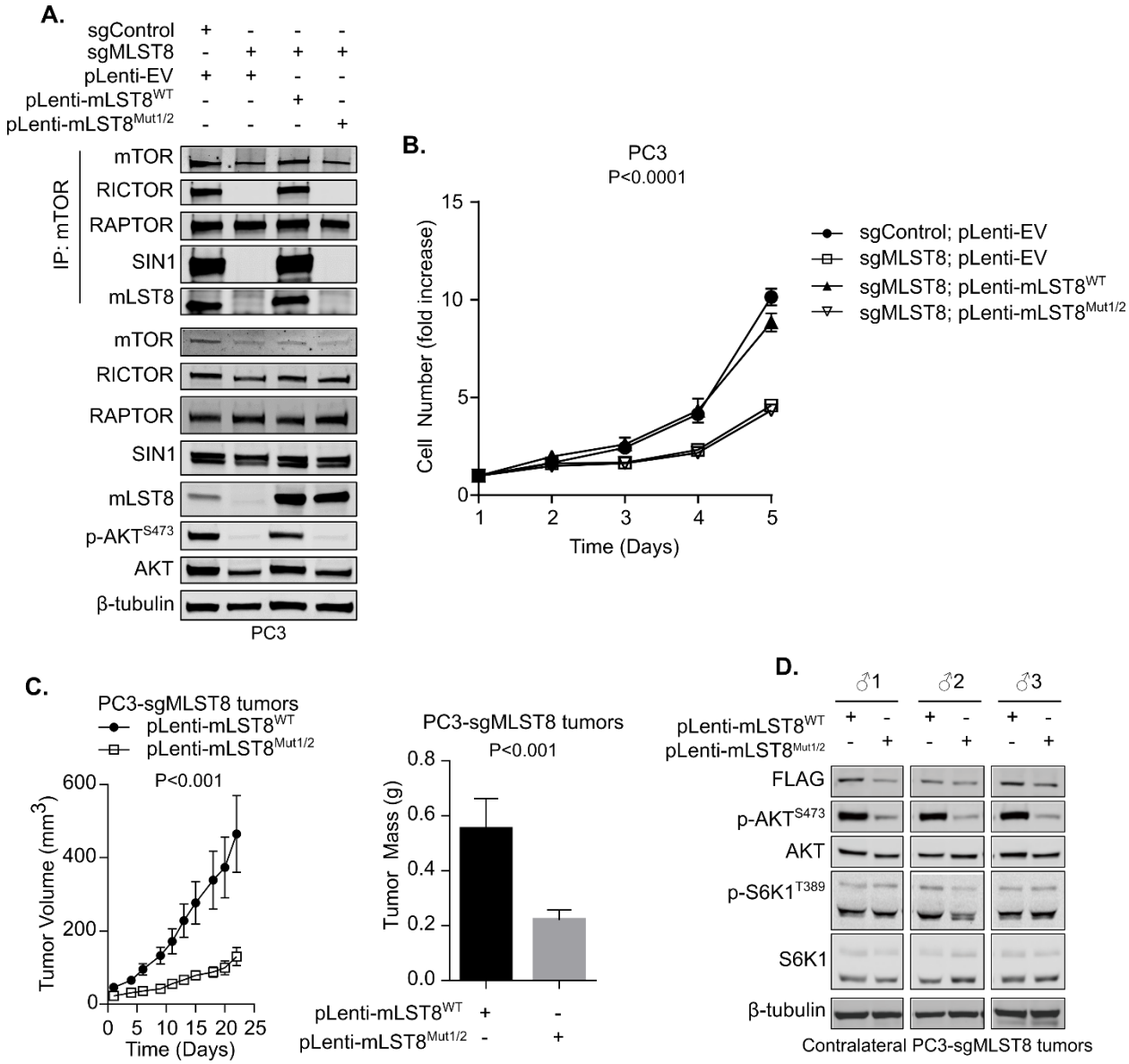

Figure 2.7. mLST8-mTOR uncoupling mutations inhibit *PTEN*-null prostate cancer growth. (A-D) PC3-sgMLST8 cells were generated by CRISPR/Cas9-mediated gene editing using sgRNA #1 and reconstituted with mLST8^{WT} or mLST8$^{Mut1/2}$. (A) mTOR IPs or whole cell lysates were assessed by western analysis. (B) Cell viability was measured by MTT assay (N=3 biological replicates). (C-D) PC3-sgMLST8 xenografts expressing mLST8^{WT} or mLST8$^{Mut1/2}$ were generated in contralateral flanks of male athymic mice. (C) Tumor volume and mass was measured. Data are presented as average ± SEM (n=10/group). (D) Tumor lysates from matched pairs of contralateral tumors were assessed by western analysis.

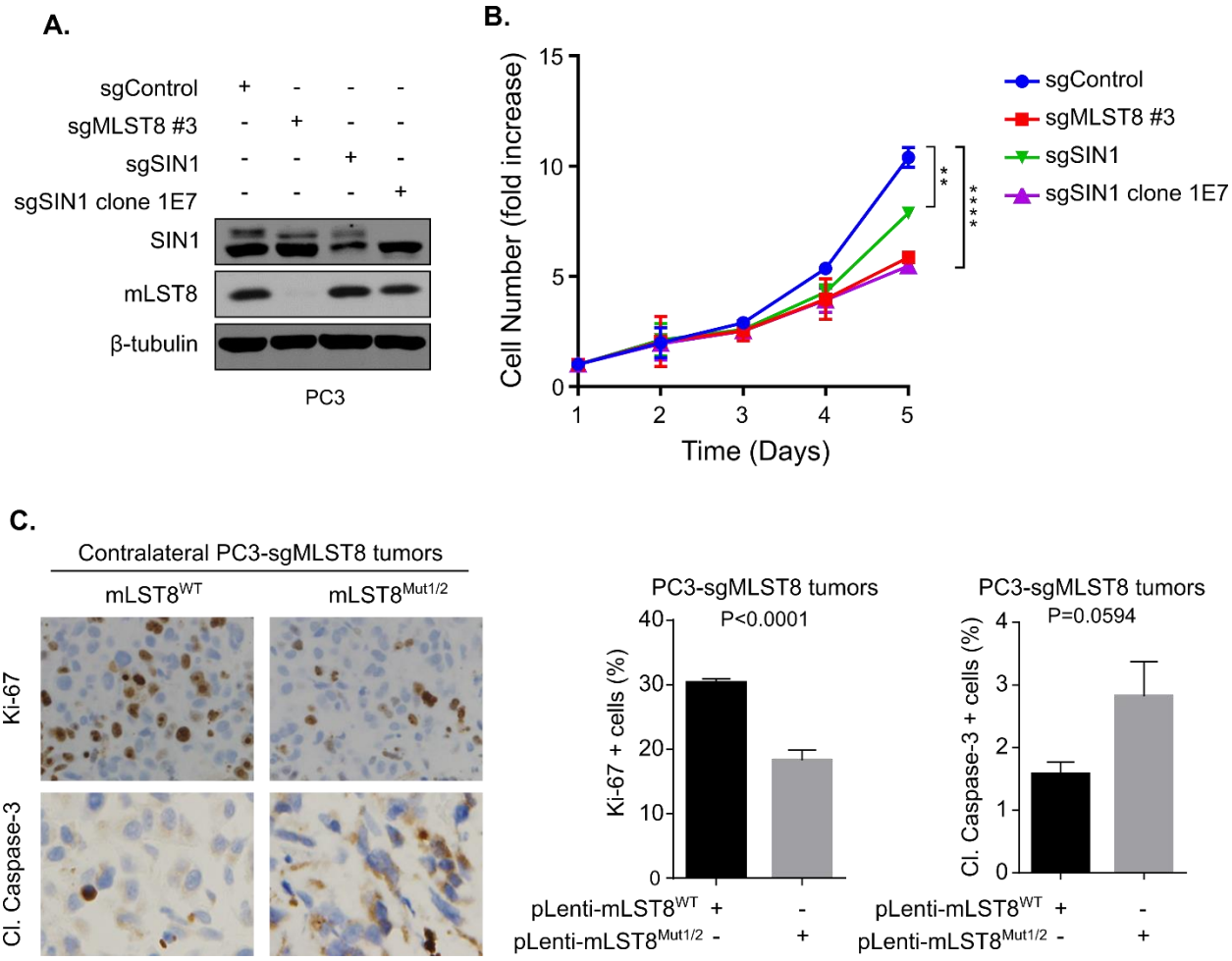

Figure 2.8. Supplemental figure related to Figure 2.7. (A-B) CRISPR/Cas9-mediated gene editing was used to target Sin1 or mLST8 in PC3 cells. sgSIN1 clone 1E7 refers to a SIN1 knockout clone generated using SIN1 sgRNA #2. (A) Whole cell lysates were assessed by western analysis using the antibodies shown to the left of each panel. (B) Cells were plated in equal numbers on Day 0, and cell viability was measured daily by MTT assay on days 1-5. Values shown are the average of N=2 biological replicates, each assessed in 6 technical replicates. **, P<0.01; ****, P<0.0001 (C) IHC analysis for Ki-67 and Cleaved Caspase-3. Representative images are shown. Quantitation of staining was performed blindly on N=6 tumors, using 3 random 400x fields per tumor.

Discussion

Recent structural analyses of the mTOR complexes revealed several intricacies of mTOR complex stability, substrate accessibility and sensitivity to Rapamycin(56,57,59,202–204). However, the role of mLST8 in assembly of the mTORC2 complex has not yet been clearly defined. Here we provide experimental evidence that distinct interaction points within mLST8 contact mTOR, and at the same time, mLST8 binds with the SIN1-RICTOR complex to generate mTORC2. This agrees with previous reports showing that mLST8 does not bind directly to RICTOR(203), but interacts strongly with SIN1, such that SIN1 deficiency abolished mTOR-Rictor interactions(205). We found that mLST8 loss, or even disruption of the mLST8 sequences required for mTOR binding, completely impaired mTORC2 assembly and function in multiple untransformed and cancer cell lines. We propose that mLST8 is the scaffold upon which the molecular components of mTORC2 assemble. As SIN1 is a key regulator of mTORC2 activity(58,117,118), the stabilizing effect of mLST8 on mTOR and SIN1 becomes critical for mTORC2 function.

Identification of the selective role of mLST8 in mTORC2 has broad implications. mTORC2 has recently been identified as a new effector for oncogenic mutant Ras(206). *RICTOR* is also amplified in several types of human cancer(130,207). Because several oncogenic mechanisms converge to activate PI3K, including growth factor overexpression, RTK activation or amplification, *PIK3CA* mutation, or *PTEN*-loss, mTORC2 is frequently activated across many cancers(58). A growing body of evidence suggests that PI3K-dependent tumors cannot develop in the absence of mTORC2 signaling(120,121,130). We have shown herein that targeting mLST8 recapitulates mTORC2-selective inhibition seen in previous studies targeting RICTOR and have identified the discrete interaction points between mTOR and mLST8 that completely abolish mTORC2 signaling when disrupted. Thus, it is possible that drug design strategies aimed at disrupting mTOR-mLST8 interactions would be an effective

approach at selective mTORC2 targeting in cancer. Further, currently available mTORC1 inhibitors relieve the potent negative feedback upon the PI3K signaling pathway, thus reviving PI3K signaling and activity of its many downstream effectors that promote tumor cell survival. There is no currently approved mTORC2-selective inhibitor, despite the significant interest in their development. The discoveries herein unveil a new approach for mTORC2-specific inhibitor design, which may hold an impact for patients with mutant Ras and/or PI3K-active cancers.

Chapter III

Rictor promotes NSCLC cell proliferation through formation and activation of mTORC2 at the expense of mTORC1

Abstract

Non-small cell lung cancer (NSCLC) is a disease typically characterized by genomic alterations, yet a targetable mutation has not been discovered in nearly half of all patients. Recent studies have identified amplification of *RICTOR*, an mTORC2-specific cofactor, as a novel actionable target in NSCLC. mTORC2 is one of two distinct complexes that the mTOR serine/threonine kinase acts in to sense environmental cues and regulate a variety of cellular processes including cell growth, proliferation, and metabolism, all of which promote tumorigenesis when aberrantly regulated. Interestingly, other components of mTORC2 are not co-amplified with *RICTOR* in human lung cancer, raising the question as to whether *RICTOR* amplification-induced changes are dependent on mTORC2 function. To model *RICTOR* amplification, we overexpressed Rictor using the Cas9 Synergistic Activator system. Overexpression of Rictor increased mTORC2 integrity and signaling, but at the expense of mTORC1, suggesting that overexpressed Rictor recruits common components away from mTORC1. Additionally, Rictor overexpression increases proliferation and growth of NSCLC 3D cultures and tumors *in vivo*. Conversely, knockout of *RICTOR* by CRISPR-Cas9-mediated genome editing leads to decreased mTORC2 formation and activity, but increased mTORC1 function. Because Rictor has mTOR-dependent and independent functions, we also knocked out mLST8, a shared mTOR co-factor but is specifically required for mTORC2 function. Inducible loss of mLST8 in *RICTOR*-amplified NSCLC cells inhibited mTORC2 integrity and

signaling, tumor cell proliferation, and tumor growth. Collectively, these data identify a mechanism for Rictor-driven tumor progression and provide further rationale for development of an mTORC2-specific inhibitor.

Introduction

Lung cancer is the leading cause of cancer-related deaths worldwide, despite significant advances in therapeutic options for these patients. Lung cancer is divided into two subtypes, non-small cell lung cancer (NSCLC) and small cell lung cancer (SCLC) which account for approximately 85% and 15% of cases, respectively. NSCLC is a disease typically characterized by its genomic alterations, although nearly half of all patients lack a known targetable alteration (208). Recent advances in tumor sequencing technologies have identified amplification of mTORC2-specific component *RICTOR* as potential targetable alteration in several types of cancer including non-small cell lung cancer (NSCLC), small cell lung cancer (SCLC), breast cancer, and gastric cancer (130,207,209,210).

The mechanistic target of Rapamycin (mTOR) is a serine/threonine kinase that acts in two distinct complexes, rapamycin-sensitive mTORC1 and rapamycin-insensitive mTORC2. Both complexes share the mTOR kinase and scaffolding protein mLST8, while mTORC1 contains scaffolding protein Raptor and mTORC2 contains Raptor-analogous scaffolding protein Rictor and regulatory component Sin1 (194,195). Growth factors, amino acids, and cellular energy activate mTORC1 which has well-characterized functions including regulation of cell growth, protein translation, metabolism, and autophagy (194,195). Although less well-understood, mTORC2 is activated by growth factors and the PI3K pathway, primarily through binding of PIP3 in the plasma membrane via the PH domain of co-factor Sin1 (58). Once localized to the membrane, mTORC2 can phosphorylate (S473) and activate its downstream effector AKT (115), also situated at the membrane. In addition to AKT, mTORC2 targets include

PKCα and SGK (54,211). mTORC2 and its downstream effectors act together to regulate cell proliferation, metabolism, and cytoskeletal organization (194,195).

Aberrant signaling of both mTOR complexes has been implicated in many types of cancer, although most studies have focused on mTORC1. mTORC2's role in cancer has also been reported- for example, mTORC2 is required for tumor formation in PTEN-null prostate cancer (120,212) and drives tumor progression and resistance in HER2-positive breast cancer (130,213). Additionally, the recent identification of *RICTOR* amplification as a potential actionable target in several cancer types suggests an additional subtype of cancer may rely on mTORC2 signaling for tumorigenesis (130,207,209,210). However, the mechanism by which amplification of a single scaffolding component within mTORC2 drives its oncogenic function remains unknown.

In this report, we investigate the roles of Rictor amplification as a driver of mTORC2 formation and promoter of NSCLC tumor growth. Using the Cas9 synergistic activation mediator (SAM) system (214) to increase expression of Rictor or the CRISPR-Cas9 system to knock out Rictor, we show that alterations in Rictor lead to corresponding changes in not only mTORC2 formation, but also mTORC1. Further, overexpression of Rictor in NSCLC cells leads to increased growth of 3D cultures and *in vivo* tumor xenografts. We also found that *RICTOR*-amplified NSCLC is sensitive to loss of mLST8, an mTOR co-factor specifically required for mTORC2 function (212), both *in vitro* and *in vivo*. Collectively, these data show that Rictor promotes NSCLC through mTORC2 formation and could potentially be targeted with an mTORC2-specific inhibitor.

Results

RICTOR is amplified and overexpressed in non-small cell lung cancer

Amplification of *RICTOR* has been identified in several different types of cancer including breast, gastric, small cell lung cancer, and non-small cell lung cancer (NSCLC) (130,207,209,210). Analysis of the TCGA PanCancer Atlas identified *RICTOR* amplification in 12% of total NSCLC cases, and 15% of squamous cell carcinoma and 11% of adenocarcinoma cases, with amplification being the most frequent alteration of RICTOR (**Figure 3.1A**). RICTOR is located on the 5p chromosome, a site of frequent copy number gain in NSCLC (215). In addition to the overall 5p gain, copy number segment and GISTIC analysis reveals a focal amplification of the chromosomal locus surrounding the RICTOR gene (**Figure 3.2A&B**). Interestingly, no other components of the mTOR complexes were co-altered with *RICTOR* amplification (**Figure 3.1B**). Further analysis of adenocarcinoma cases, which accounts for the majority of NSCLC cases, showed a positive correlation between copy-number and mRNA expression of *RICTOR*, suggesting amplification does indeed lead to an increase in Rictor expression in NSCLC cases (**Figure 3.1C**).

In order to examine how amplification of a single mTOR complex component might drive tumorigenesis, we used the Cas9 Synergistic Activation Mediator Complex system (SAM) to upregulate expression of *RICTOR* (214). This system utilizes a nucleolytically inactive Cas9 (dCas9) fused to VP64, co-expressed with MS2-P65-HSF1 activation helper proteins. A small guide RNA (sgRNA) with two MS2 aptamers targeting the promoter region of the gene of interest is also expressed, such that all components of the system co-localize and activate transcription of the targeted gene. Multiple sgRNAs targeting the promoter region of *RICTOR* (**Figure 3.1D**) were tested in a panel of non-tumorigenic, immortalized lung epithelial (BEAS-2B) and NSCLC (H1975, H358, H460, H2030) cell lines, all of which have lower copy number values compared to the H23 cell line (**Figure 3.1E**), a NSCLC cell with a verified amplification of *RICTOR* (207). Western blot analysis of these cell lines at baseline demonstrated Rictor protein levels that largely correlate with copy number values (**Figure 3.1F**). In all lines, SAM Rictor cells

exhibited increased mRNA (**Figure 3.1G**) and protein (**Figure 3.1H**) levels of Rictor compared to SAM empty vector (EV) control cells. Across all cell lines analyzed, RICTOR mRNA was upregulated approximately 2 to 4-fold with the CRISPR SAM system (**Figure 3.1G**). Analysis of mRNA expression in RICTOR-amplified samples compared diploid samples of TCGA Lung Adenocarcinoma samples (**Figure 3.1C**) showed a ~2.25 fold increase in Rictor expression. This correlates well with the expression changes in Rictor when using the CRISPR SAM system in **Figure 3.1G**.

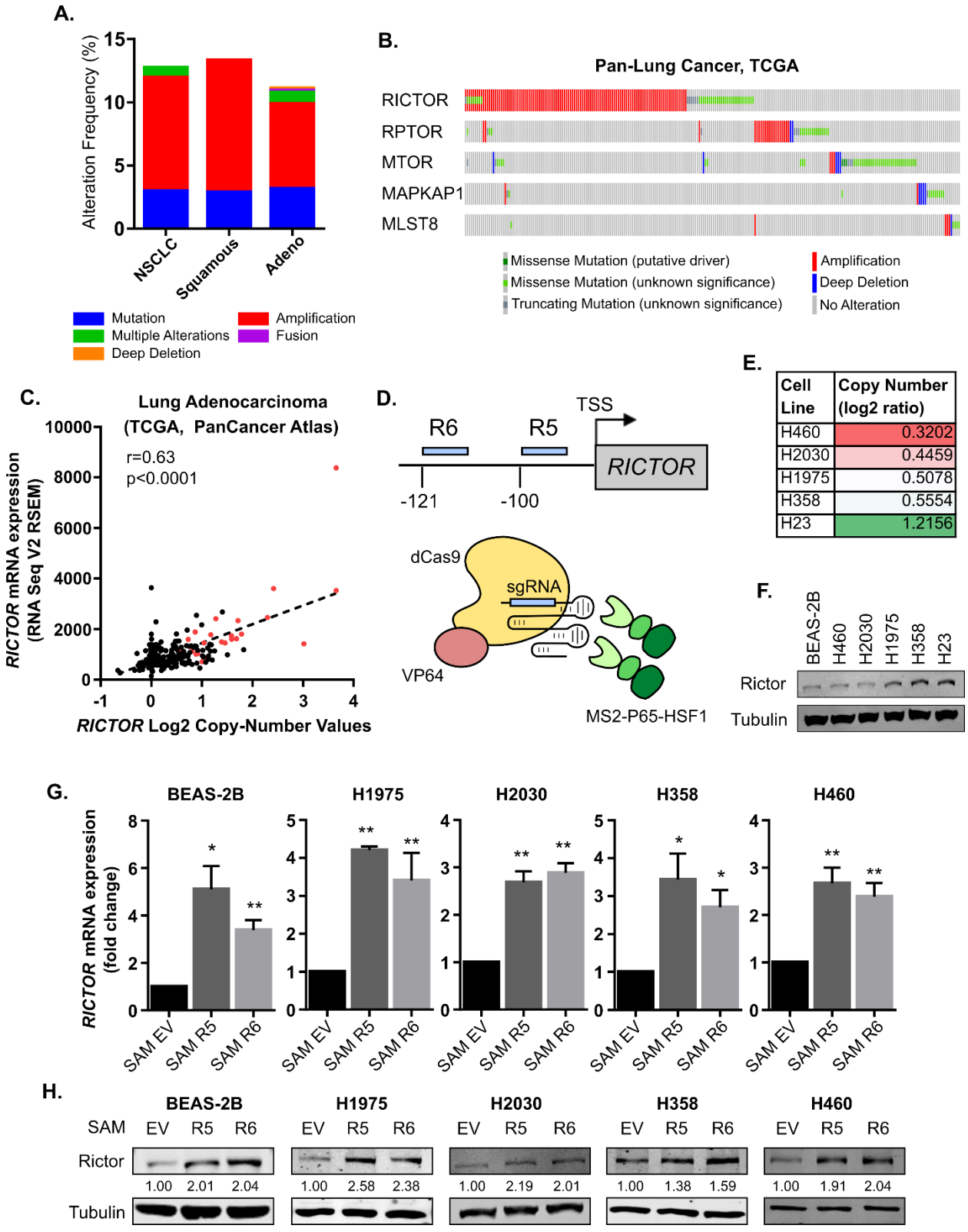

Figure 3.1. CRISPR Synergistic Activation Mediator (SAM) system can be used to model *RICTOR* amplification in NSCLC. (A-C) Patient data from the TCGA Pan-Lung Cancer Atlas

was analyzed using the online platform at cbioportal.org. (A) Alteration frequencies of *RICTOR* in non-small cell lung cancer, squamous cell carcinoma, and adenocarcinoma. (B) Alterations in mTOR complex components in patient-matched samples. (C) Correlation of *RICTOR* mRNA levels with copy number values in Lung Adenocarcinoma. Red, amplified samples based on GISTIC scoring. (D-H) CRISPR SAM (214) was used to target the promoter region of Rictor 100 bp (R5) and 121 bp (R6) upstream of the transcription start site (D) in a panel of transformed lung epithelium and NSCLC cell lines. (E) RICTOR copy number values of utilized cell lines according to CCLE database. (F) Western blot analysis of Rictor protein levels in parental cell lines. mRNA relative to Actin (G) and protein levels of Rictor (H) were measured by qRT-PCR or Western blotting, respectively.

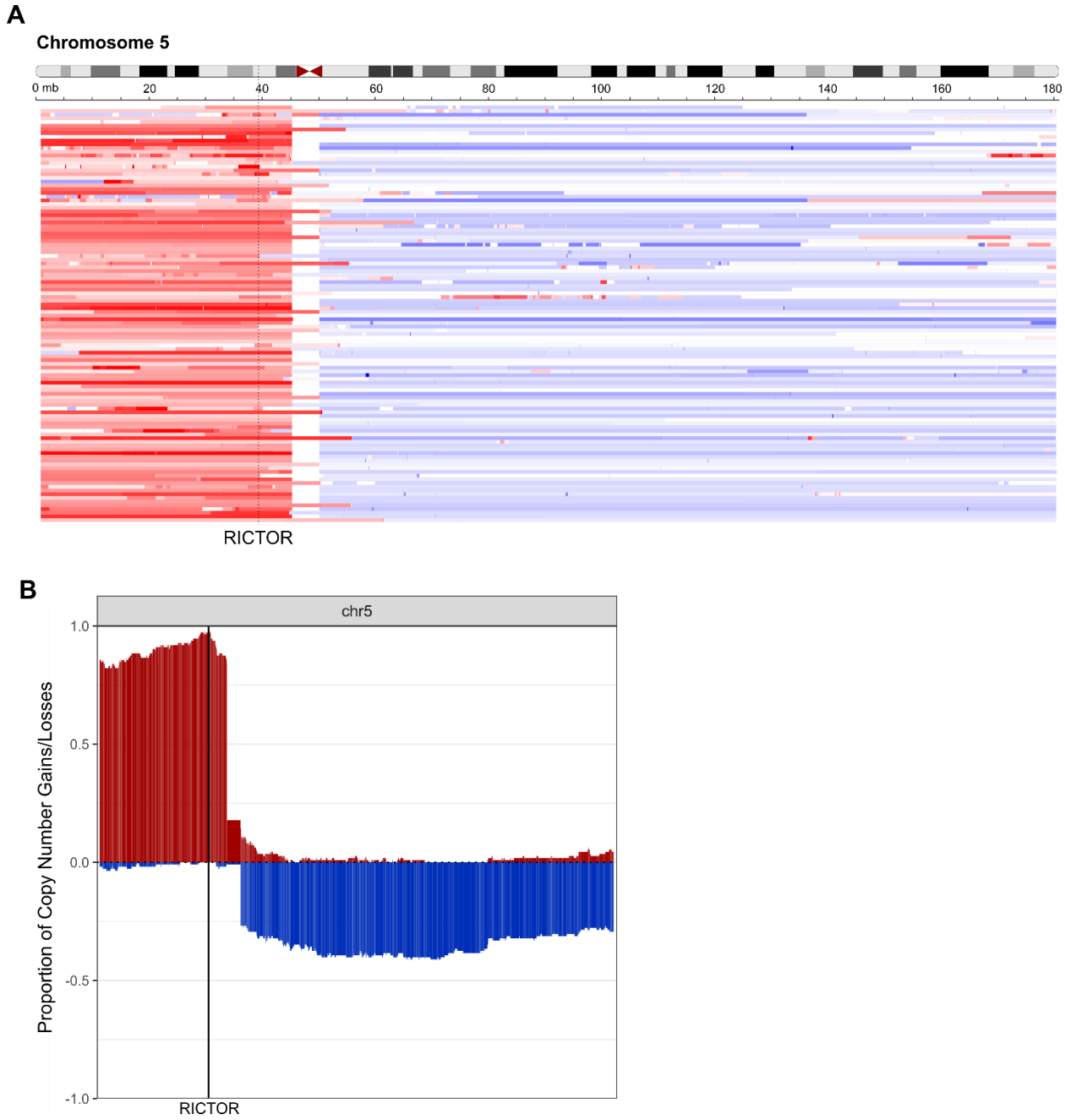

Figure 3.2. Copy number analysis of TCGA NSCLC samples with RICTOR-amplification. (A) Copy number segment levels across chromosome 5 in primary tumor samples with putative RICTOR-amplifications from the TCGA Pan-Lung Cancer database. Adapted from cbioportal.org (B) Proportion of copy number gains or losses across chromosome 5 with putative RICTOR-amplified tumor samples from the TCGA Pan-Lung Cancer database. Copy number loss cut-off = -0.3; gain cut-off = 0.3.

Alterations in Rictor expression lead to corresponding changes in mTORC2 and mTORC1

We hypothesized that amplification of *RICTOR* could promote tumorigenesis by driving formation of mTORC2. To test this hypothesis, we used the proximity ligation assay (PLA) to quantitate the interactions between mTOR and either Rictor (mTORC2) or Raptor (mTORC1). The same rabbit antibody against mTOR was used in all PLA experiments, while mouse anti-Rictor or anti-Raptor were used to differentiate between the two complexes (**Table 3.2**). Compared to SAM EV cells, SAM Rictor cells exhibited increased fluorescent foci indicating an increase in mTOR-Rictor interactions (Figure 2A), thereby suggesting an increase in the formation of mTORC2. In contrast, mTOR-Raptor interactions were decreased in Rictor-overexpressing cells, consistent with a previous report showing an increase in mTOR-Rictor precipitation when mTORC1 was inhibited (53). To complement the PLA studies, we also immunoprecipitated for mTOR and found that Rictor and Sin1 binding to mTOR was increased in SAM Rictor cells compared to control, while binding of Raptor to mTOR was reduced (**Figure 3.3B**). Furthermore, this Rictor-driven increase in mTORC2 formation increased downstream phosphorylation of AKT (S473) in Rictor overexpressing cells compared to control (**Figure 3.3C**), suggesting the increased mTORC2 was indeed functional.

In order to assess the effect of Rictor overexpression on mTORC1 activity while excluding the effects of crosstalk between the mTOR complexes, we stimulated SAM Rictor or EV cells with glutamine, a known activator of mTORC1, but not mTORC2 (216). SAM Rictor cells showed a reduction in phosphorylation of S6K1, a direct substrate of mTORC1, compared to SAM EV cells in response to glutamine stimulation (**Figure 3.3D**), confirming a reduction in mTORC1 activity caused by a loss of mTORC1 upon Rictor overexpression. These data suggest amplification of Rictor in NSCLC promotes formation and activity of mTORC2 at the expense of mTORC1.

To complement overexpression experiments, we used CRISPR-Cas9 mediated genome editing (199,217,218) to target *RICTOR* for loss-of-function in H23 cells, a cell line with verified *RICTOR* amplification (**Figure 3.1E**) (207). Rictor-deficient H23 cells showed a reduction in mTOR-Rictor interactions and an increase in mTOR-Raptor interactions compared to sgLacZ control cells when assessed by PLA (**Figure 3.3E**). Additionally, immunoprecipitation of mTOR in sgRictor cells showed a loss of Rictor and Sin1 binding to mTOR while Raptor binding was increased (**Figure 3.3F**). As expected with a loss of mTORC2, phosphorylation of AKT (S473) was reduced in H23 sgRictor compared to sgLacZ control cells in response to serum stimulation (**Figure 3.3G**). Glutamine stimulation, however, increased the levels of p-S6RP (S235/236) in Rictor deficient cells (**Figure 3.3H**), suggesting mTORC1 activity was increased. Together, these results demonstrate that changes in cellular Rictor alter the amount of mTORC2, consequently increasing or decreasing the amount of mTORC1 in the opposite direction.

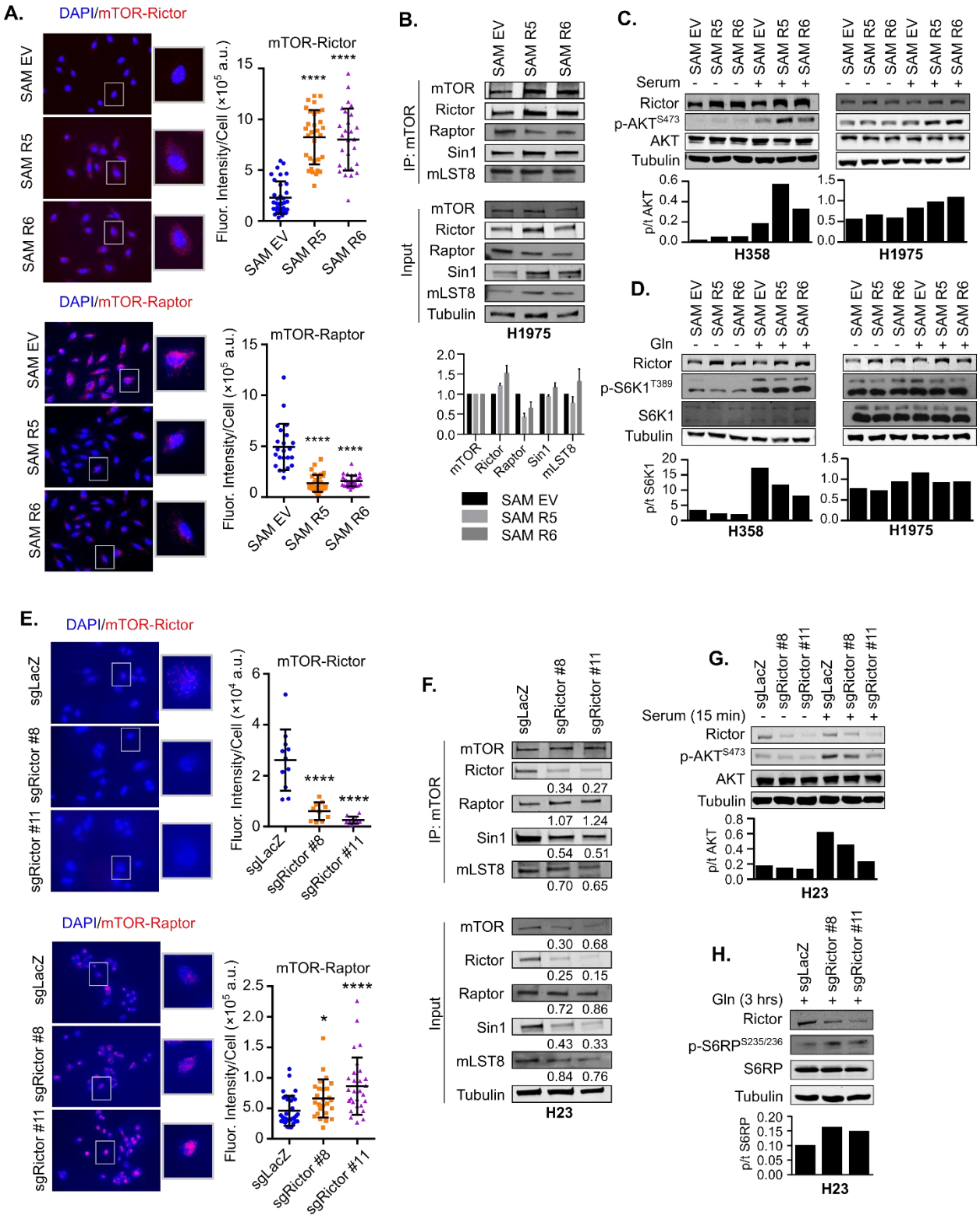

Figure 3.3. Rictor alterations promote corresponding changes in mTORC2 and mTORC1. (A) Proximity Ligation Assays (PLA) were used to assess mTOR-Rictor or mTOR-Raptor interactions in SAM Rictor or EV H1975 cells. Data presented as Mean ± S.D. (B) Interactions

among components of mTOR complexes were measured by co-immunoprecipitation followed by western blot analysis in SAM Rictor overexpressing or EV control H1975 cells with the indicated antibodies. Densitometry quantifications of the co-IP relative to mTOR pulldown, then SAM EV cells are displayed below (n=3). (C&D) SAM Rictor or SAM EV control H1975 or H358 whole cell lysates were assessed by western blot analysis using the indicated antibodies. Quantification of phospho/total AKT or S6K1 normalized to tubulin is plotted below. (C) Cells were serum starved overnight then stimulated with serum for 15 minutes. (D) Cells were starved of glutamine overnight followed by stimulation with 4mM glutamine for 3 hrs. (E) PLAs were used to assess mTOR-Rictor or mTOR-Raptor interactions in sgLacZ control or sgRictor knockout H23 cells. Data presented as Mean ± S.D. (F) Interactions among components of mTOR complexes were measured by co-immunoprecipitation followed by western blot analysis in H23 sgRictor knockout or sgLacZ control cells with the indicated antibodies. Densitometry quantifications of the co-IP are normalized to mTOR pulldown then sgLacZ are indicated below each blot. Quantification of whole cell lysate relative to tubulin levels, then normalized to sgLacZ cells are indicated below each blot. (G&H) sgLacZ control or sgRictor knockout H23 whole cell lysates were assessed by western blot analysis using the indicated antibodies. Quantification of phospho/total AKT or S6RP normalized to tubulin is plotted below. (G) Cells were serum starved overnight followed by stimulation with serum for 15 minutes. (H) Cells were starved of glutamine overnight followed by stimulated with 4mM glutamine for 3 hrs. * = $p<0.05$; **** = $p<0.0001$

Rictor promotes proliferation of NSCLC cells

mTORC2 is a known regulator of cell proliferation and promoter of tumorigenesis (194,195). To determine if Rictor-driven mTORC2 provides a growth advantage to NSCLC cells, control or Rictor overexpressing H1975 or H358 cells were grown as Matrigel-embedded 3D cultures for 20 days. Imaging of cultures on the final day showed the area of SAM Rictor cultures was significantly larger than SAM EV cultures (**Figure 3.4A**), suggesting that Rictor overexpression promotes growth of NSCLC.

Conversely, loss of Rictor in H23 Rictor-amplified cells significantly reduced cell viability compared to control when measured by MTT assay (**Figure 3.4B**). The loss of cell viability in Rictor-deficient cells was due to a reduction in cell proliferation, as judged by BrdU incorporation (**Figure 3.4C**). These results are consistent with the possibility that Rictor-driven mTORC2 formation promotes cell proliferation of NSCLC tumor cells.

Increased Rictor expression promotes NSCLC tumor growth *in vivo*

Next, we investigated whether the growth advantage conferred by Rictor overexpression would result in faster growing tumors *in vivo*. SAM Rictor #5 or EV control H1975 cells were injected into the hind flanks of Rag1-null immunodeficient mice and tumor growth was monitored for approximately 1 month. Rictor overexpression significantly increased tumor volume compared to control in the xenograft model (**Figure 3.4D**). Tumors were harvested and weighed upon removal. The mass of SAM Rictor tumors was significantly larger than control tumors (**Figure 3.4E**). Western blot analysis of tumor lysates showed that SAM R5 tumors retained the increased expression of Rictor throughout the course of tumor development and exhibited increased levels of p-AKT, a readout of mTORC2 activity (**Figure 3.4F**). Furthermore, SAM RICTOR tumors had an increase in Ki-67 staining (**Figure 3.4G**), consistent with studies showing mTORC2 activity drives cell proliferation.

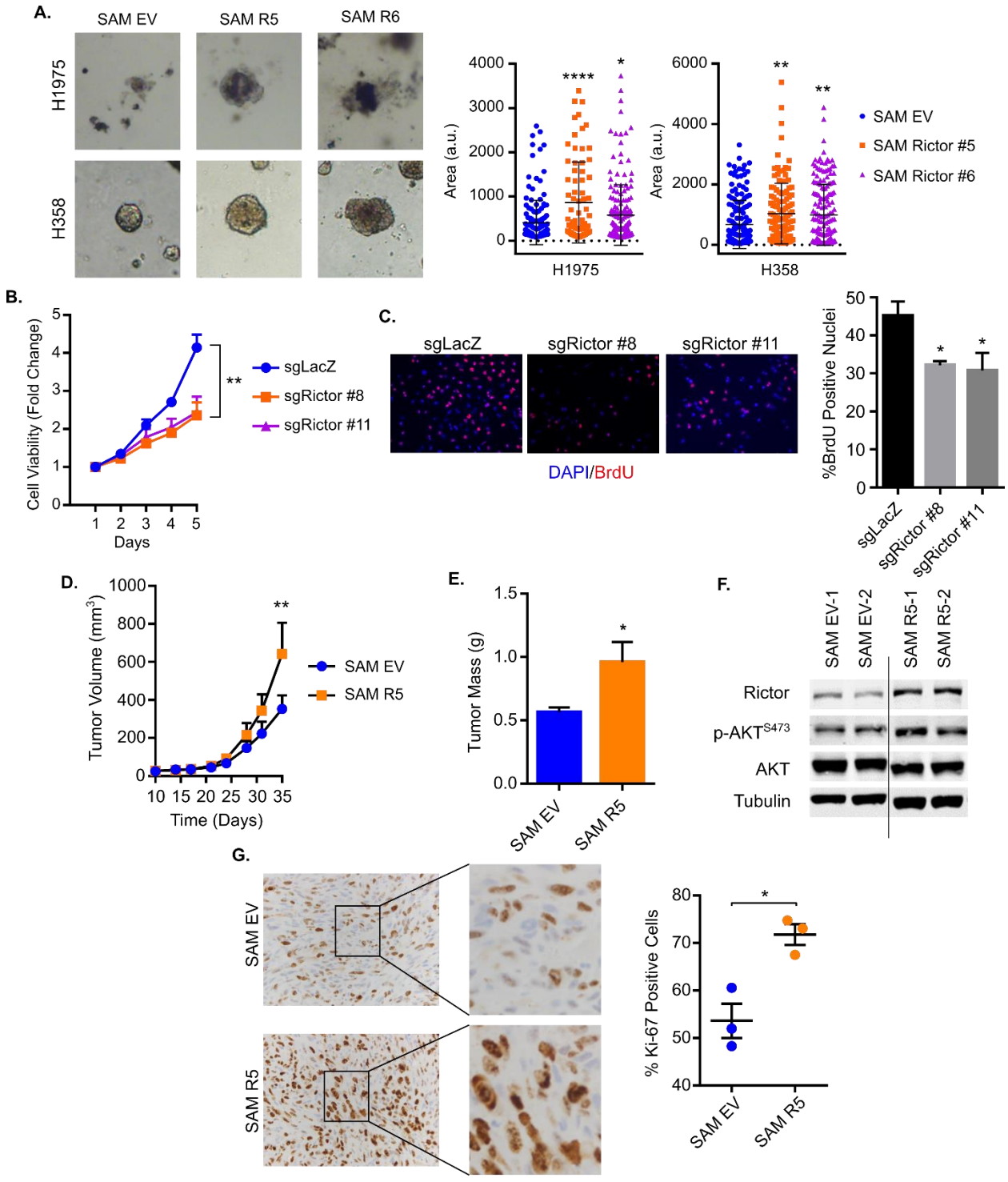

Figure 3.4. Rictor promotes NSCLC proliferation and tumor growth. (A) SAM Rictor or EV H1975 or H358 cells were grown as Matrigel-embedded 3D cultures supplemented with 5ng/mL of EGF. Representative images of cultures after 20 days are shown. Each point indicates an individual colony, with mean and SEM denoted. (B) Cell viability of sgLacZ control and sgRictor H23 knockout cells was assessed by MTT assay. (C) Proliferation of sgLacZ control and

sgRictor knockout H23 cells was measured by BrdU uptake. Representative images are shown. Data presented as mean ± S.D. (D-G) $2.5x10^6$ SAM Rictor #5 or EV control H1975 cells were generated as xenografts in hind flanks of Rag1-null immunodeficient mice. Tumor volume (D) and tumor mass (E) were measured. Data presented as mean ± SEM (n=9/group). (F) Tumor lysates from 2 individual tumors per group were analyzed by western blotting using the indicated antibodies. (G) Proliferation of tumors was assessed by immunohistochemical staining of Ki-67. Representative images are shown, and quantification is presented as mean ± SEM. *, $p<0.05$; **, $p<0.01$; ****, $p<0.0001$

Targeting mTORC2 for loss-of-function inhibits tumor growth of RICTOR-amplified NSCLC

Increased proliferation of Rictor overexpressing tumors suggested that mTORC2 inhibition might be beneficial for treatment of *RICTOR*-amplified tumors. However, an mTORC2 specific small molecule is not currently available. A previous study from our lab identified mLST8, a co-factor associated with both complexes, to be selectively required for mTORC2 integrity and function, but not mTORC1 (212), thus targeting of mLST8 could be used to specifically inhibit mTORC2. As shown in **Figure 3.5A**, CRISPR-Cas9 mediated targeting of mLST8 in H23 cells inhibited co-immunoprecipitation of mTORC2 specific components Rictor and Sin1 with the mTOR kinase, while Raptor co-immunoprecipitation increased (**Figure 3.5A**). Western blot analysis of downstream signaling also confirmed that p-AKT was decreased upon mLST8 knockout (**Figure 3.5A**). Consistent with Rictor knockout in **Figure 3.4**, mLST8 knockout also reduced cell viability and inhibited cell proliferation as measured by MTT assays and BrdU uptake assays, respectively (**Figure 3.5B&C**).

To achieve equal cell numbers between WT and mLST8 cells for implantation *in vivo*, we utilized a doxycycline inducible Cas9 system co-expressed with a sgRNA targeting mLST8 (219). *In vitro* experiments showed that a single dose of doxycycline was enough to induce Cas9-mediated LOF of mLST8, although continuous treatment was required for sustained

expression of Cas9 (**Figure 3.5D**). Inducible knockout of mLST8 in H23 resulted in a reduction in colony formation after a single dose of doxycycline in sgMLST8 cells compared to sgLacZ (**Figure 3.5E**).

For xenograft studies, H23 cells expressing a doxycycline inducible Cas9 and either sgLacZ control or sgMLST8 were injected into the hind flanks of athymic nude mice. Doxycycline was given for 10 days to induce Cas9 expression and mLST8 LOF and tumor growth was measured every 2-4 days for 2 months. At the end of the study, tumors were removed, weighed, and subjected to further analysis by immunohistochemistry. Tumor volume and weight of sgMLST8 tumors were significantly reduced compared to sgLacZ (**Figure 3.5F&G**). Western blot analysis of tumor lysates showed sustained reduction of mLST8 in tumors expressing sgMLST8 (**Figure 3.5H**). Additionally, immunohistochemistry staining of Ki-67 was reduced in sgMLST8 tumors compared to sgLacZ tumors (**Figure 3.5I**), recapitulating the in vitro results of loss of cell proliferation caused by inhibition of mTORC2 activity.

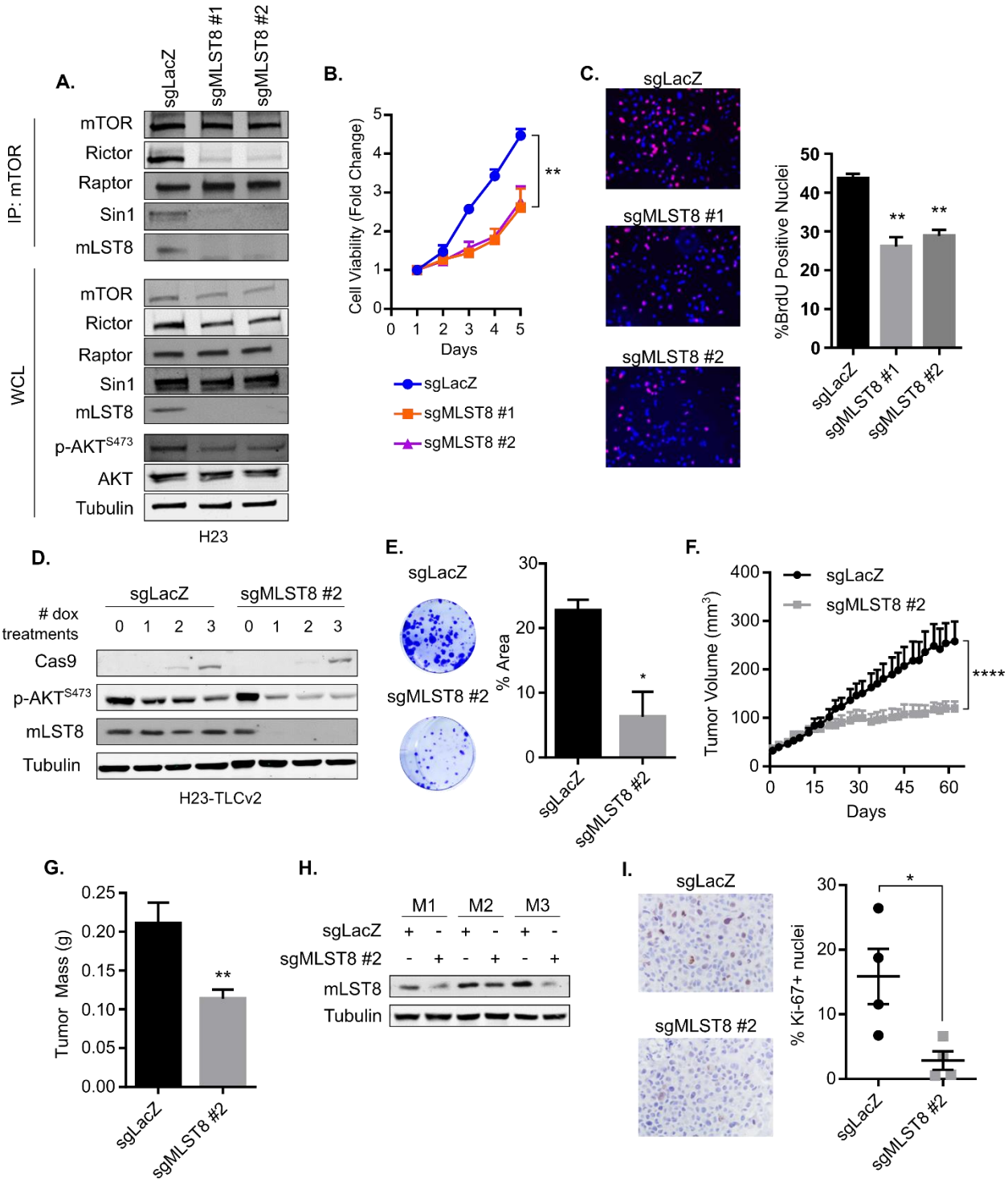

Figure 3.5. mLST8 loss-of-function inhibits growth of *RICTOR*-amplified tumors *in vivo*. (A-C) sgControl or sgMLST8 knockout H23 cells were generated. (A) Interactions among components of mTOR complexes were measured by co-immunoprecipitation followed by western blot analysis with the indicated antibodies. (B) Cell viability was measured by MTT assay. (C) Proliferation was measured by BrdU uptake assay. Representative images are

shown. Data presented as mean ± SEM. (D-I) H23 cells were generated to express a doxycycline-inducible Cas9 and either sgLacZ or sgMLST8 #2. (D) Western blot analysis of cells treated with doxycycline (1μg/mL) the indicated number of times over 10 days. (E) Colony formation assay of 2000 cells treated with doxycycline for 72 hours, then cultured for 2 weeks. Data presented as mean ± SEM. (F-I) $5x10^6$cells were implanted in the hind flanks of athymic nude mice that were fed doxycycline food for 10 days. (F) Tumor volume was monitored 3 times a week. Data presented as mean ± SEM. (G) Tumor mass was measured after tumors were removed 5 weeks after implantation. Data presented as mean ± SEM. (H) Western blot analysis of mLST8 expression 3 pairs of tumor lysates. (I) Tumor sections were analyzed by immunohistochemistry for proliferation and apoptosis by Ki-67. *, $p<0.05$ **, $p<0.01$

Discussion

Amplification of *RICTOR* has been identified as an actionable target in NSCLC, yet no other mTORC2 component is co-amplified with *RICTOR* in human lung cancer datasets (**Figure 3.1**). Because Rictor was shown to have mTOR-independent functions (220), the mechanism by which amplification of *RICTOR* could drive oncogenesis has not been clearly defined. We hypothesized that overexpression of Rictor would suppress Raptor-mTOR interactions and increase Rictor-mTOR interactions, driving activity of mTORC2, a known activator of AKT and cell proliferation. Here we show that overexpression of Rictor in NSCLC increases the amount of mTORC2 at the expense of mTORC1, thereby increasing mTORC2 downstream signaling and facilitating tumor cell proliferation.

Aberrant mTORC2 signaling has been identified as an important mediator of tumorigenesis in the context of other cancer-causing mutations such as loss of PTEN or activation of PI3K (120,221). Amplification of *RICTOR* in NSCLC also co-occurs with common oncogenic driver mutations including KRAS and EGFR (129). In this study, we performed all experiments with both KRAS (H358 and H23) and EGFR (H1975) mutant cell lines. In H358 or H1975 cells harboring these mutations, overexpression of Rictor increased 3D culture growth, yet 3D cultures of immortalized, non-tumorigenic lung epithelial cells (BEAS2B) were unchanged in response to overexpression of Rictor (data not shown). Conversely, in H23

RICTOR-amplified and KRAS mutant NSCLC, loss of mTORC2 inhibited tumor growth, suggesting that mTORC2 activity can promote tumor cell proliferation but may not be sufficient to cause cellular transformation on its own. In addition to proliferation, mTORC2 has known roles in regulation of metabolism and cytoskeletal organization. Additional studies focused on understanding the impact of *RICTOR* amplification on these other aspects of tumor biology are warranted.

Our study shows that increased mTORC2 formation occurs at the expense of mTORC1 formation, a finding that seems counter to the large body of work demonstrating the importance of mTORC1 in promoting tumor growth. It is important to note that the increased proliferative effect of Rictor overexpression was observed in 3D culture experiments, a condition that more closely mimics the nutrient gradients present in the *in vivo* tumor microenvironment. A recent study has suggested mTORC1 may inhibit tumor growth in nutrient starved conditions, offering a potential explanation to how reduced mTORC1 could still promote tumor growth (109). Thus, further investigation of nutrient availability in 3D or *in vivo* tumor settings is required to better understand how mTORC2 upregulation impacts tumor cell proliferation.

RICTOR is located on the p arm of chromosome 5 (5p13.1), a common site of copy number gain in lung cancer and other diseases (215). Recent studies, including our own analysis, show that in addition to this overall copy number gain, the loci surrounding the RICTOR gene is a site of focal amplification (Supplemental Figure 1, (129)). Amplification of *RICTOR* often co-occurs with amplification or copy number gain of several other genes along the 5p chromosome, including SKP2 and GOLPH3, both of which have been implicated in cancer progression and modulating the PI3K-mTOR-AKT signaling axis (222–224). Other co-amplified genes with known tumorigenic properties include OSMR and LIFR, also located at the 5p13.1 cytoband (225–227). While we were able to show that overexpression of Rictor alone was able to increase the proliferative capacity of lung cancer cell lines, further studies exploring

the interaction between *RICTOR* and its co-altered genes in cancer are necessary to fully understand the oncogenic effects of amplification occurring at the 5p chromosome.

The identification of Rictor overexpression as a driver of mTORC2 formation and tumor progression suggests that specific inhibition of mTORC2 would be a logical therapeutic strategy for patients with *RICTOR*-amplified cancers. However, only mTORC1-specific inhibitors (rapamycin analogs) or mTOR kinase inhibitors that block the activity of both complexes are available (228). Our data suggests that increased mTORC2 formation can reduce the levels of mTORC1, thus inhibition of both mTOR complexes may not be necessary for treatment of *RICTOR*-amplified cancers. Additionally, inhibition of mTORC1 releases a negative feedback loop on PI3K/AKT signaling (137,138), which could potentially lead to an unwanted upregulation of mTORC2 signaling. In our study, we target mLST8 to specifically inhibit mTORC2 and show that tumor growth of *RICTOR*-amplified H23 NSCLC cells is reduced, suggesting inhibition of the mTOR-mLST8 interaction (212) may be an efficacious way to specifically inhibit mTORC2 and treat *RICTOR*-amplified NSCLC.

Materials and Methods

Cell lines and cell culture

H1975, H358, H23, and H1703 cells were obtained from ATCC and maintained in RPMI-1640 media containing 10 % fetal bovine serum (FBS) and 1% Penicillin/Streptomycin. BEAS-2B and H460 cells were obtained from the Vanderbilt-Ingram Cancer Center Core Facility and maintained in the same conditions. 293T cells were obtained from ATCC and maintained in DMEM containing 10% FBS. All cells were cultured in a humidified incubator with 5% CO_2 at 37 °C. Cell lines were used between passages 1 and 50 after thaw. Cell lines from ATCC were authenticated using short tandem repeat profiling. Mycoplasma testing was performed every 6 months, most recently in January 2019, using the PlasmoTest kit (Invitrogen).

Plasmids and sgRNA sequences

CRISPR-Cas9 backbone vectors were obtained from Addgene and guide RNA sequences were cloned into the vector according to depositor's instructions. Plasmids and guide RNA primers are listed in **Table 3.1**.

Lentivirus production and transduction

CRISPR SAM, knockout, and inducible Cas9 cell lines were established using the lentiviral delivery system. Briefly, lentiviruses were packaged in HEK293T cells by transfecting cells with CRISPR or expression plasmids together with psPAX2 (lentiviral packaging) and pCMV-VSV-G (envelope) plasmids at a 1:1:1 molar ratio using the Lipofectamine 2000 Reagent. Media was changed after 16hrs of transfection and virus was collected after 24-48hrs. Indicated cells were transduced with 1:1 virus and complete growth media with polybrene (8 μg/mL) for 24hr and selected with puromycin (1-2 μg/mL), blasticidin (10 μg/mL), or hygromycin (40-50 μg/ml) for at least 48hrs to establish stable cell lines before being used for experiments.

Xenograft Assay

2.5 x 10^6 cells suspended in 100 uL of Matrigel and PBS (1:1) were injected into the hind flanks of 6-week old athymic nude ($Foxn1^{nu}$; Envigo) or $Rag1^{-/-}$ C57BL/6J mice. For xenograft experiments using an inducible Cas9, doxycycline feed (Envigo #TD.00426) was given for 10 days. Tumor measurements were started 10 days after injection and measured for 30-60 days post injection. Tumors were measured every 2-3 days with digital calipers and tumor volume calculated according to the formula ($V=4/3\pi(l/2)(h/2)(w/2)$). Data are presented as mean ± SEM. Two-way ANOVA with Bonferroni's Correction was used for statistical analysis. Experiments with mice were pre-approved by the Vanderbilt Institutional Animal Care and Use Committee and followed all state and federal rules and regulations.

Western Blot and Co-immunoprecipitation (Co-IP)

Cell lysates for western blotting only were collected in RIPA buffer. Tumor lysates were collected in Triton-X lysis buffer (1% Triton X-100, 0.5mM EDTA, 50mM Tris-Cl). All lysis buffers were supplemented with protease inhibitors and phosphatase inhibitors (Complete Mini and PhosStop inhibitor cocktail, Roche). Protein concentration was determined by Pierce BCA Protein Assay kit and equal amounts of protein extracts were mixed with 4x Laemmli sample buffer and separated by electrophoresis on an SDS-PAGE gel, and then transferred onto nitrocellulose membranes. Membranes were blocked with 5% milk in TBST buffer and incubated with corresponding primary antibodies and IRdye-conjugated or HRP-conjugated secondary antibodies. Immunoreactivity was detected using the Odyssey scanner (Li-cor Biosciences) or enhanced chemiluminescence. To perform immunoprecipitation, equal amounts of input lysates (500 ug) collected in CHAPS buffer (40 mM Tris, pH 7.5, 120 mM NaCl, 1 mM EDTA, 0.3% CHAPS), were incubated with the primary antibodies (1-2 µg) for 2 hrs to overnight at 4°C. Protein G Dynabeads (Thermo Fisher Scientific #10-003-D) were added and lysates were incubated for 1 hr and washed four times with CHAPS lysis buffer. Immunoprecipitate and whole cell lysates were then subjected to western blot analysis. All antibodies are listed in **Table 3.2**. Quantification of western blots was performed using ImageJ software.

Proximity Ligation Assay

Cells cultured on glass coverslips were fixed with 4% PFA, permeabilized with 1% Triton-X 100 in PBS, and stained with the Duolink (Sigma-Aldrich #92102) proximity ligation assay according to the manufacturer's protocol using antibodies listed in **Table 3.2** and counterstained and mounted with DAPI (Thermo Scientific #P36941). PLA puncta and DAPI-stained nuclei were enumerated using ImageJ software.

Cell Growth Assays

Cell growth was measured by MTT, colony formation, and BrdU assays. For MTT assays, 2000 cells were plated into each well of a 96-well plate in 100uL of complete growth medium. Cell viability was measured by incubating cells with 20uL of 5ug/mL Tetrazolium salt 3-(4,5-dimethylthiazol-2-yL)-2,5-diphenyltetrazolium bromide (MTT, Sigma-Aldrich) and quantified by reading absorbance at 590nm after resuspending in MTT solvent. For colony formation assay, 500 cells were plated in complete growth medium in each well of a 12-well plate. Cells were grown for 10-14 days and the media was changed every 3 days. Colonies were stained with 0.5% crystal violet in methanol and colony area was quantified. For the BrdU assay, cells were grown on glass coverslips for 24 hrs, then incubated with BrdU (10 ng/ml) for 30 min. Cells were fixed in 4% paraformaldehyde for 15 min, then permeabilized with 1% Triton X-100 in PBS for 5 min. DNA was denatured by incubation with 2N HCl for 30 min at 37 deg C, followed by rinsing in PBS. Cells were blocked for 1 hr using 2.5% goat serum in PBS, then probed with Alexa 647-conjugated anti-BrdU antibody (1:50, Invitrogen) overnight at 4 deg C. Coverslips were mounted onto slides using ProLong Gold antifade reagent with DAPI (Thermo Scientific #P36941). 40x images were quantified by counting BrdU-positive nuclei/total nuclei using ImageJ software.

3D Cultures

60uL of Matrigel (Corning #354230) was added to each well of an 8-well chamber slide (Thermo Scientific) and incubated at 37°C to solidify. 5000 cells were suspended in 400µL of complete media with 2.5% Matrigel and 5ng/mL of EGF, then added to the chamber slides. Cultures were monitored for 20 days and media was replaced every 4 days. Area of cultures was quantified using ImageJ software.

Immunohistochemistry Staining

Xenograft tumor sections were paraffin embedded and sectioned. Rehydrated paraffin sections were subjected to antigen retrieval (Retrievagen A, BD Pharmingen) and endogenous

peroxidases were blocked by 3% H_20_2 for 30min. Sections were blocked in 2.5% goat serum in PBS and stained with primary antibody and biotinylated secondary antibody, followed by avidin-peroxidase reagent and DAB. Antibodies are listed in **Table 3.2**. Sections were then counterstained with hematoxylin and mounted with Cytoseal-XYL (Thermo Scientific Richard-Allan Scientific).

TCGA Data Analysis

Alteration frequency and copy number segmentation plots and analysis were generated using the online platform cbioportal.org. Proportion of copy number gain/loss was analyzed using the GenVisR package(229).

sgRNA	**Sequence**	**Source**
SAM R5	CACCGCAGGCTCGGCCCCAGCGCTG	sam.genome-engineering.org
	AAACCAGCGCTGGGGCCGAGCCTGC	
SAM R6	CACCGGGGAGCACTGAGCCGACCCA	sam.genome-engineering.org
	AAACTGGGTCGGCTCAGTGCTCCCC	
sgLacZ	CACCGTGCGAATACGCCCACGCGAT	(217)
	AAACATCGCGTGGGCGTATTCGCAC	
sgRictor #8	CACCGGGCATAGTCGCAAACATCTG	GPP Portal
	AAACCAGATGTTTGCGACTATGCCC	
sgRictor #11	CACCGATGGTGATAACTATGTTCGT	GPP Portal
	AAACACGAACATAGTTATCACCATC	
sgMLST8 #1	CACCGCTGCAGGCTACGACCACACC	(198,199)
	AAACGGTGTGGTCGTAGCCTGCAGC	
sgMLST8 #2	CACCGCTGGATGTACACGGGCGGCG	(198,199)
	AAACCGCCGCCCGTGTACATCCAGC	
Plasmid		**Source**
lentiCRISPR v2		(199)
LentiSAM v2		(218)
LentiMPH v2		(218)
TLCV2		(219)

Table 3.1. sgRNA sequences and plasmids used in Chapter III.

Antibody	Source	Identifier	Usage
Mouse anti-Rictor (9F1.2)	Millipore Sigma	Cat #: 05-1471	WB (1:1000), PLA (1:50)
Rabbit anti-mTOR (N19-R)	Santa Cruz Biotech.	Cat #: sc-1549-R	WB (1:1000), IP, PLA (1:100)
Rabbit anti-Raptor (24C12)	Cell Signaling Technology	Cat #: 2280S	WB (1:1000)
Mouse anti-Raptor (1H6.2)	Millipore Sigma	Cat #: 05-1470	PLA (1:100)
Rabbit anti-GBL (86B8)	Cell Signaling Technology	Cat #: 3274S	WB (1:1000)
Mouse anti-Sin1 (1C7.2)	Millipore	Cat #: 05-1044	WB (1:1000)
Mouse anti-Tubulin	Sigma-Aldrich	Cat #: T4026	WB (1:1000)
Rabbit anti-phospho-AKT (S473) (D9E) XP	Cell Signaling Technology	Cat #: 4060L	WB (1:1000)
Rabbit anti-AKT (pan) (11E7)	Cell Signaling Technology	Cat #: 4685	WB (1:1000)
Rabbit anti-phospho-S6K1 (T389) (108D2)	Cell Signaling Technology	Cat #: 9234S	WB (1:1000)
Rabbit anti-S6K1	Cell Signaling Technology	Cat #: 9202S	WB (1:1000)
BrdU-Monoclonal Antibody (MoBU-1), Alexa Fluor 647	Invitrogen	Cat #: B35133	IF (1:50)
Rabbit anti-Ki67	Vector Laboratories	Cat #: VP-K451	IHC (1:100)
Anti-Rabbit IgG (H+L), HRP conjugate	Promega	Cat #: W4011	WB (1:500)
IRDye 800CW Goat anti-Mouse IgG (H+L)	Licor	Cat #: 926-32210	WB (1:10,000)
IRDye 680RD Goat anti-Rabbit IgG (H+L)	Licor	Cat #: 926-68071	WB (1:10,000)
Biotin Goat Anti-Rabbit IgG	BD Pharmingen	Cat #: 550338	IHC (1:200)

Table 3.2. List of antibodies used in Chapter III.

Chapter IV

Conclusions and Future Directions

Conclusions

Cancer continues to be the second leading cause of death worldwide despite significant advances in characterizing cancer causing mutations and development of therapies. Faster and more affordable sequencing technology combined with widespread availability of data is expected to further increase the mechanistic understanding of tumorigenesis and aid in identification of novel therapeutic targets. The mTOR signaling node has emerged as an important mediator of many disease phenotypes, including cancer, thus revealing itself as a potential target for therapeutic intervention. Both mTOR complexes integrate signals from the cellular environment to regulate a variety of downstream processes including translation, metabolism, proliferation, and autophagy- all of which can promote tumor growth when aberrantly regulated. Much of the research on mTOR signaling was focused on mTORC1, while understanding of mTORC2 lagged behind due to the lack of an mTORC2-specific inhibitor. However, several recent studies have shown that mTORC2 also plays distinct roles in cancer-related processes, demonstrating the need for better mechanistic understanding of mTORC2. In Chapter II, we identify mLST8, a co-factor present in both mTOR complexes, to be specifically required for mTORC2 integrity and function through its role as a molecular scaffold between the mTOR kinase and mTORC2 regulatory component Sin1. In Chapter III, we investigated the mechanism by which RICTOR amplification could promote tumor progression. Our data show that upregulated RICTOR expression leads to increased formation of mTORC2 at the expense of mTORC1, promoting mTORC2 downstream signaling and accelerating tumor growth. The

results described in this dissertation have contributed to our understanding of mTORC2, particularly in the context of cancer and have laid the foundation for additional investigation into the potential for mTORC2 to be targeted for cancer therapy.

Future Directions

The work described herein has contributed significantly to understanding the role of mTORC2 as a tumor promoter and as a potential target in cancer. However, this additional information has also opened many questions that remain to be answered. A few of these questions are discussed below.

How do other oncogenic alterations or co-amplified genes interact with RICTOR to promote tumorigenesis?

Although amplification of RICTOR does not co-occur with other mTOR complex alterations, analysis of TCGA mutational data in NSCLC showed that RICTOR amplification can co-occur with other well-known oncogenic mutations (**Figure 4.1**). The work described in this dissertation has demonstrated that increased expression of Rictor in NSCLC cell lines can promote proliferation and increase tumor growth in xenograft models (**Figure 3.4**). Of note, all cell lines used for the experiments described harbor additional oncogenic mutations, including the most common TP53, KRAS and EGFR mutations. When BEAS2B (transformed, “normal” lung epithelium) cells overexpressing RICTOR were grown in Matrigel, no 3D colonies were formed suggesting that RICTOR overexpression alone was not able to transform these cells (data not shown). Together, these data suggest that RICTOR can accelerate the growth and proliferation of tumors harboring other transforming mutations, rather than initiating tumor formation. Additional experiments exploring the cooperation between these oncogenic signaling pathways and the importance of RICTOR upregulation across the timeline of tumor progression are warranted.

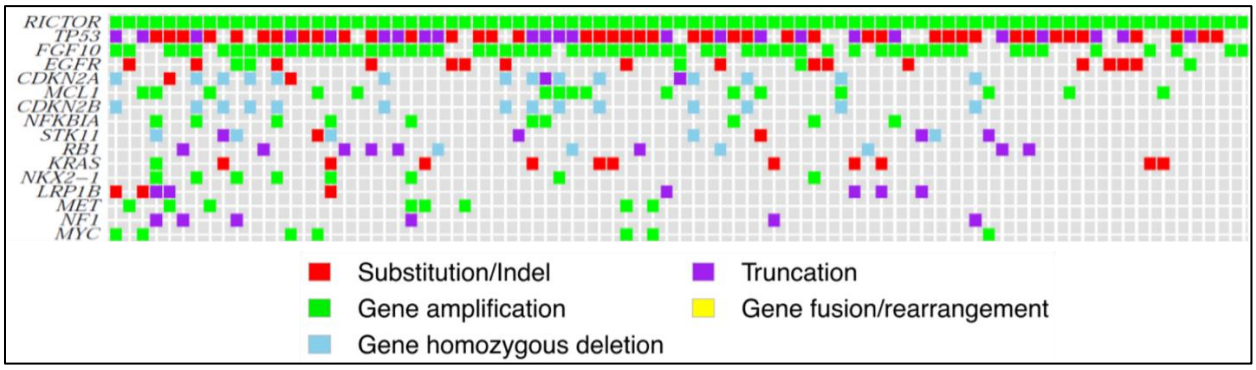

Figure 4.1. Common co-altered genes in RICTOR-amplified NSCLC. Tile plot showing the top 15 most common gene alterations in each individual with RICTOR-amplified NSCLC. Adapted from Cheng et al(129).

Additionally, as described in Chapter III, the amplification of RICTOR occurs within a focal amplification on the 5p chromosome. Interestingly, the 5p arm is a common site of copy number gain in lung cancer (215). Several other genes within region of amplification and/or copy number gain have also been implicated in promoting tumor progression, with several genes having a known connection to the PI3K/AKT/mTOR signaling pathway. For example, GOLPH3, also located on the 5p arm, has been shown to activate mTOR signaling and increase sensitivity to rapamycin in cancer cells (224). SKP2 is another gene located on this chromosome that ubiquitylates and activates AKT downstream of PI3K signaling (222,223,230,231). Since all three genes modulate different aspects of the same pathway, it will be interesting to explore how concurrent upregulation affects cancer phenotypes associated with the PI3K/AKT/mTOR pathway. Moreover, many other genes on the 5p chromosome are associated with tumor promotion and are co-amplified with RICTOR (**Table 4.1**). The SAM system used in Chapter III targeted RICTOR individually, so it is likely that the data do not fully capitulate the phenotypes

caused by an entire 5p copy number gain. This may also explain why overexpression of RICTOR alone did not transform cells, but RICTOR amplification was considered the sole actionable target in 13% of NSCLC patients (129). Further exploration of the gene networks altered by a 5p chromosomal copy number gain should reveal important details about RICTOR-amplified NSCLC.

Gene	Cytoband	Co-occurrence with *RICTOR* amplification	p-Value
FYB1	5p13.1	23 (62.16%)	2.36E-22
OSMR	5p13.1	23 (62.16%)	2.36E-22
C9	5p13.1	22 (59.46%)	3.27E-21
DAB2	5p13.1	22 (59.46%)	3.27E-21
EGFLAM	5p13.2-p13.1	22 (59.46%)	3.27E-21
EGFLAM-AS4	5p13.2	22 (59.46%)	3.27E-21
GDNF	5p13.2	22 (59.46%)	3.27E-21
LIFR	5p13.1	22 (59.46%)	3.27E-21
NUP155	5p13.2	22 (59.46%)	3.27E-21
WDR70	5p13.2	22 (59.46%)	3.27E-21
CPLANE1	5p13.2	22 (59.46%)	7.82E-19
C7	5p13.1	21 (56.76%)	8.71E-19
CARD6	5p13.1	21 (56.76%)	8.71E-19
LOC100506548	5p13.1	21 (56.76%)	8.71E-19
MROH2B	5p13.1	21 (56.76%)	8.71E-19
PRKAA1	5p13.1	21 (56.76%)	8.71E-19
PTGER4	5p13.1	21 (56.76%)	8.71E-19
RPL37	5p13.1	21 (56.76%)	8.71E-19
SNORD72	5p13.1	21 (56.76%)	8.71E-19
TTC33	5p13.1	21 (56.76%)	8.71E-19
CAPSL	5p13.2	21 (56.76%)	9.28E-18
IL7R	5p13.2	21 (56.76%)	9.28E-18
NIPBL	5p13.2	21 (56.76%)	9.28E-18
NIPBL-DT	5p13.2	21 (56.76%)	9.28E-18
SLC1A3	5p13.2	21 (56.76%)	9.28E-18
UGT3A1	5p13.2	21 (56.76%)	9.28E-18
ANXA2R	5p12	20 (54.05%)	1.02E-17
C5ORF34	5p12	20 (54.05%)	1.02E-17
C6	5p13.1	20 (54.05%)	1.02E-17
CCDC152	5p12	20 (54.05%)	1.02E-17
CCL28	5p12	20 (54.05%)	1.02E-17
HMGCS1	5p12	20 (54.05%)	1.02E-17
LOC100132356	5p12	20 (54.05%)	1.02E-17
LOC153684	5p12	20 (54.05%)	1.02E-17
LOC648987	5p12	20 (54.05%)	1.02E-17
NIM1K	5p12	20 (54.05%)	1.02E-17
SELENOP	5p12	20 (54.05%)	1.02E-17
TMEM267	5p12	20 (54.05%)	1.02E-17
ZNF131	5p12	20 (54.05%)	1.02E-17
LMBRD2	5p13.2	21 (56.76%)	6.88E-17
RANBP3L	5p13.2	21 (56.76%)	6.88E-17
UGT3A2	5p13.2	21 (56.76%)	6.88E-17
NNT	5p12	20 (54.05%)	1.04E-16
PAIP1	5p12	20 (54.05%)	1.04E-16
SPEF2	5p13.2	20 (54.05%)	1.04E-16

C5ORF51	5p13.1	19 (51.35%)	1.14E-16
FBXO4	5p13.1	19 (51.35%)	1.14E-16
GHR	5p13.1-p12	19 (51.35%)	1.14E-16
OXCT1	5p13.1	19 (51.35%)	1.14E-16
PLCXD3	5p13.1	19 (51.35%)	1.14E-16
NADK2	5p13.2	21 (56.76%)	3.98E-16
SKP2	5p13.2	21 (56.76%)	3.98E-16
MRPS30	5p12	20 (54.05%)	7.34E-16
FGF10	5p12	19 (51.35%)	1.10E-15
AGXT2	5p13.2	18 (48.65%)	1.20E-15
BRIX1	5p13.2	18 (48.65%)	1.20E-15
DNAJC21	5p13.2	18 (48.65%)	1.20E-15
PRLR	5p13.2	18 (48.65%)	1.20E-15
RAD1	5p13.2	18 (48.65%)	1.20E-15
TARS	5p13.3	18 (48.65%)	1.20E-15
ADAMTS12	5p13.3-p13.2	18 (48.65%)	1.10E-14
LINC02120	5p13.3	18 (48.65%)	1.10E-14
RAI14	5p13.2	18 (48.65%)	1.10E-14
RXFP3	5p13.2	18 (48.65%)	1.10E-14
TTC23L	5p13.2	18 (48.65%)	1.10E-14
AMACR	5p13.2	18 (48.65%)	7.03E-14
C1QTNF3	5p13.2	18 (48.65%)	7.03E-14
C1QTNF3-AMACR	5p13.2	18 (48.65%)	7.03E-14
NPR3	5p13.3	18 (48.65%)	7.03E-14
SLC45A2	5p13.2	18 (48.65%)	7.03E-14
SUB1	5p13.3	18 (48.65%)	7.03E-14
GOLPH3	5p13.3	18 (48.65%)	3.53E-13
MTMR12	5p13.3	18 (48.65%)	3.53E-13
PDZD2	5p13.3	18 (48.65%)	3.53E-13
ZFR	5p13.3	18 (48.65%)	3.53E-13
HCN1	5p12	17 (45.95%)	6.34E-13
CDH6	5p13.3	18 (48.65%)	1.48E-12
C5ORF22	5p13.3	18 (48.65%)	5.42E-12
DROSHA	5p13.3	18 (48.65%)	5.42E-12
ANKRD33B	5p15.2	18 (48.65%)	1.77E-11
DAP	5p15.2	18 (48.65%)	1.77E-11
ANKH	5p15.2	20 (54.05%)	4.44E-11
LOC100130744	5p15.2	20 (54.05%)	4.44E-11
OTULIN	5p15.2	20 (54.05%)	4.44E-11
OTULINL	5p15.2	20 (54.05%)	4.44E-11
CCT5	5p15.2	18 (48.65%)	5.24E-11
CDH10	5p14.2-p14.1	18 (48.65%)	5.24E-11
CMBL	5p15.2	18 (48.65%)	5.24E-11
MARCH6	5p15.2	18 (48.65%)	5.24E-11
ROPN1L	5p15.2	18 (48.65%)	5.24E-11
TRIO	5p15.2	19 (51.35%)	1.31E-10
ATPSCKMT	5p15.2	18 (48.65%)	1.44E-10
CDH12	5p14.3	18 (48.65%)	1.44E-10

LINC01194	5p15.2	18 (48.65%)	1.44E-10
SNORD123	5p15.31	18 (48.65%)	1.44E-10
TAS2R1	5p15.31	18 (48.65%)	1.44E-10
LINC02111	5p15.1	19 (51.35%)	3.09E-10
GUSBP1	5p14.3	18 (48.65%)	3.66E-10
PMCHL1	5p14.3	18 (48.65%)	3.66E-10
CTNND2	5p15.2	17 (45.95%)	3.74E-10
LINC02239	5p14.1	17 (45.95%)	3.74E-10
FBXL7	5p15.1	19 (51.35%)	6.95E-10
LINC02226	5p15.31	19 (51.35%)	6.95E-10
MARCH11	5p15.1	19 (51.35%)	6.95E-10
CDH18	5p14.3	18 (48.65%)	8.80E-10
DNAH5	5p15.2	18 (48.65%)	8.80E-10
LINC02112	5p15.31-p15.2	18 (48.65%)	8.80E-10
SEMA5A	5p15.31	18 (48.65%)	8.80E-10
CDH9	5p14.1	17 (45.95%)	9.81E-10
CLPTM1L	5p15.33	21 (56.76%)	1.25E-09
IRX4	5p15.33	21 (56.76%)	1.25E-09
LOC728613	5p15.33	21 (56.76%)	1.25E-09
LPCAT1	5p15.33	21 (56.76%)	1.25E-09
MRPL36	5p15.33	21 (56.76%)	1.25E-09
NDUFS6	5p15.33	21 (56.76%)	1.25E-09
SDHAP3	5p15.33	21 (56.76%)	1.25E-09
SLC6A3	5p15.33	21 (56.76%)	1.25E-09
ADAMTS16	5p15.32	19 (51.35%)	1.50E-09
BASP1	5p15.1	18 (48.65%)	2.00E-09
BASP1-AS1	5p15.1	18 (48.65%)	2.00E-09
C5ORF49	5p15.31	18 (48.65%)	2.00E-09
FASTKD3	5p15.31	18 (48.65%)	2.00E-09
MTRR	5p15.31	18 (48.65%)	2.00E-09
ZNF622	5p15.1	18 (48.65%)	2.00E-09
AHRR	5p15.33	21 (56.76%)	2.35E-09
BRD9	5p15.33	21 (56.76%)	2.35E-09
CCDC127	5p15.33	21 (56.76%)	2.35E-09
CEP72	5p15.33	21 (56.76%)	2.35E-09
EXOC3	5p15.33	21 (56.76%)	2.35E-09
EXOC3-AS1	5p15.33	21 (56.76%)	2.35E-09
LOC100506688	5p15.33	21 (56.76%)	2.35E-09
LRRC14B	5p15.33	21 (56.76%)	2.35E-09
NKD2	5p15.33	21 (56.76%)	2.35E-09
PDCD6	5p15.33	21 (56.76%)	2.35E-09
PLEKHG4B	5p15.33	21 (56.76%)	2.35E-09
PP7080	5p15.33	21 (56.76%)	2.35E-09
SDHA	5p15.33	21 (56.76%)	2.35E-09
SLC12A7	5p15.33	21 (56.76%)	2.35E-09
SLC6A18	5p15.33	21 (56.76%)	2.35E-09
SLC6A19	5p15.33	21 (56.76%)	2.35E-09
SLC9A3	5p15.33	21 (56.76%)	2.35E-09
TERT	5p15.33	21 (56.76%)	2.35E-09

TPPP	5p15.33	21 (56.76%)	2.35E-09
TRIP13	5p15.33	21 (56.76%)	2.35E-09
ZDHHC11	5p15.33	21 (56.76%)	2.35E-09
ICE1	5p15.32	18 (48.65%)	4.35E-09
MYO10	5p15.1	18 (48.65%)	4.35E-09
RETREG1	5p15.1	18 (48.65%)	4.35E-09
PRDM9	5p14.2	16 (43.24%)	6.30E-09
ADCY2	5p15.31	17 (45.95%)	1.22E-08
LOC442132	5p15.31	17 (45.95%)	1.22E-08
LINC02145	5p15.31	17 (45.95%)	2.55E-08
MED10	5p15.31	17 (45.95%)	2.55E-08
NSUN2	5p15.31	17 (45.95%)	2.55E-08
SRD5A1	5p15.31	17 (45.95%)	2.55E-08
TENT4A	5p15.31	17 (45.95%)	2.55E-08
UBE2QL1	5p15.31	17 (45.95%)	2.55E-08
C5ORF38	5p15.33	18 (48.65%)	6.56E-08
IRX2	5p15.33	18 (48.65%)	6.56E-08
IRX1	5p15.33	17 (45.95%)	1.85E-07

Table 4.1. Significantly co-amplified genes with RICTOR in TCGA Lung Adenocarcinoma samples.

How does RICTOR amplification alter tumor metabolism?

Altered cellular metabolism has long been recognized as a hallmark of cancer. Much of the current interest in tumor metabolism stemmed from the discovery that tumors cells had increased reliance on glycolysis even in the presence of oxygen. Since then, the field of tumor metabolism has expanded greatly, and we now recognize that there are many more metabolic alterations than just increased aerobic glycolysis. The mTOR signaling node is a master regulator of cellular metabolism, sensing nutrient and energy availability and regulating several downstream metabolic processes including glycolysis, lipid metabolism, and autophagy. While most of the current understanding of mTOR signaling in metabolism regulation is focused on mTORC1, several reports suggest that mTORC2 also plays an important role in regulating distinct downstream metabolic pathways. With the discovery that RICTOR amplification can promote tumor growth by increasing mTORC2 formation at the expense of mTORC1, it will be important to dissect the role of each mTOR complex in tumor metabolism, and understand how the balance and interaction between both complexes affects overall tumor growth.

AKT, the most well-studied mTORC2 downstream effector, was identified as an upstream kinase and activator of ATP Citrate Lyase (ACLY), an enzyme responsible for production of Acetyl-CoA(232,233). Acetyl-CoA can be used as precursor for several cellular events including lipogenesis, cholesterol synthesis, and histone acetylation (234). Interestingly, in brown adipocytes, the AKT-ACLY axis was identified to be specific to mTORC2 activation, suggesting that these downstream processes could all be altered in mTORC2-dependent tumors (235). mTORC2 was shown to promote hepatocellular carcinoma (HCC) through increased de novo lipid synthesis (236), but the mTORC2-AKT-ACLY axis was not directly tested as the mechanism for this increased reliance on lipids. Preliminary experiments show that loss of mLST8 can inhibit ACLY phosphorylation in lung cancer cell lines as well, suggesting mTORC2 regulation of lipid synthesis is not specific to adipose or hepatic tissue

(**Figure 4.2**). Importantly, other studies show mTORC1 is required for SREBP-dependent lipid synthesis downstream of AKT (102), suggesting coordination of both mTOR complexes is important for complete regulation of lipid synthesis. The distinct roles of each complex in lipid metabolism are particularly interesting in the context of RICTOR-amplified cancers. The data herein show that amplification of RICTOR increases the amount of mTORC2 at the expense of mTORC1. Since both mTOR complexes regulate lipid metabolism, this begs the question- do RICTOR-amplified tumors exhibit increased reliance on de novo lipogenesis and could lipid metabolism be a potential therapeutic target in RICTOR-amplified cancers? Or, could the increased mTORC2-dependent lipogenesis be counteracted by the loss of mTORC1 and SREBP-dependent transcription? Additionally, RICTOR-amplification has been identified in tumors arising from many different tissue types. Does increased mTORC2-mediated lipogenesis have implications in tissues with already high levels of fat such as breast or gastric tissue? What are the implications of altered lipid metabolism for cancers arising in tissues that are not considered to be fatty, such as the lung? Metabolomic studies across a variety of tumor types with RICTOR amplification could provide valuable information that help to dissect the roles of mTORC1 and mTORC2 on tumor metabolism.

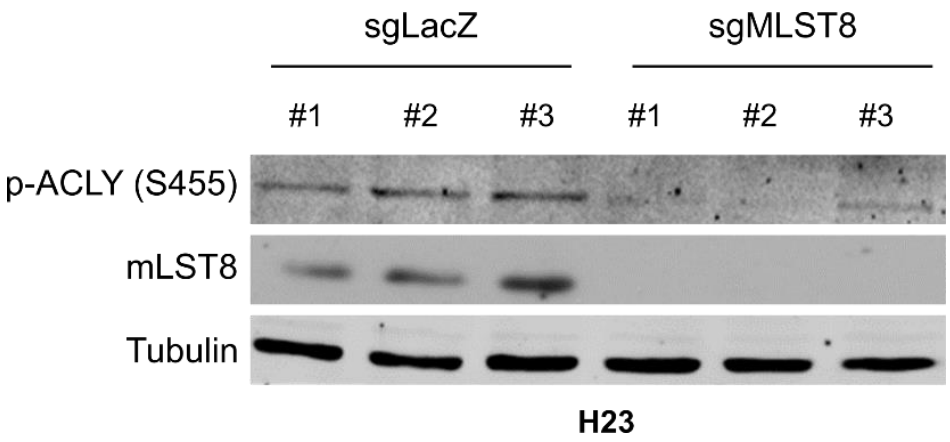

Figure 4.2. Loss of mLST8 inhibits phosphorylation of ACLY. Western blot analysis of 3 individual clones of H23 cells co-expressing Cas9 and either sgLacZ or sgmLST8, probed with the indicated antibodies.

In addition to the cell intrinsic effects of altered mTOR complex ratios caused by RICTOR amplification, nutrient gradients in the global context of a tumor may also affect the way mTOR signaling could promote tumor growth. As solid tumors grow, the center of the mass becomes starved, while the periphery of the tumor continues to have access to nutrients, thus creating a gradient in nutrient availability. Since the mTOR complexes respond to extracellular signals such as growth factors and nutrients, it is likely the cells in the center of the tumor respond very differently to their environments compared to cells located at the edge of the tumor. Macropinocytosis is used by tumor cells to scavenge larger proteins for nutrients, yet this process is inhibited by mTORC1 (109). This suggests that in additional to the proliferative effects of upregulated mTORC2 activity, the reduction of mTORC1 in RICTOR-amplified tumors might promote tumor growth through upregulation of macropinocytosis. In addition to nutrient availability gradients, oxygen gradients are also formed as the growth of tumors prevents access to the vasculature (169). Hypoxia at the center of the tumor stabilizes the HIFs, leading to increased expression of HIF target genes, many of which are related to cellular metabolism, and tumor growth. Interestingly, the two HIF isoforms are regulated independently by the two

mTOR complexes, with HIF1α regulated at the translational level by mTORC1 and HIF2α regulated transcriptionally by mTORC2 (100,237). It will be interesting to see how the activity and crosstalk between the mTOR complexes affect the tumor hypoxia response and the resulting changes in tumor metabolism. Additional experiments exploring the role of RICTOR amplification in in vivo mouse models better recapitulating the nutrient and oxygen gradients present in the tumor microenvironment should provide much needed information about how increased RICTOR expression alters tumor metabolism.

How is mTORC2 regulated and how does mTORC2 regulation impact cancer?

The mechanisms of mTORC2 regulation (summarized in Chapter I) are still relatively unknown, especially when compared to what is known about upstream regulation of mTORC1. The results described in **Figure 3.3**, suggest there may be an additional mechanism of mTORC2 regulation that has not been previously described. Although only RICTOR was targeted for LOF, Sin1 whole cell lysate levels were also reduced, indicating mTORC2 co-factors might be co-regulated. Preliminary qPCR data show that Rictor and Sin1 expression levels are not co-regulated at the level of transcription (**Figure 4.3**), suggesting the regulation could happen at the protein level. A previous study demonstrated that Sin1 could be targeted for degradation by the Cullin-RING protein ubiquitin ligase (CRL) 5 complex (238). Pilot experiments using a doxycycline inducible Cas9 and sgRNA targeting Rictor show that there is a time delay between loss of Rictor and reduction in Sin1 protein levels (**Figure 4.4**), providing additional evidence supporting the hypothesis that Sin1 protein levels are degraded upon loss of mTORC2 stability. Further investigation into how expression of RICTOR or other mTORC2 co-factors might regulate the CRL5 complex or another mechanism of Sin1 degradation could provide valuable information about mTORC2 regulation. Understanding these mechanisms may lead to important translational discoveries as well. For example, activation of the degradation mechanism of Sin1, perhaps through inhibition of deubiquitinating enzymes, may provide

therapeutic value for inhibiting mTORC2 when RICTOR is amplified. Although direct regulation of translation by Rictor expression has not been explored, this could also be a potential mechanism of mTORC2 co-factor regulation.

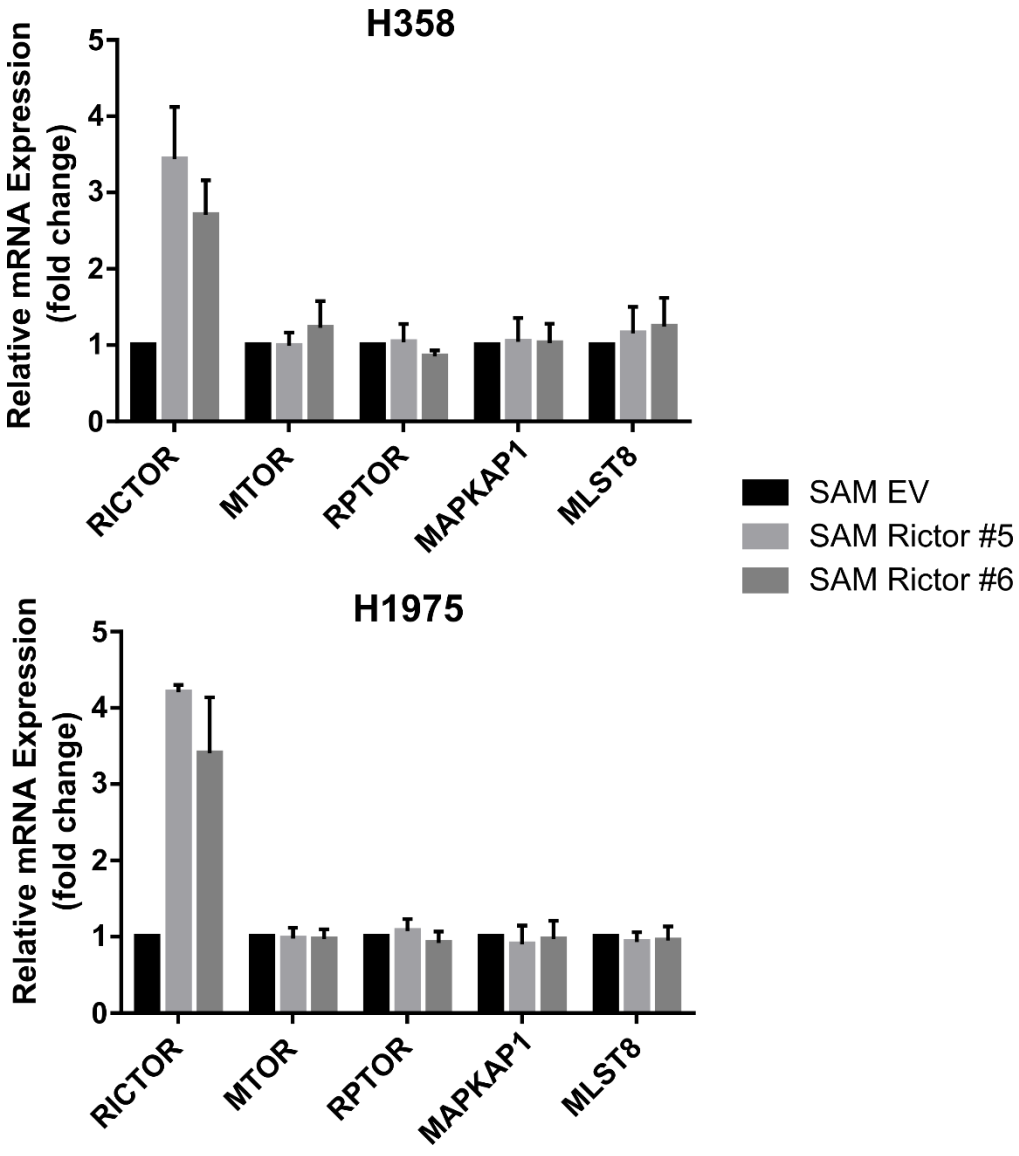

Figure 4.3. mRNA expression levels of mTOR complex components are unchanged in Rictor overexpressing NSCLC cells. qRT-PCR analysis of mTOR complex components in H358 or H1975 SAM EV or Rictor cells. mRNA levels are normalized to actin, and data are displayed as fold change relative to SAM EV cells.

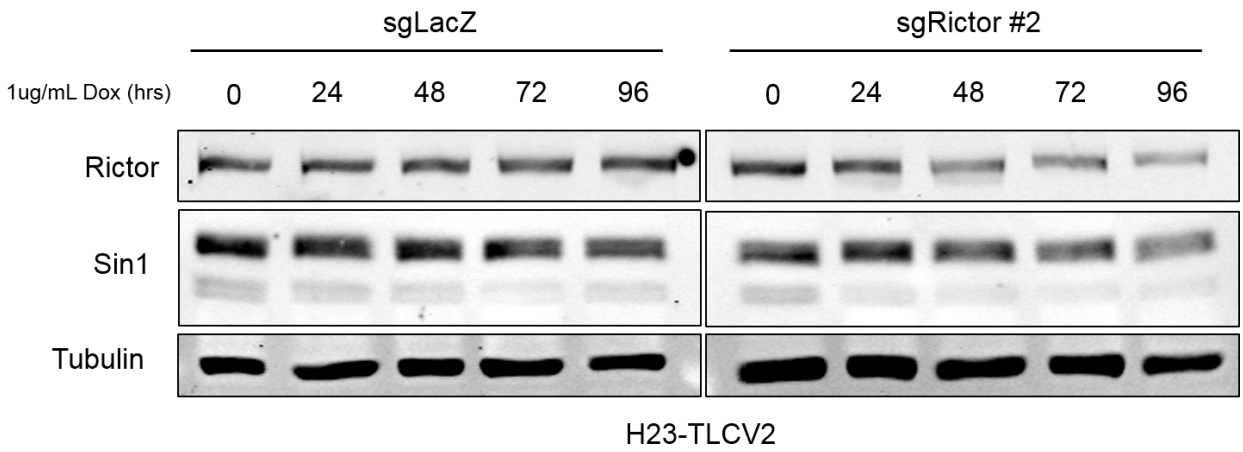

Figure 4.4. Reduction in Sin1 expression occurs 24hrs after reduction in Rictor expression. Western blot analysis of H23 cells expressing a doxycycline inducible Cas9 with either sgLacZ or sgRictor #2. Cells were treated with 1ug/mL of doxycycline for the indicated times then probed for Rictor or Sin1.

What are the feasible strategies for development of mTORC2-specific inhibitors?

Several studies, including the work described in this dissertation, provide evidence of a subset of cancer with particular dependence on mTORC2, underscoring the importance of developing an mTORC2-specific inhibitor. While some effort has been made on this front, an effective inhibitor is not currently available. In Chapter II, we identified mLST8, a shared mTOR co-factor, to be selectively required for mTORC2, not mTORC1, integrity and function, suggesting that targeting of mLST8 could be a novel strategy for mTORC2-specific inhibition. Additionally, our data show that disruption of mTOR-mLST8 or mLST8-Sin1 binding is sufficient to block activity of the entire mTORC2 (**Figures 2.3&2.5**). Thus, the interface between mTOR and mLST8 can be explored for designing small molecule inhibitors that selectively inhibit mTORC2 (see discussion below).

Several therapeutic strategies to deplete oncogenic proteins have been developed in recent years. With the advent of CRISPR-mediated gene therapy for in-human use on the

horizon, we suspect that this technology could be useful for mTORC2-specific inhibition. Our in vitro studies have shown that knockout of mLST8 halted the proliferation of both PTEN-null prostate cancer and RICTOR-amplified lung cancer cells (**Figures 2.7&3.5**). Furthermore, nanoparticle-mediated siRNA targeting of Rictor in pre-clinical breast cancer models showed promising results (213). Studies exploring the use of targeted gene therapy against mLST8 or Rictor in orthotopic tumor models in immune-competent systems could provide evidence for additional effort into developing this technology. Development of Proteolysis Targeting Chimeras (PROTACs) targeting mLST8 or other mTORC2-specific co-factors is also a potential strategy for mTORC2 inhibition for cancer therapy. PROTACS are heterobifunctional molecules that bind a protein of interest while also engaging an E3 ubiquitin ligase, activating intracellular proteolysis of the specified protein (239). Recent success of PROTACS designed against oncogenic proteins such as AKT and BET family members (240,241), suggests that further development of this strategy may become an efficacious way to inhibit mTORC2.

In addition to targeting these molecules for complete loss-of-function, disruption of the protein-protein interaction (PPI) between mLST8 and mTOR or Sin1 could be a viable strategy for mTORC2 inhibition. mLST8 is a WD40 repeat (WDR) domain-containing protein, a large class of proteins that are often involved in scaffolding of large protein complexes, consistent with the function of mLST8 determined in Chapter II. WDR domains consist of seven beta-propeller blades in the shape of a donut, often mediating protein-protein interactions at the central pore. PPIs have been notoriously difficult to target, but several small molecule inhibitors blocking the activity of WDR domain-containing proteins have recently been reported (242). Although there is significant sequence diversity between the various WDR domains, these inhibitors provide promise for continued effort in development of small molecule inhibitors against WDR domain-containing proteins including against mLST8 for mTORC2-specific inhibition.

Concluding Remarks

The results reported in this dissertation mark a significant step forward in the understanding of RICTOR and mTORC2 signaling in cancer. Still, much work is required to fully understand how alterations of this important signaling node modulates cancer phenotypes and to determine effective ways to inhibit mTORC2 for cancer therapy. As technology for studying these mechanisms continues to evolve, we anticipate the exciting new discoveries in the field of mTORC2 and cancer biology that are sure to emerge.

REFERENCES

1. Hanahan D, Weinberg RA. Hallmarks of cancer: the next generation. Cell. 2011;144:646–74.

2. Brown EJ, Albers MW, Bum Shin T, ichikawa K, Keith CT, Lane WS, et al. A mammalian protein targeted by G1-arresting rapamycin–receptor complex. Nature. 1994;369:756–8.

3. Sabatini DM, Erdjument-Bromage H, Lui M, Tempst P, Snyder SH. RAFT1: A mammalian protein that binds to FKBP12 in a rapamycin-dependent fashion and is homologous to yeast TORs. Cell. 1994;78:35–43.

4. Siegel RL, Miller KD, Jemal A. Cancer statistics, 2020. CA Cancer J Clin. Wiley; 2020;70:7–30.

5. Herbst RS, Morgensztern D, Boshoff C. The biology and management of non-small cell lung cancer. Nature. Nature Publishing Group; 2018. page 446–54.

6. Sharma S V., Bell DW, Settleman J, Haber DA. Epidermal growth factor receptor mutations in lung cancer. Nat. Rev. Cancer. 2007. page 169–81.

7. Lynch TJ, Bell DW, Sordella R, Gurubhagavatula S, Okimoto RA, Brannigan BW, et al. Activating Mutations in the Epidermal Growth Factor Receptor Underlying Responsiveness of Non-Small-Cell Lung Cancer to Gefitinib. N Engl J Med. 2004;350:2129–39.

8. Paez JG, Jänne PA, Lee JC, Tracy S, Greulich H, Gabriel S, et al. EGFR mutations in lung, cancer: Correlation with clinical response to gefitinib therapy. Science (80-). 2004;304:1497–500.

9. Kobayashi S, Boggon TJ, Dayaram T, Jänne PA, Kocher O, Meyerson M, et al. EGFR

mutation and resistance of non-small-cell lung cancer to gefitinib. N Engl J Med. 2005;352:786–92.

10. Jänne PA, Yang JC-H, Kim D-W, Planchard D, Ohe Y, Ramalingam SS, et al. AZD9291 in EGFR Inhibitor–Resistant Non–Small-Cell Lung Cancer. N Engl J Med. Massachussetts Medical Society; 2015;372:1689–99.

11. Soria JC, Ohe Y, Vansteenkiste J, Reungwetwattana T, Chewaskulyong B, Lee KH, et al. Osimertinib in untreated EGFR-Mutated advanced non-small-cell lung cancer. N Engl J Med. Massachussetts Medical Society; 2018;378:113–25.

12. Thress KS, Paweletz CP, Felip E, Cho BC, Stetson D, Dougherty B, et al. Acquired EGFR C797S mutation mediates resistance to AZD9291 in non-small cell lung cancer harboring EGFR T790M. Nat Med. Nature Publishing Group; 2015;21:560–2.

13. Niederst MJ, Hu H, Mulvey HE, Lockerman EL, Garcia AR, Piotrowska Z, et al. The Allelic Context of the C797S Mutation Acquired upon Treatment with Third-Generation EGFR Inhibitors Impacts Sensitivity to Subsequent Treatment Strategies. Clin Cancer Res. American Association for Cancer Research Inc.; 2015;21:3924–33.

14. Jia Y, Yun C-H, Park E, Ercan D, Manuia M, Juarez J, et al. Overcoming EGFR(T790M) and EGFR(C797S) resistance with mutant-selective allosteric inhibitors. Nature. Nature Publishing Group; 2016;534:129–32.

15. Uchibori K, Inase N, Araki M, Kamada M, Sato S, Okuno Y, et al. Brigatinib combined with anti-EGFR antibody overcomes osimertinib resistance in EGFR-mutated non-small-cell lung cancer. Nat Commun. Nature Publishing Group; 2017;8:14768.

16. Sequist L V., Waltman BA, Dias-Santagata D, Digumarthy S, Turke AB, Fidias P, et al. Genotypic and histological evolution of lung cancers acquiring resistance to EGFR

inhibitors. Sci Transl Med. 2011;3.

17. Camidge DR, Pao W, Sequist L V. Acquired resistance to TKIs in solid tumours: Learning from lung cancer. Nat. Rev. Clin. Oncol. Nature Publishing Group; 2014. page 473–81.

18. Amato KR, Wang S, Tan L, Hastings AK, Song W, Lovly CM, et al. EPHA2 Blockade Overcomes Acquired Resistance to EGFR Kinase Inhibitors in Lung Cancer. Cancer Res. American Association for Cancer Research; 2016;76:305–18.

19. Pao W, Wang TY, Riely GJ, Miller VA, Pan Q, Ladanyi M, et al. KRAS mutations and primary resistance of lung adenocarcinomas to gefitinib or erlotinib. PLoS Med. 2005;2:0057–61.

20. Katayama R, Lovly CM, Shaw AT. Therapeutic targeting of anaplastic lymphoma kinase in lung cancer: A paradigm for precision cancer medicine. Clin Cancer Res. American Association for Cancer Research Inc.; 2015;21:2227–35.

21. Kwak EL, Bang YJ, Camidge DR, Shaw AT, Solomon B, Maki RG, et al. Anaplastic lymphoma kinase inhibition in non-small-cell lung cancer.[Erratum appears in N Engl J Med. 2011 Feb 10;364(6):588]. N Engl J Med. 2010;363:1693–703.

22. Gainor JF, Dardaei L, Yoda S, Friboulet L, Leshchiner I, Katayama R, et al. Molecular mechanisms of resistance to first- and second-generation ALK inhibitors in ALK - rearranged lung cancer. Cancer Discov. American Association for Cancer Research Inc.; 2016;6:1118–33.

23. Shaw AT, Felip E, Bauer TM, Besse B, Navarro A, Postel-Vinay S, et al. Lorlatinib in non-small-cell lung cancer with ALK or ROS1 rearrangement: an international, multicentre, open-label, single-arm first-in-man phase 1 trial. Lancet Oncol. Lancet Publishing Group; 2017;18:1590–9.

24. Non-Small Cell Lung Carcinoma - My Cancer Genome [Internet]. [cited 2020 Apr 3]. Available from: https://www.mycancergenome.org/content/disease/non-small-cell-lung-carcinoma/

25. Sweeney SM, Cerami E, Baras A, Pugh TJ, Schultz N, Stricker T, et al. AACR project genie: Powering precision medicine through an international consortium. Cancer Discov. American Association for Cancer Research Inc.; 2017;7:818–31.

26. Cox AD, Fesik SW, Kimmelman AC, Luo J, Der CJ. Drugging the undruggable RAS: Mission possible? Nat Rev Drug Discov. Nature Publishing Group; 2014;13:828–51.

27. Karachaliou N, Mayo C, Costa C, Magrí I, Gimenez-Capitan A, Molina-Vila MA, et al. KRAS mutations in lung cancer. Clin. Lung Cancer. 2013. page 205–14.

28. Wood K, Hensing T, Malik R, Salgia R. Prognostic and predictive value in KRAS in non-small-cell lung cancer. JAMA Oncol. American Medical Association; 2016. page 805–12.

29. Cox AD, Der CJ, Philips MR. Targeting RAS membrane association: Back to the future for anti-RAS drug discovery? Clin Cancer Res. American Association for Cancer Research Inc.; 2015;21:1819–27.

30. Lito P, Solomon M, Li LS, Hansen R, Rosen N. Cancer therapeutics: Allele-specific inhibitors inactivate mutant KRAS G12C by a trapping mechanism. Science (80-). American Association for the Advancement of Science; 2016;351:604–8.

31. Patricelli MP, Janes MR, Li LS, Hansen R, Peters U, Kessler L V., et al. Selective inhibition of oncogenic KRAS output with small molecules targeting the inactive state. Cancer Discov. American Association for Cancer Research Inc.; 2016;6:316–29.

32. Janes MR, Zhang J, Li LS, Hansen R, Peters U, Guo X, et al. Targeting KRAS Mutant

Cancers with a Covalent G12C-Specific Inhibitor. Cell. Cell Press; 2018;172:578-589.e17.

33. Canon J, Rex K, Saiki AY, Mohr C, Cooke K, Bagal D, et al. The clinical KRAS(G12C) inhibitor AMG 510 drives anti-tumour immunity. Nature. Nature Publishing Group; 2019;575:217–23.

34. Xue JY, Zhao Y, Aronowitz J, Mai TT, Vides A, Qeriqi B, et al. Rapid non-uniform adaptation to conformation-specific KRAS(G12C) inhibition. Nature. Nature Research; 2020;577:421–5.

35. Ryan MB, Fece de la Cruz F, Phat S, Myers DT, Wong E, Shahzade HA, et al. Vertical Pathway Inhibition Overcomes Adaptive Feedback Resistance to KRAS G12C Inhibition . Clin Cancer Res. American Association for Cancer Research (AACR); 2019;26:1633–43.

36. Rizvi NA, Hellmann MD, Snyder A, Kvistborg P, Makarov V, Havel JJ, et al. Mutational landscape determines sensitivity to PD-1 blockade in non-small cell lung cancer. Science (80-). American Association for the Advancement of Science; 2015;348:124–8.

37. Leach DR, Krummel MF, Allison JP. Enhancement of antitumor immunity by CTLA-4 blockade. Science (80-). American Association for the Advancement of Science; 1996;271:1734–6.

38. Hodi FS, O'Day SJ, McDermott DF, Weber RW, Sosman JA, Haanen JB, et al. Improved survival with ipilimumab in patients with metastatic melanoma. N Engl J Med. Massachussetts Medical Society; 2010;363:711–23.

39. Iwai Y, Ishida M, Tanaka Y, Okazaki T, Honjo T, Minato N. Involvement of PD-L1 on tumor cells in the escape from host immune system and tumor immunotherapy by PD-L1 blockade. Proc Natl Acad Sci U S A. 2002;99:12293–7.

40. Topalian SL, Hodi FS, Brahmer JR, Gettinger SN, Smith DC, McDermott DF, et al. Safety, activity, and immune correlates of anti-PD-1 antibody in cancer. N Engl J Med. Massachussetts Medical Society; 2012;366:2443–54.

41. Garon EB, Rizvi NA, Hui R, Leighl N, Balmanoukian AS, Eder JP, et al. Pembrolizumab for the treatment of non-small-cell lung cancer. N Engl J Med. Massachussetts Medical Society; 2015;372:2018–28.

42. Reck M, Rodriguez-Abreu D, Robinson AG, Hui R, Csöszi T, Fülöp A, et al. Pembrolizumab versus Chemotherapy for PD-L1-Positive Non-Small-Cell Lung Cancer. N Engl J Med. Massachussetts Medical Society; 2016;375:1823–33.

43. Gandhi L, Rodríguez-Abreu D, Gadgeel S, Esteban E, Felip E, De Angelis F, et al. Pembrolizumab plus chemotherapy in metastatic non-small-cell lung cancer. N Engl J Med. Massachussetts Medical Society; 2018;378:2078–92.

44. Paz-Ares L, Luft A, Vicente D, Tafreshi A, Gümüş M, Mazières J, et al. Pembrolizumab plus chemotherapy for squamous non-small-cell lung cancer. N Engl J Med. Massachussetts Medical Society; 2018;379:2040–51.

45. Saab S, Zalzale H, Rahal Z, Khalifeh Y, Sinjab A, Kadara H. Insights Into Lung Cancer Immune-Based Biology, Prevention, and Treatment. Front. Immunol. NLM (Medline); 2020. page 159.

46. Zitvogel L, Galluzzi L, Smyth MJ, Kroemer G. Mechanism of Action of Conventional and Targeted Anticancer Therapies: Reinstating Immunosurveillance. Immunity. Elsevier; 2013. page 74–88.

47. Chang CH, Qiu J, O'Sullivan D, Buck MD, Noguchi T, Curtis JD, et al. Metabolic Competition in the Tumor Microenvironment Is a Driver of Cancer Progression. Cell. Cell

Press; 2015;162:1229–41.

48. Fukumura D, Kloepper J, Amoozgar Z, Duda DG, Jain RK. Enhancing cancer immunotherapy using antiangiogenics: Opportunities and challenges. Nat. Rev. Clin. Oncol. Nature Publishing Group; 2018. page 325–40.

49. Loo Yau H, Ettayebi I, De Carvalho DD. The Cancer Epigenome: Exploiting Its Vulnerabilities for Immunotherapy. Trends Cell Biol. Elsevier Ltd; 2019. page 31–43.

50. Sahin U, Derhovanessian E, Miller M, Kloke BP, Simon P, Löwer M, et al. Personalized RNA mutanome vaccines mobilize poly-specific therapeutic immunity against cancer. Nature. Nature Publishing Group; 2017;547:222–6.

51. Rodriguez PC, Popa X, Martínez O, Mendoza S, Santiesteban E, Crespo T, et al. A Phase III Clinical Trial of the Epidermal Growth Factor Vaccine CIMAvax-EGF as Switch Maintenance Therapy in Advanced Non-Small Cell Lung Cancer Patients. Clin Cancer Res. American Association for Cancer Research Inc.; 2016;22:3782–90.

52. Sharma P, Hu-Lieskovan S, Wargo JA, Ribas A. Primary, Adaptive, and Acquired Resistance to Cancer Immunotherapy. Cell. Cell Press; 2017. page 707–23.

53. Sarbassov DD, Ali SM, Kim D-H, Guertin DA, Latek RR, Erdjument-Bromage H, et al. Rictor, a novel binding partner of mTOR, defines a rapamycin-insensitive and raptor-independent pathway that regulates the cytoskeleton. Curr Biol. 2004;14:1296–302.

54. Jacinto E, Loewith R, Schmidt A, Lin S, Rüegg MA, Hall A, et al. Mammalian TOR complex 2 controls the actin cytoskeleton and is rapamycin insensitive. Nat Cell Biol. 2004;6:1122–8.

55. Laplante M, Sabatini DM. mTOR signaling in growth control and disease. Cell.

2012;149:274–93.

56. Yang H, Rudge DG, Koos JD, Vaidialingam B, Yang HJ, Pavletich NP. mTOR kinase structure, mechanism and regulation. Nature. 2013;497:217–23.

57. Aylett CHS, Sauer E, Imseng S, Boehringer D, Hall MN, Ban N, et al. Architecture of human mTOR complex 1. Science (80-). American Association for the Advancement of Science; 2015;351:48–52.

58. Liu P, Gan W, Chin YR, Ogura K, Guo J, Zhang J, et al. PtdIns(3,4,5)P3-Dependent Activation of the mTORC2 Kinase Complex. Cancer Discov. 2015;

59. Gaubitz C, Oliveira TM, Prouteau M, Leitner A, Karuppasamy M, Konstantinidou G, et al. Molecular Basis of the Rapamycin Insensitivity of Target Of Rapamycin Complex 2. Mol Cell. 2015;58:977–88.

60. Zinzalla V, Stracka D, Oppliger W, Hall MN. Activation of mTORC2 by association with the ribosome. Cell. 2011;144:757–68.

61. Thorpe LM, Yuzugullu H, Zhao JJ. PI3K in cancer: divergent roles of isoforms, modes of activation and therapeutic targeting. Nat Rev Cancer. Nature Publishing Group; 2014;15:7–24.

62. Inoki K, Li Y, Zhu T, Wu J, Guan K-L. TSC2 is phosphorylated and inhibited by Akt and suppresses mTOR signalling. Nat Cell Biol. Nature Publishing Group; 2002;4:648–57.

63. Manning BD, Tee AR, Logsdon MN, Blenis J, Cantley LC. Identification of the Tuberous Sclerosis Complex-2 Tumor Suppressor Gene Product Tuberin as a Target of the Phosphoinositide 3-Kinase/Akt Pathway. Mol Cell. 2002;10:151–62.

64. Potter CJ, Pedraza LG, Xu T. Akt regulates growth by directly phosphorylating Tsc2. Nat

Cell Biol. 2002;4:658–65.

65. Inoki K, Li Y, Xu T, Guan K-L. Rheb GTPase is a direct target of TSC2 GAP activity and regulates mTOR signaling. Genes Dev. 2003;17:1829–34.

66. Tee AR, Manning BD, Roux PP, Cantley LC, Blenis J. Tuberous Sclerosis Complex Gene Products, Tuberin and Hamartin, Control mTOR Signaling by Acting as a GTPase-Activating Protein Complex toward Rheb. Curr Biol. 2003;13:1259–68.

67. Sancak Y, Thoreen CC, Peterson TR, Lindquist RA, Kang SA, Spooner E, et al. PRAS40 Is an Insulin-Regulated Inhibitor of the mTORC1 Protein Kinase. Mol Cell. 2007;25:903–15.

68. Thedieck K, Polak P, Kim ML, Molle KD, Cohen A, Jenö P, et al. PRAS40 and PRR5-like protein are new mTOR interactors that regulate apoptosis. PLoS One. 2007;2:e1217.

69. Vander Haar E, Lee S-I, Bandhakavi S, Griffin TJ, Kim D-H. Insulin signalling to mTOR mediated by the Akt/PKB substrate PRAS40. Nat Cell Biol. 2007;9:316–23.

70. Wang L, Harris TE, Roth RA, Lawrence JC. PRAS40 regulates mTORC1 kinase activity by functioning as a direct inhibitor of substrate binding. J Biol Chem. 2007;282:20036–44.

71. Ma L, Chen Z, Erdjument-Bromage H, Tempst P, Pandolfi PP. Phosphorylation and Functional Inactivation of TSC2 by Erk: Implications for Tuberous Sclerosisand Cancer Pathogenesis. Cell. 2005;121:179–93.

72. Roux PP, Ballif BA, Anjum R, Gygi SP, Blenis J. Tumor-promoting phorbol esters and activated Ras inactivate the tuberous sclerosis tumor suppressor complex via p90 ribosomal S6 kinase. Proc Natl Acad Sci U S A. 2004;101:13489–94.

73. Carrière A, Cargnello M, Julien L-A, Gao H, Bonneil É, Thibault P, et al. Oncogenic

MAPK Signaling Stimulates mTORC1 Activity by Promoting RSK-Mediated Raptor Phosphorylation. Curr Biol. 2008;18:1269–77.

74. Inoki K, Zhu T, Guan K-L. TSC2 Mediates Cellular Energy Response to Control Cell Growth and Survival. Cell. 2003;115:577–90.

75. Blommaart EF, Luiken JJ, Blommaart PJ, van Woerkom GM, Meijer AJ. Phosphorylation of ribosomal protein S6 is inhibitory for autophagy in isolated rat hepatocytes. J Biol Chem. 1995;270:2320–6.

76. Hara K, Yonezawa K, Weng QP, Kozlowski MT, Belham C, Avruch J. Amino acid sufficiency and mTOR regulate p70 S6 kinase and eIF-4E BP1 through a common effector mechanism. J Biol Chem. 1998;273:14484–94.

77. Shimobayashi M, Hall MN. Multiple amino acid sensing inputs to mTORC1. Cell Res. Nature Publishing Group; 2016;26:7–20.

78. Wang S, Tsun Z-Y, Wolfson RL, Shen K, Wyant GA, Plovanich ME, et al. Metabolism. Lysosomal amino acid transporter SLC38A9 signals arginine sufficiency to mTORC1. Science. American Association for the Advancement of Science; 2015;347:188–94.

79. Han JM, Jeong SJ, Park MC, Kim G, Kwon NH, Kim HK, et al. Leucyl-tRNA Synthetase Is an Intracellular Leucine Sensor for the mTORC1-Signaling Pathway. Cell. 2012;149:410–24.

80. Bonfils G, Jaquenoud M, Bontron S, Ostrowicz C, Ungermann C, De Virgilio C. Leucyl-tRNA Synthetase Controls TORC1 via the EGO Complex. Mol. Cell. 2012.

81. Wolfson RL, Chantranupong L, Saxton RA, Shen K, Scaria SM, Cantor JR, et al. Sestrin2 is a leucine sensor for the mTORC1 pathway. Science (80-). American Association for

the Advancement of Science; 2015;351:43–8.

82. Sancak Y, Peterson TR, Shaul YD, Lindquist RA, Thoreen CC, Bar-Peled L, et al. The Rag GTPases bind raptor and mediate amino acid signaling to mTORC1. Science. 2008;320:1496–501.

83. Stracka D, Jozefczuk S, Rudroff F, Sauer U, Hall MN. Nitrogen source activates TOR (target of rapamycin) complex 1 via glutamine and independently of Gtr/Rag proteins. J Biol Chem. 2014;289:25010–20.

84. Plouffe SW, Park HW, Tagliabracci VS, Jewell JL, Russell RC, Kim YC, et al. Differential regulation of mTORC1 by leucine and glutamine. Science (80-). 2015;347:194–8.

85. Fingar DC, Salama S, Tsou C, Harlow E, Blenis J. Mammalian cell size is controlled by mTOR and its downstream targets S6K1 and 4EBP1/eIF4E. Genes Dev. 2002;16:1472–87.

86. Dowling RJO, Topisirovic I, Alain T, Bidinosti M, Fonseca BD, Petroulakis E, et al. mTORC1-mediated cell proliferation, but not cell growth, controlled by the 4E-BPs. Science. 2010;328:1172–6.

87. Ma XM, Blenis J. Molecular mechanisms of mTOR-mediated translational control. Nat Rev Mol Cell Biol. Nature Publishing Group; 2009;10:307–18.

88. Holz MK, Ballif BA, Gygi SP, Blenis J. mTOR and S6K1 mediate assembly of the translation preinitiation complex through dynamic protein interchange and ordered phosphorylation events. Cell. Elsevier; 2005;123:569–80.

89. Browne GJ, Proud CG. A novel mTOR-regulated phosphorylation site in elongation factor 2 kinase modulates the activity of the kinase and its binding to calmodulin. Mol Cell Biol.

2004;24:2986–97.

90. Hsieh AC, Liu Y, Edlind MP, Ingolia NT, Janes MR, Sher A, et al. The translational landscape of mTOR signalling steers cancer initiation and metastasis. Nature. Nature Publishing Group, a division of Macmillan Publishers Limited. All Rights Reserved.; 2012;485:55–61.

91. Mayer C, Zhao J, Yuan X, Grummt I. mTOR-dependent activation of the transcription factor TIF-IA links rRNA synthesis to nutrient availability. Genes Dev. 2004;18:423–34.

92. Kantidakis T, Ramsbottom BA, Birch JL, Dowding SN, White RJ. mTOR associates with TFIIIC, is found at tRNA and 5S rRNA genes, and targets their repressor Maf1. Proc Natl Acad Sci U S A. 2010;107:11823–8.

93. Shor B, Wu J, Shakey Q, Toral-Barza L, Shi C, Follettie M, et al. Requirement of the mTOR kinase for the regulation of Maf1 phosphorylation and control of RNA polymerase III-dependent transcription in cancer cells. J Biol Chem. 2010;285:15380–92.

94. Harrington LS, Findlay GM, Gray A, Tolkacheva T, Wigfield S, Rebholz H, et al. The TSC1-2 tumor suppressor controls insulin-PI3K signaling via regulation of IRS proteins. J Cell Biol. 2004;166:213–23.

95. Um SH, Frigerio F, Watanabe M, Picard F, Joaquin M, Sticker M, et al. Absence of S6K1 protects against age- and diet-induced obesity while enhancing insulin sensitivity. Nature. 2004;431:200–5.

96. Shah OJ, Wang Z, Hunter T. Inappropriate activation of the TSC/Rheb/mTOR/S6K cassette induces IRS1/2 depletion, insulin resistance, and cell survival deficiencies. Curr Biol. 2004;14:1650–6.

97. Hsu PP, Kang SA, Rameseder J, Zhang Y, Ottina KA, Lim D, et al. The mTOR-regulated phosphoproteome reveals a mechanism of mTORC1-mediated inhibition of growth factor signaling. Science. American Association for the Advancement of Science; 2011;332:1317–22.

98. Yu Y, Yoon S-O, Poulogiannis G, Yang Q, Ma XM, Villén J, et al. Phosphoproteomic analysis identifies Grb10 as an mTORC1 substrate that negatively regulates insulin signaling. Science. American Association for the Advancement of Science; 2011;332:1322–6.

99. Majumder PK, Febbo PG, Bikoff R, Berger R, Xue Q, McMahon LM, et al. mTOR inhibition reverses Akt-dependent prostate intraepithelial neoplasia through regulation of apoptotic and HIF-1-dependent pathways. Nat Med. 2004;10:594–601.

100. Düvel K, Yecies JL, Menon S, Raman P, Lipovsky AI, Souza AL, et al. Activation of a metabolic gene regulatory network downstream of mTOR complex 1. Mol Cell. 2010;39:171–83.

101. Peterson TR, Sengupta SS, Harris TE, Carmack AE, Kang SA, Balderas E, et al. mTOR complex 1 regulates lipin 1 localization to control the SREBP pathway. Cell. 2011;146:408–20.

102. Porstmann T, Santos CR, Griffiths B, Cully M, Wu M, Leevers S, et al. SREBP activity is regulated by mTORC1 and contributes to Akt-dependent cell growth. Cell Metab. 2008;8:224–36.

103. Ricoult SJH, Yecies JL, Ben-Sahra I, Manning BD. Oncogenic PI3K and K-Ras stimulate de novo lipid synthesis through mTORC1 and SREBP. Oncogene. 2016;35:1250–60.

104. Ben-Sahra I, Howell JJ, Asara JM, Manning BD. Stimulation of de novo pyrimidine

synthesis by growth signaling through mTOR and S6K1. Science. 2013;339:1323–8.

105. Robitaille AM, Christen S, Shimobayashi M, Cornu M, Fava LL, Moes S, et al. Quantitative phosphoproteomics reveal mTORC1 activates de novo pyrimidine synthesis. Science. American Association for the Advancement of Science; 2013;339:1320–3.

106. Ben-Sahra I, Hoxhaj G, Ricoult SJH, Asara JM, Manning BD. mTORC1 induces purine synthesis through control of the mitochondrial tetrahydrofolate cycle. Science (80-). American Association for the Advancement of Science; 2016;351:728–33.

107. Raez LE, Papadopoulos K, Ricart AD, Chiorean EG, Dipaola RS, Stein MN, et al. A phase I dose-escalation trial of 2-deoxy-D-glucose alone or combined with docetaxel in patients with advanced solid tumors. Cancer Chemother Pharmacol. 2013;71:523–30.

108. Pusapati RV, Daemen A, Wilson C, Sandoval W, Gao M, Haley B, et al. mTORC1-Dependent Metabolic Reprogramming Underlies Escape from Glycolysis Addiction in Cancer Cells. Cancer Cell. Elsevier; 2016;29:548–62.

109. Palm W, Park Y, Wright K, Pavlova NN, Tuveson DA, Thompson CB. The Utilization of Extracellular Proteins as Nutrients Is Suppressed by mTORC1. Cell. 2015;162:259–70.

110. Kim YC, Guan K-L. mTOR: a pharmacologic target for autophagy regulation. J Clin Invest. American Society for Clinical Investigation; 2015;125:25–32.

111. White E. The role for autophagy in cancer. J Clin Invest. American Society for Clinical Investigation; 2015;125:42–6.

112. Yue Z, Jin S, Yang C, Levine AJ, Heintz N. Beclin 1, an autophagy gene essential for early embryonic development, is a haploinsufficient tumor suppressor. Proc Natl Acad Sci U S A. 2003;100:15077–82.

113. Qu X, Yu J, Bhagat G, Furuya N, Hibshoosh H, Troxel A, et al. Promotion of tumorigenesis by heterozygous disruption of the beclin 1 autophagy gene. J Clin Invest. 2003;112:1809–20.

114. Degenhardt K, Mathew R, Beaudoin B, Bray K, Anderson D, Chen G, et al. Autophagy promotes tumor cell survival and restricts necrosis, inflammation, and tumorigenesis. Cancer Cell. 2006;10:51–64.

115. Sarbassov DD, Guertin DA, Ali SM, Sabatini DM. Phosphorylation and regulation of Akt/PKB by the rictor-mTOR complex. Science. American Association for the Advancement of Science; 2005;307:1098–101.

116. Humphrey SJ, Yang G, Yang P, Fazakerley DJ, Stöckli J, Yang JY, et al. Dynamic adipocyte phosphoproteome reveals that Akt directly regulates mTORC2. Cell Metab. 2013;17:1009–20.

117. Yang G, Murashige DS, Humphrey SJ, James DE. A Positive Feedback Loop between Akt and mTORC2 via SIN1 Phosphorylation. Cell Rep. 2015;12:937–43.

118. Liu P, Gan W, Inuzuka H, Lazorchak AS, Gao D, Arojo O, et al. Sin1 phosphorylation impairs mTORC2 complex integrity and inhibits downstream Akt signalling to suppress tumorigenesis. Nat Cell Biol. Nature Publishing Group, a division of Macmillan Publishers Limited. All Rights Reserved.; 2013;15:1340–50.

119. Zhang J, Xu K, Liu P, Geng Y, Wang B, Gan W, et al. Inhibition of Rb Phosphorylation Leads to mTORC2-Mediated Activation of Akt. Mol Cell. 2016;

120. Guertin DA, Stevens DM, Saitoh M, Kinkel S, Crosby K, Sheen J-H, et al. mTOR complex 2 is required for the development of prostate cancer induced by Pten loss in mice. Cancer Cell. 2009;15:148–59.

121. Tanaka K, Babic I, Nathanson D, Akhavan D, Guo D, Gini B, et al. Oncogenic EGFR signaling activates an mTORC2-NF-κB pathway that promotes chemotherapy resistance. Cancer Discov. American Association for Cancer Research; 2011;1:524–38.

122. Masui K, Tanaka K, Akhavan D, Babic I, Gini B, Matsutani T, et al. mTOR complex 2 controls glycolytic metabolism in glioblastoma through FoxO acetylation and upregulation of c-Myc. Cell Metab. 2013;18:726–39.

123. Gasser JA, Inuzuka H, Lau AW, Wei W, Beroukhim R, Toker A. SGK3 mediates INPP4B-dependent PI3K signaling in breast cancer. Mol Cell. 2014;56:595–607.

124. Weiler M, Blaes J, Pusch S, Sahm F, Czabanka M, Luger S, et al. mTOR target NDRG1 confers MGMT-dependent resistance to alkylating chemotherapy. Proc Natl Acad Sci U S A. 2014;111:409–14.

125. Sommer EM, Dry H, Cross D, Guichard S, Davies BR, Alessi DR. Elevated SGK1 predicts resistance of breast cancer cells to Akt inhibitors. Biochem J. 2013;452:499–508.

126. Bakker WJ, Harris IS, Mak TW. FOXO3a is activated in response to hypoxic stress and inhibits HIF1-induced apoptosis via regulation of CITED2. Mol Cell. 2007;28:941–53.

127. Morrison MM, Young CD, Wang S, Sobolik T, Sanchez VM, Hicks DJ, et al. mTOR Directs Breast Morphogenesis through the PKC-alpha-Rac1 Signaling Axis. PLoS Genet. Public Library of Science; 2015;11:e1005291.

128. Lee K, Nam KT, Cho SH, Gudapati P, Hwang Y, Park D-S, et al. Vital roles of mTOR complex 2 in Notch-driven thymocyte differentiation and leukemia. J Exp Med. 2012;209:713–28.

129. Cheng H, Zou Y, Ross JS, Wang K, Liu X, Halmos B, et al. RICTOR amplification defines

a novel subset of lung cancer patients who may benefit from treatment with mTOR1/2 inhibitors. Cancer Discov. 2015;

130. Morrison-Joly M, Hicks DJ, Jones B, Sanchez V, Estrada MV, Young C, et al. Rictor/mTORC2 drives progression and therapeutic resistance of HER2-amplified breast cancers. Cancer Res. 2016;76:0008-5472.CAN-15-3393-.

131. Balko JM, Giltnane JM, Wang K, Schwarz LJ, Young CD, Cook RS, et al. Molecular profiling of the residual disease of triple-negative breast cancers after neoadjuvant chemotherapy identifies actionable therapeutic targets. Cancer Discov. 2014;4:232–45.

132. Masri J, Bernath A, Martin J, Jo OD, Vartanian R, Funk A, et al. mTORC2 activity is elevated in gliomas and promotes growth and cell motility via overexpression of rictor. Cancer Res. 2007;67:11712–20.

133. Sarbassov DD, Ali SM, Sengupta S, Sheen J-H, Hsu PP, Bagley AF, et al. Prolonged rapamycin treatment inhibits mTORC2 assembly and Akt/PKB. Mol Cell. 2006;22:159–68.

134. Benjamin D, Colombi M, Moroni C, Hall MN. Rapamycin passes the torch: a new generation of mTOR inhibitors. Nat Rev Drug Discov. 2011;10:868–80.

135. Hudes G, Carducci M, Tomczak P, Dutcher J, Figlin R, Kapoor A, et al. Temsirolimus, interferon alfa, or both for advanced renal-cell carcinoma. N Engl J Med. 2007;356:2271–81.

136. Yu K, Toral-Barza L, Shi C, Zhang W-G, Lucas J, Shor B, et al. Biochemical, cellular, and in vivo activity of novel ATP-competitive and selective inhibitors of the mammalian target of rapamycin. Cancer Res. 2009;69:6232–40.

137. Sun S-Y, Rosenberg LM, Wang X, Zhou Z, Yue P, Fu H, et al. Activation of Akt and

eIF4E survival pathways by rapamycin-mediated mammalian target of rapamycin inhibition. Cancer Res. 2005;65:7052–8.

138. O'Reilly KE, Rojo F, She Q-B, Solit D, Mills GB, Smith D, et al. mTOR inhibition induces upstream receptor tyrosine kinase signaling and activates Akt. Cancer Res. 2006;66:1500–8.

139. Hsieh AC, Costa M, Zollo O, Davis C, Feldman ME, Testa JR, et al. Genetic dissection of the oncogenic mTOR pathway reveals druggable addiction to translational control via 4EBP-eIF4E. Cancer Cell. 2010;17:249–61.

140. Naing A, Aghajanian C, Raymond E, Olmos D, Schwartz G, Oelmann E, et al. Safety, tolerability, pharmacokinetics and pharmacodynamics of AZD8055 in advanced solid tumours and lymphoma. Br J Cancer. Cancer Research UK; 2012;107:1093–9.

141. Basu B, Dean E, Puglisi M, Greystoke A, Ong M, Burke W, et al. First-in-Human Pharmacokinetic and Pharmacodynamic Study of the Dual m-TORC 1/2 Inhibitor AZD2014. Clin Cancer Res. 2015;21:3412–9.

142. Rodrik-Outmezguine VS, Okaniwa M, Yao Z, Novotny CJ, McWhirter C, Banaji A, et al. Overcoming mTOR resistance mutations with a new-generation mTOR inhibitor. Nature. 2016;534:272–6.

143. Britten CD, Adjei AA, Millham R, Houk BE, Borzillo G, Pierce K, et al. Phase I study of PF-04691502, a small-molecule, oral, dual inhibitor of PI3K and mTOR, in patients with advanced cancer. Invest New Drugs. 2014;32:510–7.

144. Jänne PA, Cohen RB, Laird AD, Macé S, Engelman JA, Ruiz-Soto R, et al. Phase I safety and pharmacokinetic study of the PI3K/mTOR inhibitor SAR245409 (XL765) in combination with erlotinib in patients with advanced solid tumors. J Thorac Oncol.

2014;9:316–23.

145. Mateo J, Olmos D, Dumez H, Poondru S, Samberg NL, Barr S, et al. A first in man, dose-finding study of the mTORC1/mTORC2 inhibitor OSI-027 in patients with advanced solid malignancies. Br J Cancer. 2016;114:889–96.

146. Powles T, Wheater M, Din O, Geldart T, Boleti E, Stockdale A, et al. A Randomised Phase 2 Study of AZD2014 Versus Everolimus in Patients with VEGF-Refractory Metastatic Clear Cell Renal Cancer. Eur Urol. 2016;69:450–6.

147. Bendell JC, Kelley RK, Shih KC, Grabowsky JA, Bergsland E, Jones S, et al. A phase I dose-escalation study to assess safety, tolerability, pharmacokinetics, and preliminary efficacy of the dual mTORC1/mTORC2 kinase inhibitor CC-223 in patients with advanced solid tumors or multiple myeloma. Cancer. 2015;121:3481–90.

148. Bendell JC, Kurkjian C, Infante JR, Bauer TM, Burris HA, Greco FA, et al. A phase 1 study of the sachet formulation of the oral dual PI3K/mTOR inhibitor BEZ235 given twice daily (BID) in patients with advanced solid tumors. Invest New Drugs. 2015;33:463–71.

149. Fazio N, Buzzoni R, Baudin E, Antonuzzo L, Hubner RA, Lahner H, et al. A Phase II Study of BEZ235 in Patients with Everolimus-resistant, Advanced Pancreatic Neuroendocrine Tumours. Anticancer Res. 2016;36:713–9.

150. Seront E, Rottey S, Filleul B, Glorieux P, Goeminne J, Verschaeve V, et al. Phase II study of dual phosphoinositol-3-kinase (PI3K) and mammalian target of rapamycin (mTOR) inhibitor BEZ235 in patients with locally advanced or metastatic transitional cell carcinoma (TCC). BJU Int. 2016;

151. Wen PY, Omuro A, Ahluwalia MS, Fathallah-Shaykh HM, Mohile N, Lager JJ, et al. Phase I dose-escalation study of the PI3K/mTOR inhibitor voxtalisib (SAR245409, XL765)

plus temozolomide with or without radiotherapy in patients with high-grade glioma. Neuro Oncol. 2015;17:1275–83.

152. Papadopoulos KP, Egile C, Ruiz-Soto R, Jiang J, Shi W, Bentzien F, et al. Efficacy, safety, pharmacokinetics and pharmacodynamics of SAR245409 (voxtalisib, XL765), an orally administered phosphoinositide 3-kinase/mammalian target of rapamycin inhibitor: a phase 1 expansion cohort in patients with relapsed or refractory lymphoma. Leuk Lymphoma. 2015;56:1763–70.

153. Papadopoulos KP, Tabernero J, Markman B, Patnaik A, Tolcher AW, Baselga J, et al. Phase I safety, pharmacokinetic, and pharmacodynamic study of SAR245409 (XL765), a novel, orally administered PI3K/mTOR inhibitor in patients with advanced solid tumors. Clin Cancer Res. 2014;20:2445–56.

154. Dolly SO, Wagner AJ, Bendell JC, Kindler HL, Krug LM, Seiwert TY, et al. Phase I Study of Apitolisib (GDC-0980), Dual Phosphatidylinositol-3-Kinase and Mammalian Target of Rapamycin Kinase Inhibitor, in Patients with Advanced Solid Tumors. Clin Cancer Res. 2016;

155. Powles T, Lackner MR, Oudard S, Escudier B, Ralph C, Brown JE, et al. Randomized Open-Label Phase II Trial of Apitolisib (GDC-0980), a Novel Inhibitor of the PI3K/Mammalian Target of Rapamycin Pathway, Versus Everolimus in Patients With Metastatic Renal Cell Carcinoma. J Clin Oncol. 2016;34:1660–8.

156. Shapiro GI, Bell-McGuinn KM, Molina JR, Bendell J, Spicer J, Kwak EL, et al. First-in-Human Study of PF-05212384 (PKI-587), a Small-Molecule, Intravenous, Dual Inhibitor of PI3K and mTOR in Patients with Advanced Cancer. Clin Cancer Res. 2015;21:1888–95.

157. Munster P, Aggarwal R, Hong D, Schellens JHM, van der Noll R, Specht J, et al. First-in-

Human Phase I Study of GSK2126458, an Oral Pan-Class I Phosphatidylinositol-3-Kinase Inhibitor, in Patients with Advanced Solid Tumor Malignancies. Clin Cancer Res. 2015;22:1932–9.

158. Del Campo JM, Birrer M, Davis C, Fujiwara K, Gollerkeri A, Gore M, et al. A randomized phase II non-comparative study of PF-04691502 and gedatolisib (PF-05212384) in patients with recurrent endometrial cancer. Gynecol Oncol. 2016;

159. Mahadevan D, Chiorean EG, Harris WB, Von Hoff DD, Stejskal-Barnett A, Qi W, et al. Phase I pharmacokinetic and pharmacodynamic study of the pan-PI3K/mTORC vascular targeted pro-drug SF1126 in patients with advanced solid tumours and B-cell malignancies. Eur J Cancer. 2012;48:3319–27.

160. Markman B, Tabernero J, Krop I, Shapiro GI, Siu L, Chen LC, et al. Phase I safety, pharmacokinetic, and pharmacodynamic study of the oral phosphatidylinositol-3-kinase and mTOR inhibitor BGT226 in patients with advanced solid tumors. Ann Oncol. 2012;23:2399–408.

161. Viñals F, Chambard JC, Pouysségur J. p70 S6 kinase-mediated protein synthesis is a critical step for vascular endothelial cell proliferation. J Biol Chem. 1999;274:26776–82.

162. Guba M, von Breitenbuch P, Steinbauer M, Koehl G, Flegel S, Hornung M, et al. Rapamycin inhibits primary and metastatic tumor growth by antiangiogenesis: involvement of vascular endothelial growth factor. Nat Med. Nature Publishing Group; 2002;8:128–35.

163. Hudson CC, Liu M, Chiang GG, Otterness DM, Loomis DC, Kaper F, et al. Regulation of Hypoxia-Inducible Factor 1 Expression and Function by the Mammalian Target of Rapamycin. Mol Cell Biol. 2002;22:7004–14.

164. Bernardi R, Guernah I, Jin D, Grisendi S, Alimonti A, Teruya-Feldstein J, et al. PML inhibits HIF-1alpha translation and neoangiogenesis through repression of mTOR. Nature. 2006;442:779–85.

165. Sun S, Chen S, Liu F, Wu H, McHugh J, Bergin IL, et al. Constitutive Activation of mTORC1 in Endothelial Cells Leads to the Development and Progression of Lymphangiosarcoma through VEGF Autocrine Signaling. Cancer Cell. 2015;28:758–72.

166. Wang S, Amato KR, Song W, Youngblood V, Lee K, Boothby M, et al. Regulation of endothelial cell proliferation and vascular assembly through distinct mTORC2 signaling pathways. Mol Cell Biol. 2015;35:1299–313.

167. Roy D, Sin S-H, Lucas A, Venkataramanan R, Wang L, Eason A, et al. mTOR inhibitors block Kaposi sarcoma growth by inhibiting essential autocrine growth factors and tumor angiogenesis. Cancer Res. 2013;73:2235–46.

168. Chatterjee S, Heukamp LC, Siobal M, Schöttle J, Wieczorek C, Peifer M, et al. Tumor VEGF:VEGFR2 autocrine feed-forward loop triggers angiogenesis in lung cancer. J Clin Invest. American Society for Clinical Investigation; 2013;123:1732–40.

169. LaGory EL, Giaccia AJ. The ever-expanding role of HIF in tumour and stromal biology. Nat Cell Biol. Nature Publishing Group, a division of Macmillan Publishers Limited. All Rights Reserved.; 2016;18:356–65.

170. Mayerhofer M, Valent P, Sperr WR, Griffin JD, Sillaber C. BCR/ABL induces expression of vascular endothelial growth factor and its transcriptional activator, hypoxia inducible factor-1alpha, through a pathway involving phosphoinositide 3-kinase and the mammalian target of rapamycin. Blood. American Society of Hematology; 2002;100:3767–75.

171. Brugarolas JB, Vazquez F, Reddy A, Sellers WR, Kaelin WG. TSC2 regulates VEGF through mTOR-dependent and -independent pathways. Cancer Cell. 2003;4:147–58.

172. Phung TL, Ziv K, Dabydeen D, Eyiah-Mensah G, Riveros M, Perruzzi C, et al. Pathological angiogenesis is induced by sustained Akt signaling and inhibited by rapamycin. Cancer Cell. 2006;10:159–70.

173. Guertin DA, Stevens DM, Thoreen CC, Burds AA, Kalaany NY, Moffat J, et al. Ablation in mice of the mTORC components raptor, rictor, or mLST8 reveals that mTORC2 is required for signaling to Akt-FOXO and PKCalpha, but not S6K1. Dev Cell. 2006;11:859–71.

174. Farhan MA, Carmine-Simmen K, Lewis JD, Moore RB, Murray AG. Endothelial Cell mTOR Complex-2 Regulates Sprouting Angiogenesis. PLoS One. Public Library of Science; 2015;10:e0135245.

175. Guo F, Wang Y, Liu J, Mok SC, Xue F, Zhang W. CXCL12/CXCR4: a symbiotic bridge linking cancer cells and their stromal neighbors in oncogenic communication networks. Oncogene. Nature Publishing Group; 2016;35:816–26.

176. Zhuang G, Yu K, Jiang Z, Chung A, Yao J, Ha C, et al. Phosphoproteomic analysis implicates the mTORC2-FoxO1 axis in VEGF signaling and feedback activation of receptor tyrosine kinases. Sci Signal. American Association for the Advancement of Science; 2013;6:ra25.

177. Paik J-H, Kollipara R, Chu G, Ji H, Xiao Y, Ding Z, et al. FoxOs are lineage-restricted redundant tumor suppressors and regulate endothelial cell homeostasis. Cell. 2007;128:309–23.

178. Wilhelm K, Happel K, Eelen G, Schoors S, Oellerich MF, Lim R, et al. FOXO1 couples

metabolic activity and growth state in the vascular endothelium. Nature. Nature Publishing Group, a division of Macmillan Publishers Limited. All Rights Reserved.; 2016;advance on.

179. Lane HA, Wood JM, McSheehy PMJ, Allegrini PR, Boulay A, Brueggen J, et al. mTOR inhibitor RAD001 (everolimus) has antiangiogenic/vascular properties distinct from a VEGFR tyrosine kinase inhibitor. Clin Cancer Res. 2009;15:1612–22.

180. Shinohara ET, Cao C, Niermann K, Mu Y, Zeng F, Hallahan DE, et al. Enhanced radiation damage of tumor vasculature by mTOR inhibitors. Oncogene. 2005;24:5414–22.

181. Fokas E, Im JH, Hill S, Yameen S, Stratford M, Beech J, et al. Dual inhibition of the PI3K/mTOR pathway increases tumor radiosensitivity by normalizing tumor vasculature. Cancer Res. 2012;72:239–48.

182. Sharma P, Allison JP, Curtin JA, Fridlyand J, Kageshita T, Patel HN, et al. The future of immune checkpoint therapy. Science. American Association for the Advancement of Science; 2015;348:56–61.

183. Lastwika KJ, Wilson W, Li QK, Norris J, Xu H, Ghazarian SR, et al. Control of PD-L1 Expression by Oncogenic Activation of the AKT-mTOR Pathway in Non-Small Cell Lung Cancer. Cancer Res. 2016;76:227–38.

184. Kleffel S, Posch C, Barthel SR, Mueller H, Schlapbach C, Guenova E, et al. Melanoma Cell-Intrinsic PD-1 Receptor Functions Promote Tumor Growth. Cell. 2015;162:1242–56.

185. Granot Z, Fridlender ZG. Plasticity beyond cancer cells and the “immunosuppressive switch”. Cancer Res. 2015;75:4441–5.

186. Delgoffe GM, Kole TP, Zheng Y, Zarek PE, Matthews KL, Xiao B, et al. The mTOR

kinase differentially regulates effector and regulatory T cell lineage commitment. Immunity. 2009;30:832–44.

187. Lee K, Gudapati P, Dragovic S, Spencer C, Joyce S, Killeen N, et al. Mammalian target of rapamycin protein complex 2 regulates differentiation of Th1 and Th2 cell subsets via distinct signaling pathways. Immunity. 2010;32:743–53.

188. Heikamp EB, Patel CH, Collins S, Waickman A, Oh M-H, Sun I-H, et al. The AGC kinase SGK1 regulates TH1 and TH2 differentiation downstream of the mTORC2 complex. Nat Immunol. 2014;15:457–64.

189. Pollizzi KN, Patel CH, Sun I-H, Oh M-H, Waickman AT, Wen J, et al. mTORC1 and mTORC2 selectively regulate $CD8^+$ T cell differentiation. J Clin Invest. 2015;125:2090–108.

190. Araki K, Turner AP, Shaffer VO, Gangappa S, Keller SA, Bachmann MF, et al. mTOR regulates memory CD8 T-cell differentiation. Nature. 2009;460:108–12.

191. Zhang L, Tschumi BO, Lopez-Mejia IC, Oberle SG, Meyer M, Samson G, et al. Mammalian Target of Rapamycin Complex 2 Controls CD8 T Cell Memory Differentiation in a Foxo1-Dependent Manner. Cell Rep. 2016;14:1206–17.

192. Byles V, Covarrubias AJ, Ben-Sahra I, Lamming DW, Sabatini DM, Manning BD, et al. The TSC-mTOR pathway regulates macrophage polarization. Nat Commun. 2013;4:2834.

193. Lee K, Heffington L, Jellusova J, Nam KT, Raybuck A, Cho SH, et al. Requirement for Rictor in homeostasis and function of mature B lymphoid cells. Blood. American Society of Hematology; 2013;122:2369–79.

194. Saxton RA, Sabatini DM. mTOR Signaling in Growth, Metabolism, and Disease. Cell. Cell

Press; 2017;168:960–76.

195. Kim LC, Cook RS, Chen J. MTORC1 and mTORC2 in cancer and the tumor microenvironment. Oncogene. Nature Publishing Group; 2017;36:2191–201.

196. Kim D-H, Sarbassov DD, Ali SM, Latek RR, Guntur KVP, Erdjument-Bromage H, et al. GbetaL, a positive regulator of the rapamycin-sensitive pathway required for the nutrient-sensitive interaction between raptor and mTOR. Mol Cell. 2003;11:895–904.

197. Wang T, Blumhagen R, Lao U, Kuo Y, Edgar BA. LST8 regulates cell growth via target-of-rapamycin complex 2 (TORC2). Mol Cell Biol. American Society for Microbiology; 2012;32:2203–13.

198. Wang T, Wei JJ, Sabatini DM, Lander ES. Genetic screens in human cells using the CRISPR-Cas9 system. Science (80-). American Association for the Advancement of Science; 2014;343:80–4.

199. Sanjana NE, Shalem O, Zhang F. Improved vectors and genome-wide libraries for CRISPR screening. Nat Methods. 2014;11:783–4.

200. Karuppasamy M, Kusmider B, Oliveira TM, Gaubitz C, Prouteau M, Loewith R, et al. Cryo-EM structure of Saccharomyces cerevisiae target of rapamycin complex 2. Nat Commun. 2017;8:1729.

201. Tatebe H, Murayama S, Yonekura T, Hatano T, Richter D, Furuya T, et al. Substrate specificity of TOR complex 2 is determined by a ubiquitin-fold domain of the Sin1 subunit. Elife. 2017;6.

202. Yang H, Wang J, Liu M, Chen X, Huang M, Tan D, et al. 4.4 Å Resolution Cryo-EM structure of human mTOR Complex 1. Protein Cell. 2016;7:878–87.

203. Stuttfeld E, Aylett CH, Imseng S, Boehringer D, Scaiola A, Sauer E, et al. Architecture of the human mTORC2 core complex. Elife. 2018;7.

204. Chen X, Liu M, Tian Y, Li J, Qi Y, Zhao D, et al. Cryo-EM structure of human mTOR complex 2. Cell Res. 2018;28:518–28.

205. Jacinto E, Facchinetti V, Liu D, Soto N, Wei S, Jung SY, et al. SIN1/MIP1 maintains rictor-mTOR complex integrity and regulates Akt phosphorylation and substrate specificity. Cell. Elsevier; 2006;127:125–37.

206. Kovalski JR, Bhaduri A, Zehnder AM, Neela PH, Che Y, Wozniak GG, et al. The Functional Proximal Proteome of Oncogenic Ras Includes mTORC2. Mol Cell. 2019;73:830-844.e12.

207. Cheng H, Zou Y, Ross JS, Wang K, Liu X, Halmos B, et al. RICTOR Amplification Defines a Novel Subset of Patients with Lung Cancer Who May Benefit from Treatment with mTORC1/2 Inhibitors. Cancer Discov. 2015;5:1262–70.

208. Pao W, Girard N. New driver mutations in non-small-cell lung cancer. Lancet Oncol. 2011;12:175–80.

209. Sakre N, Wildey G, Behtaj M, Kresak A, Yang M, Fu P, et al. RICTOR amplification identifies a subgroup in small cell lung cancer and predicts response to drugs targeting mTOR. Oncotarget. 2017;8:5992–6002.

210. Kim ST, Kim SY, Klempner SJ, Yoon J, Kim N, Ahn S, et al. Rapamycin-insensitive companion of mTOR (*RICTOR*) Amplification Defines a Subset of Advanced Gastric Cancer and is Sensitive to AZD2014-mediated mTORC1/2 Inhibition. Ann Oncol. 2016;28:mdw669.

211. García-Martínez JM, Alessi DR. mTOR complex 2 (mTORC2) controls hydrophobic motif phosphorylation and activation of serum- and glucocorticoid-induced protein kinase 1 (SGK1). Biochem J. 2008;416:375–85.

212. Hwang Y, Kim LC, Song W, Edwards DN, Cook RS, Chen J. Disruption of the Scaffolding Function of mLST8 Selectively Inhibits mTORC2 Assembly and Function and Suppresses mTORC2-Dependent Tumor Growth *In Vivo*. Cancer Res. 2019;79:3178–84.

213. Werfel TA, Wang S, Jackson MA, Kavanaugh TE, Joly MM, Lee LH, et al. Selective mTORC2 Inhibitor Therapeutically Blocks Breast Cancer Cell Growth and Survival. Cancer Res. 2018;78:1845–58.

214. Konermann S, Brigham MD, Trevino AE, Joung J, Abudayyeh OO, Barcena C, et al. Genome-scale transcriptional activation by an engineered CRISPR-Cas9 complex. Nature. 2015;517:583–8.

215. Garnis C, Davies JJ, Buys TPH, Tsao M-S, MacAulay C, Lam S, et al. Chromosome 5p aberrations are early events in lung cancer: implication of glial cell line-derived neurotrophic factor in disease progression. Oncogene. Nature Publishing Group; 2005;24:4806–12.

216. Tan HWS, Sim AYL, Long YC. Glutamine metabolism regulates autophagy-dependent mTORC1 reactivation during amino acid starvation. Nat Commun. Nature Publishing Group; 2017;8:338.

217. Platt RJ, Chen S, Zhou Y, Yim MJ, Swiech L, Kempton HR, et al. CRISPR-Cas9 Knockin Mice for Genome Editing and Cancer Modeling. Cell. 2014;159:440–55.

218. Joung J, Konermann S, Gootenberg JS, Abudayyeh OO, Platt RJ, Brigham MD, et al. Genome-scale CRISPR-Cas9 knockout and transcriptional activation screening. Nat

Protoc. 2017;12:828–63.

219. Barger C, Branick C, Chee L, Karpf A. Pan-Cancer Analyses Reveal Genomic Features of FOXM1 Overexpression in Cancer. Cancers (Basel). 2019;11:251.

220. McDonald PC, Oloumi A, Mills J, Dobreva I, Maidan M, Gray V, et al. Rictor and Integrin-Linked Kinase Interact and Regulate Akt Phosphorylation and Cancer Cell Survival. Cancer Res. 2008;68:1618–24.

221. Janku F, Yap TA, Meric-Bernstam F. Targeting the PI3K pathway in cancer: are we making headway? Nat Rev Clin Oncol. Nature Publishing Group; 2018;15:273–91.

222. Yokoi S, Yasui K, Mori M, Iizasa T, Fujisawa T, Inazawa J. Amplification and Overexpression of SKP2 Are Associated with Metastasis of Non-Small-Cell Lung Cancers to Lymph Nodes. Am J Pathol. 2004;165:175–80.

223. Clement E, Inuzuka H, Nihira NT, Wei W, Toker A. Skp2-dependent reactivation of AKT drives resistance to PI3K inhibitors. Sci Signal. American Association for the Advancement of Science; 2018;11:eaao3810.

224. Scott KL, Kabbarah O, Liang M-C, Ivanova E, Anagnostou V, Wu J, et al. GOLPH3 modulates mTOR signalling and rapamycin sensitivity in cancer. Nature. Nature Publishing Group; 2009;459:1085–90.

225. Chen DR, Chu CY, Chen CY, Yang HC, Chiang YY, Lin TY, et al. Expression of short-form oncostatin M receptor as a decoy receptor in lung adenocarcinomas. J Pathol. J Pathol; 2008;215:290–9.

226. Kucia-Tran JA, Tulkki V, Smith S, Scarpini CG, Hughes K, Araujo AM, et al. Overexpression of the oncostatin-M receptor in cervical squamous cell carcinoma is

associated with epithelial-mesenchymal transition and poor overall survival. Br J Cancer. Nature Publishing Group; 2016;115:212–22.

227. Shien K, Papadimitrakopoulou VA, Ruder D, Behrens C, Shen L, Kalhor N, et al. JAK1/STAT3 activation through a proinflammatory cytokine pathway leads to resistance to molecularly targeted therapy in non–small cell lung cancer. Mol Cancer Ther. American Association for Cancer Research Inc.; 2017;16:2234–45.

228. Xie J, Wang X, Proud CG. mTOR inhibitors in cancer therapy. F1000Research. Faculty of 1000 Ltd; 2016;5.

229. Skidmore ZL, Wagner AH, Lesurf R, Campbell KM, Kunisaki J, Griffith OL, et al. GenVisR: Genomic Visualizations in R. Bioinformatics. 2016;32:3012–4.

230. Li C-F, Wang J-M, Kang H-Y, Huang C-K, Wang J-W, Fang F-M, et al. Characterization of Gene Amplification-Driven SKP2 Overexpression in Myxofibrosarcoma: Potential Implications in Tumor Progression and Therapeutics. Clin Cancer Res. American Association for Cancer Research; 2012;18:1598–610.

231. Wang X-C, Wu Y-P, Ye B, Lin D-C, Feng Y-B, Zhang Z-Q, et al. Suppression of Anoikis by *SKP2* Amplification and Overexpression Promotes Metastasis of Esophageal Squamous Cell Carcinoma. Mol Cancer Res. 2009;7:12–22.

232. Migita T, Narita T, Nomura K, Miyagi E, Inazuka F, Matsuura M, et al. ATP citrate lyase: Activation and therapeutic implications in non-small cell lung cancer. Cancer Res. 2008;68:8547–54.

233. Lee J V, Carrer A, Shah S, Snyder NW, Wei S, Venneti S, et al. Akt-dependent metabolic reprogramming regulates tumor cell histone acetylation. Cell Metab. NIH Public Access; 2014;20:306–19.

234. Carrer A, Trefely S, Zhao S, Campbell S, Norgard RJ, Schultz KC, et al. Acetyl-CoA metabolism supports multi-step pancreatic tumorigenesis. Cancer Discov. American Association for Cancer Research; 2019;CD-18-0567.

235. Martinez Calejman C, Trefely S, Entwisle SW, Luciano A, Jung SM, Hsiao W, et al. mTORC2-AKT signaling to ATP-citrate lyase drives brown adipogenesis and de novo lipogenesis. Nat Commun. Nature Research; 2020;11:1–16.

236. Guri Y, Colombi M, Dazert E, Hindupur SK, Roszik J, Moes S, et al. mTORC2 Promotes Tumorigenesis via Lipid Synthesis. Cancer Cell. Elsevier Inc.; 2017;32:807-823.e12.

237. Mohlin S, Hamidian A, von Stedingk K, Bridges E, Wigerup C, Bexell D, et al. PI3K-mTORC2 but not PI3K-mTORC1 regulates transcription of HIF2A/EPAS1 and vascularization in neuroblastoma. Cancer Res. 2015;75:4617–28.

238. Cui B, Gong L, Chen M, Zhang Y, Yuan H, Qin J, et al. CUL5-SOCS6 complex regulates mTORC2 function by targeting Sin1 for degradation. Cell Discov. Nature Publishing Groups; 2019. page 1–4.

239. Paiva SL, Crews CM. Targeted protein degradation: elements of PROTAC design. Curr. Opin. Chem. Biol. Elsevier Ltd; 2019. page 111–9.

240. You I, Erickson EC, Donovan KA, Eleuteri NA, Fischer ES, Gray NS, et al. Discovery of an AKT Degrader with Prolonged Inhibition of Downstream Signaling. Cell Chem Biol. Elsevier Ltd; 2020;27:66-73.e7.

241. Raina K, Lu J, Qian Y, Altieri M, Gordon D, Rossi AMK, et al. PROTAC-induced BET protein degradation as a therapy for castration-resistant prostate cancer. Proc Natl Acad Sci U S A. National Academy of Sciences; 2016;113:7124–9.

242. Schapira M, Tyers M, Torrent M, Arrowsmith CH. WD40 repeat domain proteins: A novel target class? Nat. Rev. Drug Discov. Nature Publishing Group; 2017. page 773–86.

243. Mayekar MK, Bivona TG. Current Landscape of Targeted Therapy in Lung Cancer. Clin Pharmacol Ther. John Wiley & Sons, Ltd; 2017;102:757–64.

244. Rikova K, Guo A, Zeng Q, Possemato A, Yu J, Haack H, et al. Global Survey of Phosphotyrosine Signaling Identifies Oncogenic Kinases in Lung Cancer. Cell. Cell Press; 2007;131:1190–203.

245. Pasquale EB. Eph receptors and ephrins in cancer: bidirectional signalling and beyond. Nat Rev Cancer. Nature Publishing Group; 2010;10:165–80.

246. Amato KR, Wang S, Hastings AK, Youngblood VM, Santapuram PR, Chen H, et al. Genetic and pharmacologic inhibition of EPHA2 promotes apoptosis in NSCLC. J Clin Invest. American Society for Clinical Investigation; 2014;124:2037–49.

247. Barquilla A, Pasquale EB. Eph Receptors and Ephrins: Therapeutic Opportunities. Annu Rev Pharmacol Toxicol. Annual Reviews ; 2015;55:465–87.

248. Suh P-G, Park J-I, Manzoli L, Cocco L, Peak JC, Katan M, et al. Multiple roles of phosphoinositide-specific phospholipase C isozymes. BMB Rep. 2008;41:415–34.

249. Jang H-J, Suh P-G, Lee YJ, Shin KJ, Chae YC. PLCγ1: Potential arbitrator of cancer progression. Adv Biol Regul. Pergamon; 2018;67:179–89.

250. Yang YR, Follo MY, Cocco L, Suh P-G. The physiological roles of primary phospholipase C. Adv Biol Regul. 2013;53:232–41.

251. Ji QS, Winnier GE, Niswender KD, Horstman D, Wisdom R, Magnuson MA, et al. Essential role of the tyrosine kinase substrate phospholipase C-gamma1 in mammalian

growth and development. Proc Natl Acad Sci U S A. National Academy of Sciences; 1997;94:2999–3003.

252. Faccio R, Cremasco V. PLCγ2: where bone and immune cells find their common ground. Ann N Y Acad Sci. John Wiley & Sons, Ltd (10.1111); 2010;1192:124–30.

253. Sala G, Dituri F, Raimondi C, Previdi S, Maffucci T, Mazzoletti M, et al. Phospholipase Cγ1 Is Required for Metastasis Development and Progression. Cancer Res. American Association for Cancer Research; 2008;68:10187–96.

254. Arteaga CL, Johnson MD, Todderud G, Coffey RJ, Carpenter G, Page DL. Elevated content of the tyrosine kinase substrate phospholipase C-gamma 1 in primary human breast carcinomas. Proc Natl Acad Sci U S A. National Academy of Sciences; 1991;88:10435–9.

255. Lattanzio R, Iezzi M, Sala G, Tinari N, Falasca M, Alberti S, et al. PLC-gamma-1 phosphorylation status is prognostic of metastatic risk in patients with early-stage Luminal-A and -B breast cancer subtypes. BMC Cancer. BioMed Central; 2019;19:747.

256. Gouaze-Andersson V, Delmas C, Taurand M, Martinez-Gala J, Evrard S, Mazoyer S, et al. FGFR1 Induces Glioblastoma Radioresistance through the PLCγ/Hif1 Pathway. Cancer Res. American Association for Cancer Research; 2016;76:3036–44.

257. Elkabets M, Pazarentzos E, Juric D, Sheng Q, Pelossof RA, Brook S, et al. AXL Mediates Resistance to PI3Kα Inhibition by Activating the EGFR/PKC/mTOR Axis in Head and Neck and Esophageal Squamous Cell Carcinomas. Cancer Cell. 2015;27:533–46.

258. Liu T-M, Woyach JA, Zhong Y, Lozanski A, Lozanski G, Dong S, et al. Hypermorphic mutation of phospholipase C, γ2 acquired in ibrutinib-resistant CLL confers BTK independency upon B-cell receptor activation. Blood. American Society of Hematology;

2015;126:61–8.

259. Hunter SG, Zhuang G, Brantley-Sieders D, Swat W, Cowan CW, Chen J. Essential Role of Vav Family Guanine Nucleotide Exchange Factors in EphA Receptor-Mediated Angiogenesis. Mol Cell Biol. 2006;26:4830–42.

260. Zhuang G, Hunter S, Hwang Y, Chen J. Regulation of EphA2 Receptor Endocytosis by SHIP2 Lipid Phosphatase via Phosphatidylinositol 3-Kinase-dependent Rac1 Activation. J Biol Chem. 2007;282:2683–94.

261. Carpenter G, Ji Q. Phospholipase C-γ as a Signal-Transducing Element. Exp Cell Res. Academic Press; 1999;253:15–24.

262. Fang W Bin, Brantley-Sieders DM, Hwang Y, Ham A-JL, Chen J. Identification and Functional Analysis of Phosphorylated Tyrosine Residues within EphA2 Receptor Tyrosine Kinase. J Biol Chem. 2008;283:16017–26.

263. Koss H, Bunney TD, Behjati S, Katan M. Dysfunction of phospholipase Cγ in immune disorders and cancer. Trends Biochem Sci. 2014;39:603–11.

264. Emmanouilidi A, Lattanzio R, Sala G, Piantelli M, Falasca M. The role of phospholipase Cγ1 in breast cancer and its clinical significance. Futur Oncol. 2017;13:1991–7.

265. Song W, Ma Y, Wang J, Brantley-Sieders D, Chen J. JNK Signaling Mediates EPHA2-Dependent Tumor Cell Proliferation, Motility, and Cancer Stem Cell-like Properties in Non-Small Cell Lung Cancer. Cancer Res. American Association for Cancer Research; 2014;74:2444–54.

266. Song W, Hwang Y, Youngblood VM, Cook RS, Balko JM, Chen J, et al. Targeting EphA2 impairs cell cycle progression and growth of basal-like/triple-negative breast cancers.

Oncogene. Nature Publishing Group; 2017;36:5620–30.

267. Brantley-Sieders DM, Zhuang G, Hicks D, Fang W Bin, Hwang Y, Cates JMM, et al. The receptor tyrosine kinase EphA2 promotes mammary adenocarcinoma tumorigenesis and metastatic progression in mice by amplifying ErbB2 signaling. J Clin Invest. 2008;118:64–78.

268. Paraiso KHT, Das Thakur M, Fang B, Koomen JM, Fedorenko I V, John JK, et al. Ligand-independent EPHA2 signaling drives the adoption of a targeted therapy-mediated metastatic melanoma phenotype. Cancer Discov. 2015;5:264–73.

269. Qazi MA, Vora P, Venugopal C, Adams J, Singh M, Hu A, et al. Cotargeting Ephrin Receptor Tyrosine Kinases A2 and A3 in Cancer Stem Cells Reduces Growth of Recurrent Glioblastoma. Cancer Res. 2018;78:5023–37.

270. Faoro L, Singleton PA, Cervantes GM, Lennon FE, Choong NW, Kanteti R, et al. EphA2 mutation in lung squamous cell carcinoma promotes increased cell survival, cell invasion, focal adhesions, and mammalian target of rapamycin activation. J Biol Chem. 2010;285:18575–85.

271. Brannan JM, Sen B, Saigal B, Prudkin L, Behrens C, Solis L, et al. EphA2 in the Early Pathogenesis and Progression of Non-Small Cell Lung Cancer. Cancer Prev Res. 2009;2:1039–49.

272. Giaccone G, Zucali PA. Src as a potential therapeutic target in non-small-cell lung cancer. Ann Oncol. Narnia; 2008;19:1219–23.

273. Taniguchi CM, Winnay J, Kondo T, Bronson RT, Guimaraes AR, Alemán JO, et al. The Phosphoinositide 3-Kinase Regulatory Subunit p85α Can Exert Tumor Suppressor Properties through Negative Regulation of Growth Factor Signaling. Cancer Res.

2010;70:5305–15.

274. Peng Y, Dai Y, Hitchcock C, Yang X, Kassis ES, Liu L, et al. Insulin growth factor signaling is regulated by microRNA-486, an underexpressed microRNA in lung cancer. Proc Natl Acad Sci. 2013;110:15043–8.

275. Li M-Y, Lai P-L, Chou Y-T, Chi A-P, Mi Y-Z, Khoo K-H, et al. Protein tyrosine phosphatase PTPN3 inhibits lung cancer cell proliferation and migration by promoting EGFR endocytic degradation. Oncogene. 2015;34:3791–803.

276. Li M-Y, Peng W-H, Wu C-H, Chang Y-M, Lin Y-L, Chang G-D, et al. PTPN3 suppresses lung cancer cell invasiveness by counteracting Src-mediated DAAM1 activation and actin polymerization. Oncogene. 2019;38:7002–16.

277. Wang Z, Glück S, Zhang L, Moran MF. Requirement for Phospholipase C-γ1 Enzymatic Activity in Growth Factor-Induced Mitogenesis. Mol Cell Biol. 1998;18:590–7.

278. Browaeys-Poly E, Perdereau D, Lescuyer A, Burnol A-F, Cailliau K. Akt interaction with PLC(gamma) regulates the G(2)/M transition triggered by FGF receptors from MDA-MB-231 breast cancer cells. Anticancer Res. 2009;29:4965–9.

279. Choi JH, Kim HS, Kim S-H, Yang YR, Bae YS, Chang J-S, et al. Phospholipase Cgamma1 negatively regulates growth hormone signalling by forming a ternary complex with Jak2 and protein tyrosine phosphatase-1B. Nat Cell Biol. 2006;8:1389–97.

280. Miao B, Ji Z, Tan L, Taylor M, Zhang J, Choi HG, et al. EPHA2 Is a Mediator of Vemurafenib Resistance and a Novel Therapeutic Target in Melanoma. Cancer Discov. American Association for Cancer Research; 2015;5:274–87.

281. Cheng F, Desai RJ, Handy DE, Wang R, Schneeweiss S, Barabási A-L, et al. Network-

based approach to prediction and population-based validation of in silico drug repurposing. Nat Commun. 2018;9:2691.

282. Cheng F, Kovács IA, Barabási A-L. Network-based prediction of drug combinations. Nat Commun. 2019;10:1197.

283. Cheng F, Lu W, Liu C, Fang J, Hou Y, Handy DE, et al. A genome-wide positioning systems network algorithm for in silico drug repurposing. Nat Commun. 2019;10:3476.

284. Youngblood VM, Kim LC, Edwards DN, Hwang Y, Santapuram PR, Stirdivant SM, et al. The ephrin-A1/EPHA2 signaling axis regulates glutamine metabolism in HER2-positive breast cancer. Cancer Res. 2016;0008-5472.CAN-15-0847-.

285. Brantley-Sieders DM, Zhuang G, Vaught D, Freeman T, Hwang Y, Hicks D, et al. Host Deficiency in Vav2/3 Guanine Nucleotide Exchange Factors Impairs Tumor Growth, Survival, and Angiogenesis In vivo. Mol Cancer Res. 2009;7:615–23.

Appendix A

Phosphorylation of PLCγ1 by EphA2 receptor tyrosine kinase promotes tumor growth in lung cancer

Abstract

EphA2 receptor tyrosine kinase (RTK) is often expressed at high levels in cancer and has been shown to regulate tumor growth and metastasis across multiple tumor types, including non-small cell lung cancer. A number of signaling pathways downstream of EphA2 RTK have been identified; however, mechanisms of EphA2's proximal downstream signals are less well-characterized. In this study, we used a yeast-two-hybrid screen to identify PLCγ1 as a novel EphA2 interactor. Biochemical analysis showed that EphA2 binds to PLCγ1 and the kinase activity of EphA2 was required for phosphorylation of PLCγ1. In human lung cancer cells, genetic or pharmacological inhibition of EphA2 decreased phosphorylation of PLCγ1 and loss of PLCγ1 inhibited tumor cell growth in vitro. Knockout of PLCγ1 by CRISPR-mediated genome editing also impaired tumor growth in a $Kras^{G12D}$-p53-Lkb1 murine lung tumor model. Collectively, these data show that the EphA2-PLCγ1 signaling axis promotes tumor growth of lung cancer and provides rationale for disruption of this signaling axis as a potential therapeutic option.

Implications

The EphA2-PLCG1 signaling axis promotes tumor growth of non-small cell lung cancer and can potentially be targeted as a therapeutic option.

Introduction

Receptor tyrosine kinases (RTKs) regulate signal transduction pathways that control cell proliferation, survival, and motility. Dysregulation of RTKs by mutations, amplifications, or

overexpression can lead to oncogenic transformation and malignant progression (243). A number of RTKs have been identified as potential drivers of non-small cell lung cancer (NSCLC), one of which is EphA2 (244). The EphA2 RTK belongs to the EPH family, the largest family of RTKs, and is commonly overexpressed in NSCLC and associated with poor clinical outcomes (245). Targeted disruption of EphA2 impairs tumor growth in KRAS-mutant mouse models and in human NSCLC xenografts(246). Further, EphA2 is overexpressed in EGFR tyrosine kinase inhibitor (TKI)-resistant tumor cells (18). Loss of EphA2 reduced viability of erlotinib-resistant tumor cells harboring $EGFR^{T790M}$ mutations in vitro and inhibited tumor growth in an inducible $EGFR^{L858R+T790M}$-mutant lung cancer model in vivo (18). Several EphA2 inhibitors including an antibody, a peptide, and a small molecule inhibitor have been developed recently (247). An EphA2-targeting DOPC-encapsulated siRNA is currently in Phase I clinical trials for advanced or recurrent solid tumors (NCT01591356). However, despite the interest in EphA2 as a therapeutic target, molecular mechanisms mediating EphA2 function, particularly its proximal downstream signals, are not well-characterized.

Phospholipase C Gamma (PLCγ) is a lipase activated by receptors in the cellular membrane, including RTKs and adhesion receptors. Once activated, PLCγ hydrolyzes phosphatidylinositol 4,5-bisphosphate (PIP2) to form diacylglycerol (DAG) and inositol 1,4,5-trisphosphate (IP3), the latter promoting the transient release of intracellular Ca^{2+}, another important signaling molecule. PLCγ is ubiquitously expressed and exists in two isoforms, PLCG1 and PLCG2, each with distinct functions in a variety of cell types and disease states(248,249). PLCG1 plays a role in vasculogenesis and erythrogenesis as well as T-cell development and activity(250). Importantly, loss of PLCG1 is embryonic lethal in mice(251). PLCG2, meanwhile, is critical for B-cell development and maturation (249,252). Both PLCγ isoforms are enriched and mutated in many cancers (249). Elevated PLCγ1 has been shown to drive metastasis and progression of breast cancer (253,254), and its phosphorylation status is

prognostic for metastatic risk (255). PLCγ has also been implicated in resistance to cancer treatment. In glioblastoma, PLCγ/HIF-1α mediated FGFR1-induced radioresistance (256), while in head and neck and esophageal squamous cell carcinoma the AXL-EGFR- PLCγ1 axis mediated resistance to PI3K inhibition (257). An acquired PLCG2 mutation also caused resistance to ibrutinib in chronic lymphocytic leukemia (258). While important roles for PLCγ have been identified in several cancer types, PLCγ's role in lung cancer has yet to be elucidated.

In this report, we show that PLCγ is a novel target of the EphA2 RTK in lung cancer. We show that EphA2 interacts with and directly phosphorylates PLCγ for activation. Additionally, knockdown of PLCG1 significantly reduces the growth of KRAS-mutant lung cancer cells in vitro and inhibits lung tumor growth in an orthotopic Kras-p53-Lkb1 mutant mouse model in vivo. Collectively, these studies identify the EphA2-PLCγ1 axis as a potential therapeutic target for KRAS-mutant lung cancer.

Results

EphA2 interacts with PLCγ

To identify EphA2 interacting partners in human lung cancer cells, the intracellular domain (AA 559-976) of EphA2 was used as bait for a yeast-two-hybrid (Y2H) screen against the cDNA library of lung cancer cells (www.hybrigenics-services.com). 79 positive clones were screened, resulting in 15 total candidates. The candidates were stratified into three categories based on confidence of interaction- very high confidence (3 proteins, orange), high confidence (4 proteins, blue), and moderate confidence (8 proteins, green) (**Figure 5.1A**). 1-2 candidates were identified in each category that have been previously reported to interact with EphA2, validating the efficacy and accuracy of the Y2H screen (259,260). We chose to explore PLCG1 and PLCG2 further, since both are PLCγ family members and novel interactors with EphA2 identified in this screen with very high confidence and high confidence, respectively.

To verify the interaction between EphA2 and PLCγ (PLCγ1 and PLCγ2) identified in the Y2H screen, EphA2 and PLCG1 or PLCG2 were ectopically expressed in COS-7 cells. Both PLCγ isoforms were immunoprecipitated with EphA2, however in the reverse direction, only immunoprecipitation of PLCγ1 was able to co-immunoprecipitate EphA2 (**Figure 5.1B**), suggesting a weaker interaction between EphA2 and PLCγ2 compared to PLCγ1.

PLCγ1 and PLCγ2 are important mediators of intracellular signal transduction and are activated by phosphorylation by upstream kinases (261). To determine if EphA2 is required for PLCγ activation, we assessed phosphorylation by immunoblotting. Ectopic expression of EphA2 increased the overall phosphorylation levels of both PLCγ1 and PLCγ2 including two different tyrosine sites on each protein (Y783 and Y1253 for PLCγ1, Y759 and Y1217 for PLCγ2) (**Figure 5.1C**). We also observed enhanced phosphorylation of Y783 on endogenous PLCγ1 in EphA2 overexpressing samples. Conversely, overexpression of PLCγ had no effect on the phosphorylation of EphA2 (**Figure 5.1C**), suggesting signaling proceeds from EphA2 to PLCγ.

Additional analysis of the PLCγ protein-protein interactome identified 57 interacting proteins for PLCγ1, far more than the 14 interacting proteins of PLCγ2 (**Figure 5.1D**). Interestingly, KEGG (Kyoto Encyclopedia of Genes and Genomes) enrichment analysis of the PLCγ1 interactome identified 22 proteins that were significantly enriched in the Ras signaling pathway (adjusted p value = 2.1e-22, **Figure 5.1E**), a pathway known to be important in driving a significant portion of NSCLC.

Since PLCγ1 had a stronger interaction with EphA2 (**Figure 5.1B**) and protein-protein interaction analysis of PLCG1 showed a broader functional network than PLCγ2, we focused on PLCγ1's interaction with EphA2 in KRAS-mutant lung cancer for the remainder of the study.

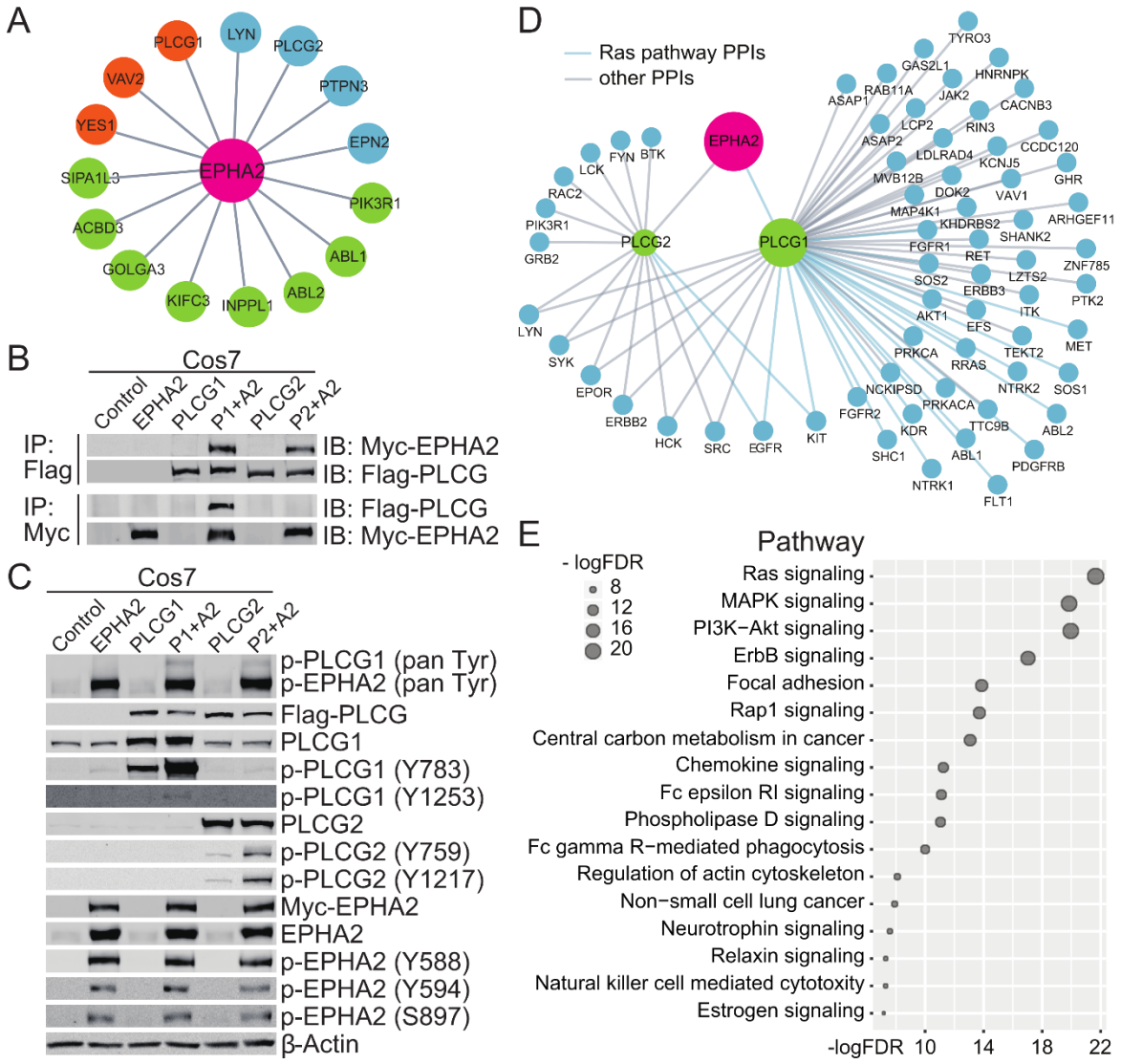

Figure 5.1. EphA2 interacts with PLCγ. (A) A yeast-two-hybrid screen identified potential EphA2 interactors based on a lung cancer cDNA library. Orange, very high confidence; Blue, high confidence; Green, moderate confidence. (B&C) Combinations of EphA2 and either PLCG1 or PLCG2 were expressed in COS-7 cells. (B) Flag-PLCγ or Myc-EphA2 were immunoprecipitated and co-immunoprecipitating EphA2 or PLCγ was probed by western blotting. (C) Phosphorylation levels of EphA2 and PLCγ were measured by western blotting. (D) Map of the human EphA2-PLCγ1/PLCγ2 subnetwork analysis. Proteins in the Ras pathway are delineated by a blue line. (E) KEGG pathway enrichment analysis of the PLCγ interactome. FDR, False Discovery Rate.

EphA2 kinase activity is required for PLCγ1 phosphorylation

PLCγ is a well-known downstream effector of several receptor tyrosine kinases (RTKs), including EGFR, PDGFR, VEGFR, and TrkB(250). Phospho-tyrosine sites on the RTKs interact with the SH2 domain of PLCγ for activation(250). Consistent with other RTKs, our results from the Y2H screen indicated that the SH2 domain of PLCγ1 was involved in the interaction with the EphA2 intracellular domain. To characterize the interaction between EphA2 and PLCγ1, a series of EphA2 mutants were made, including two kinase dead mutants (K646M, D739N), four tyrosine phosphorylation site mutants (Y588F, Y594F, Y735F, Y930F) and one serine phosphorylation site mutant (S897A) (**Figure 5.2A**). These phosphorylation sites were chosen based on the literature and analysis of EphA2 in the PhosphoSitePlus PTM Resource (https://www.phosphosite.org/homeAction.action) as putative sites most likely to be involved in EphA2 kinase activity or its cellular function.

In EphA2 and PLCG1 co-expressing COS-7 cells (**Figure 5.2B&C**), wild-type EphA2 increased the level of phospho-PLCγ1, whereas the ability to phosphorylate PLCγ1 was impaired in cells expressing kinase dead or the two tyrosine mutants (Y588F and Y594F) that are situated within the juxtamembrane domain of EphA2 and are known to be required for proper kinase activity(262). Mutation of the other two tyrosine sites in the kinase domain and SAM domain as well as the serine site had little effect on PLCγ1 phosphorylation. Furthermore, the level of phospho-PLCγ1 was dependent on the level of EphA2 expression in the cells (**Figure 5.2D**). Consistent with **Figure 5.2C**, expression of the EphA2 kinase dead mutant (K646M) had no effect on phosphorylation of PLCγ1 even at very high doses. The Y588F mutant, which exhibited reduced kinase activity, only weakly affected phosphorylation of PLCγ1 at high expression levels.

We also expressed EphA2 in BEAS2B cells, a normal bronchial epithelial cell line with low endogenous EphA2 expression and analyzed the phosphorylation levels of endogenous PLCγ1 (**Figure 5.2E**). The result here showed that only wild-type EphA2, but not K646M or Y588F mutants, could phosphorylate PLCγ1, demonstrating that PLCγ1 phosphorylation is dependent on the kinase activity of EphA2.

EphA2 activates PLCγ1 in human lung cancer cells

EphA2 is highly expressed in many KRAS-mutant lung cancer cells and has been shown to regulate tumor malignancy(246), prompting us to investigate if PLCγ1 is regulated by EphA2 in these cells. Ectopic expression of wild-type EphA2 in H23 cells led to phosphorylation of PLCγ1, while kinase-dead EphA2 had no effect on p-PLCγ1 levels (**Figure 5.3A**). Corresponding experiments knocking down EphA2 by siRNA in a panel of KRAS-mutant lung cancer cell lines (H23, H2009, A549, HCC44, H2030, H358) led to a decrease of p-PLCγ1 (**Figure 5.3B&C**). Further, loss of EphA2 by shRNA or siRNA in either H23 or H2009 cells diminished p-PLCγ1 in serum-starved, stimulated, or normal growth conditions (**Figure 5.3B&D**). Pharmacological inhibition of EphA2 kinase activity using the small molecule inhibitor ALW-II-41-27(246) (ALW) also inhibited phosphorylation of PLCγ1, with increasing doses of ALW inhibiting both p-EphA2 and p-PLCγ1 in H23 and H2009 cells (**Figure 5.3E**).

To verify that EphA2 phosphorylates PLCγ1 via a direct interaction between the two proteins in lung cancer cells, we performed DuoLink proximity ligation assay (PLA). We showed that loss of either EphA2 or PLCγ1 by shRNA reduced the number of EphA2-PLCγ1 interactions compared to control shGFP (**Figure 5.3F&G**). Additionally, we observed a higher number of baseline interactions in H2009 cells compared to H23 cells which correlated with higher EphA2 and p-PLCγ1 levels in this cell line (**Figure 5.3C&F**). Together, these data show that EphA2 interacts with and phosphorylates PLCγ1 in human KRAS-mutant lung cancer cell lines.

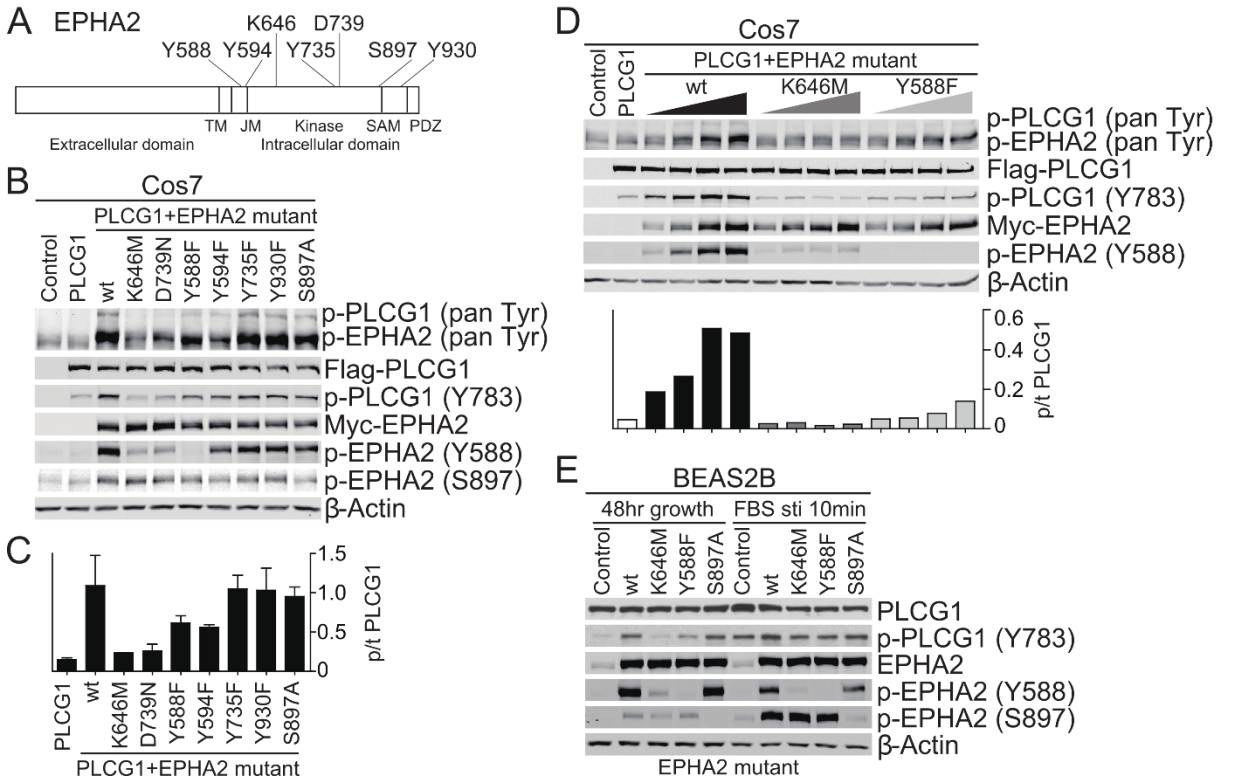

Figure 5.2. EphA2 kinase activity is required for phosphorylation of PLCγ. Wild-type (wt) or mutant EphA2 was expressed in COS-7 or BEAS2B cells to assess their ability to phosphorylate PLCγ1. (A) Diagram showing the domains of EphA2 and the mutants used in the following experiments. (B) Whole cell lysates of COS-7 cells 48 hours post-transfection were analyzed by western blotting for phosphorylation of EphA2 and PLCγ1. (C) Quantification of the ratio of phospho-PLCγ to total PLCγ in EphA2 and PLCγ co-expressing cells from two independent experiments. p/t, phospho/total (D) PLCG1 and EphA2 were co-transfected into COS-7 cells at a ratio of 1:0.1, 1:0.2, 1:0.4, and 1:1 and whole cell lysates were collected 48 hours post-transfection. Lysates were analyzed by western blotting and quantified in the bottom panel. (E) BEAS2B cells overexpressing EphA2 were cultured for 48 hours in growth medium or serum-starved and FBS-stimulated for 10 min before collection of lysates. Whole cell lysates were analyzed by western blotting using the indicated antibodies.

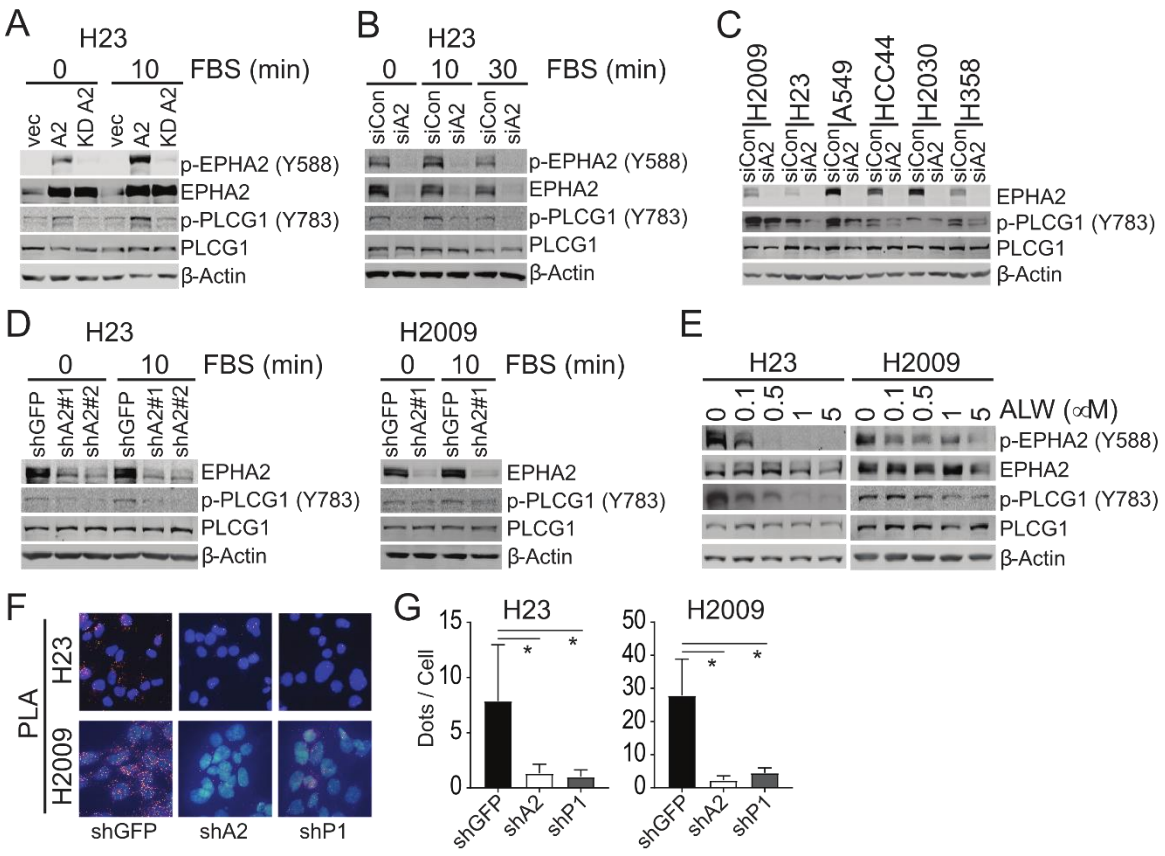

Figure 5.3. PLCγ1 is activated by EphA2 in human lung cancer cell lines. PLCγ1 activity was evaluated by its Y783 phosphorylation in human KRAS-mutant lines. A2: EphA2; P1: PLCγ1 (A) Wild-type or kinase dead (KD) EphA2 was expressed in H23 cells. Cells were serum-starved and FBS-stimulated for 10 min and whole cell lysates were analyzed by western blotting with the indicated antibodies. (B&C) EphA2 was knocked down by pooled siRNA in the indicated cell lines and whole cell lysates were analyzed by western blotting. (B) H23 cells were serum-starved and stimulated with FBS for 10 or 30 minutes. (C) Cell lines were cultured in complete growth media for 24 hours post-transfection. (D) EphA2 was knocked down by two different shRNA sequences (#1 and #2) in H23 and H2009 cell lines which were serum-starved and stimulated with FBS for 10 minutes. Whole cell lysates were analyzed by western blotting with the indicated antibodies. (E) H23 or H2009 cells were treated with increasing concentrations of ALW for 24 hours. Whole cell lysates were analyzed by western blotting with the indicated antibodies. (F&G) Endogenous interactions between EphA2 and PLCγ1 in H23 and H2009 cells were analyzed by Duolink proximity ligation assay (PLA) in shGFP control cells compared to either shEphA2 or shPLCG1 knockdown cells. PLA signals (dots) were quantified from 3-6 40× fields. Data are presented as mean ± SD. *, $p<0.05$, Student's t-test.

Loss of PLCγ1 blocks cell growth of human lung cancer cells

Despite PLCγ1's well-known roles in regulating T-cell development and homeostasis (263) and breast cancer cell migration and invasion (264), a role for PLCγ1 in lung cancer remains unclear. We used three independent siRNAs to knockdown PLCG1 in H23 and H2009 cells (**Figure 5.4A**). In both cell lines, transient loss of PLCγ1 significantly reduced cell viability compared to control (**Figure 5.4B**). Long term effects of PLCγ1 loss on cell proliferation were assessed by stable knockdown or knockout of PLCG1 by four independent shRNAs or CRISPR-Cas9 mediated genome editing followed by MTT and colony formation assays (**Figure 5.4C-E**). shPLCG1 cells showed a much slower growth rate and rarely formed colonies even after two weeks in culture compared to shGFP control. Similarly, PLCγ1 loss significantly hindered colony formation in sgPLCG1 cells compared to sgLacZ control, with the reduction in colony formation correlating with the efficiency of knockout (**Figure 5.4F&G**). Thus, we demonstrate that PLCG1 promotes the growth of human lung cancer cells *in vitro*.

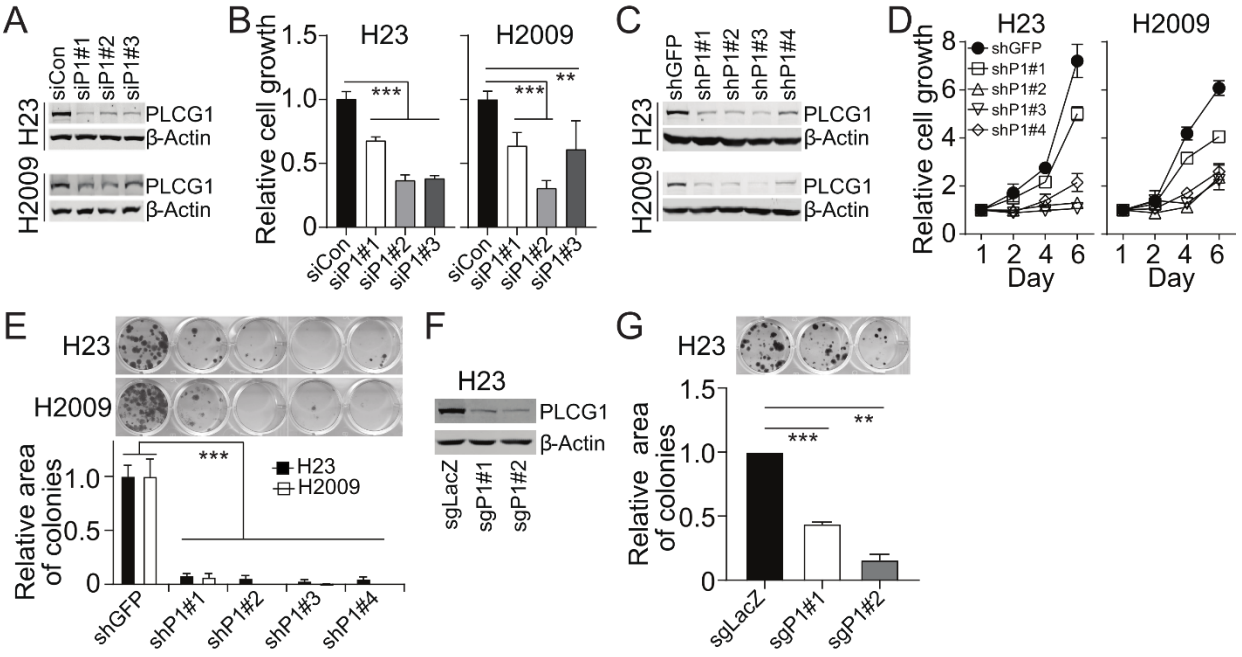

Figure 5.4. PLCγ1 loss inhibits human KRAS-mutant lung cancer cell growth. (A) Western blot of PLCγ1 levels in H23 cells upon siPLCG1 targeting. (B) Cell viability of H23 and H2009 cells upon knockdown of PLCG1 by siRNA was measured by MTT assay. Representative data are presented as mean ± SD. **, p<0.01; ***, p<0.001, Student's t-test. (C) Western blot of PLCγ1 levels in H23 and H2009 cells upon knockdown of PLCG1 by shRNA. (D) MTT assays measuring the relative cell viability of H23 and H2009 upon targeting of PLCG1 by shRNA. Representative data are presented as mean ± SD. ***, p<0.001, Two-way ANOVA. (E) Colony growth of shGFP or shPLCG1 H23 and H2009 cells. Quantification of colony area below. Representative data are presented as mean ± SD. ***, p<0.001, Student's t-test. (F) Western blot of H23 cells upon targeting of PLCG1 by CRISPR-Cas9 mediated genome editing. (G) Colony growth of sgLacZ or sgPLCG1 H23 cells. Quantification of colony area below. Representative data are presented as mean ± SD. **, p<0.01; ***, p<0.001, Student's t-test.

PLCγ1 deficiency decreases tumor growth in a mouse KPL lung tumor model

To evaluate the *in vivo* role of PLCγ1 in tumor growth within a competent immune environment, a mouse KPL lung tumor model was established (**Figure 5.5A-C**) based on the report from Platt et al(217). An adeno-associated virus (AAV) carrying three adjacent sgRNAs targeting Kras, p53, and Lkb1 genes (KPL), together with a Cre expression cassette and a mutant $Kras^{G12D}$ genomic template, was purified and delivered into the lungs of Rosa26-LSL-Cas9-EGFP knock-in recipient mice via intratracheal instillation (**Figure 5.5A**). Cre-mediated recombination allows for EGFP and Cas9 expression in target cells, which leads to mutation of the three target genes via non-homologous end joining (p53 or Lkb1) or homology-directed repair (Kras G12D). The mice developed abundant lung nodules approximately 2-3 weeks after viral instillation, as monitored by MRI (**Figure 5.5B**). Tumor nodules were also visible by EGFP after lung dissection (**Figure 5.5C**). EGFP-positive tumor cell populations were then isolated from the tumor mass and single cell clones were established (**Figure 5.5C**). Western blots were used to confirm KPL mutations in the clones (**Figure 5.5D**), and clone KPL-C2 was selected for use in the following experiments.

In addition to the targeted KPL mutations, KPL-C2 cells had high EphA2 and p-EphA2 expression. Pharmacologic inhibition of EphA2 by ALW effectively blocked both p-EphA2 and p-PLCγ1 (**Figure 5E, arrow**) and colony growth of KPL cells in a dose dependent manner (**Figure 5.5F**), indicating EphA2 might modulate PLCγ1 activity to regulate KPL tumor cell growth. CRISPR-Cas9 mediated genome editing was used to generate PLCγ1 knockout KPL cells (**Figure 5.5G**). PLCγ1-deficient KPL cells showed a significant decrease in colony growth *in vitro* (**Figure 5.5H**). sgLacZ control and sgPLCG1 knockout cells were subsequently injected into the tail veins of immune competent mice (Rosa26-LSL-Cas9-EGFP). sgLacZ cells developed a significant number of tumors in the lungs at week three, while PLCG1-deficient cells formed a very limited number of tumors compared to the control cells (**Figure 5.5I&J**). In

some mice, loss of PLCγ1 completely inhibited tumor formation. PCNA and cleaved-Caspase-3 IHC staining of the tumors showed that PLCγ1 deficiency in these KPL cells inhibited tumor cell proliferation but had little effect on apoptosis (**Figure 5.5K-M**), respectively, in agreement with our previous findings that EphA2 knockdown affected tumor cell proliferation but not apoptosis(265,266). Collectively, these data show that PLCγ1 promotes KPL lung tumor growth.

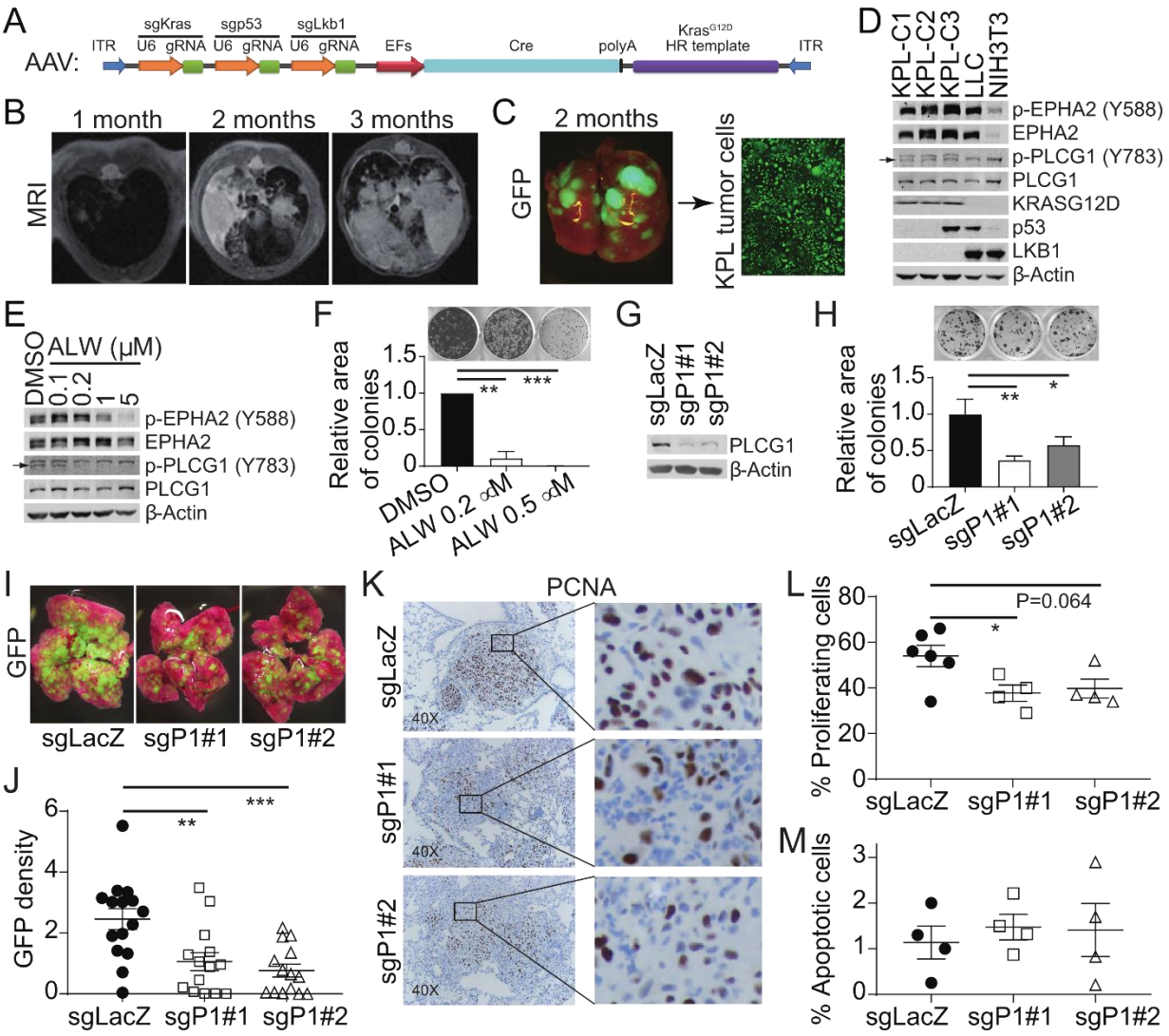

Figure 5. PLCγ1 deficiency hinders mouse KPL lung tumor growth. (A) Schematic of AAV vector used for expression of sgKras, sgp53, sgLkb1, Cre and Kras^{G12D} template. (B) MRI images of tumor formation in KPL mice up to 3 months after viral instillation. (C) Representative image of GFP expression in KPL lung tumors. Cells were isolated from tumors to create KPL tumor cell lines. (D) Single cell clones from KPL tumors were grown to create KPL tumor cell lines (ex. KPL-C1, clone 1). Whole cell lysates were analyzed by western blotting using the indicated antibodies. (E) KPL-C2 cells were treated with increasing doses of ALW. Cell lysates were analyzed by western blotting using the indicated antibodies. (F) Colony assay of KPL-C2 cells with increasing doses of ALW. Quantification in the bottom panel. Data are presented as mean ± SEM. **, p<0.01; ***, p<0.001, Student's t-test. (G) Western blot showing loss of PLCγ1 upon targeting of KPL-C2 cells with CRISPR-Cas9 sgPLCG1. (H) Colony assay of KPL-C2 cells targeted with sgPLCG1. Quantification in bottom panel. Representative data are presented as mean ± SD. *, p<0.05; **, p<0.01, Student's t-test. (I-M) sgPLCG1 KPL-C2 cells were injected via tail vein injection back into Rosa26-LSL-Cas9-GFP mice. (I) Tumor formation was visible by GFP expression. (J) Quantification of GFP density of sgLacZ or sgPLCG1 KPL-C2 tumors. Data

are presented as mean ± SEM. **, p<0.01; ***, p<0.001, Student's t-test. (K) Proliferation of sgLacZ or sgPLCG1 KPL-C2 tumors was measured by PCNA immunohistochemistry staining. (L) Quantification of PCNA staining. Data are presented as mean ± SEM. *, p<0.05, Student's t-test. (M) Apoptosis was measured by TUNEL immunohistochemistry staining. Quantified data are presented as mean ± SEM, Student's t-test.

Discussion

EphA2 has emerged as a promising target in several tumor types including lung, pancreatic, breast, and glioblastoma (246,265–269), yet understanding of its proximal downstream signals is not comprehensive. In this report, we identify PLCγ as a novel downstream effector of EphA2 capable of promoting tumor progression in the context of KRAS-mutant lung cancer. In addition to PLCγ1, several other well-known signaling molecules, including S6K1-pBAD, JNK-c-JUN, mTOR, and ERK, are also known to function downstream of EphA2 in lung cancer (246,265,270,271). How cells precisely regulate timing and localization of these interactions downstream of EphA2 remains unanswered. Along with PLCγ, our Y2H screen also identified other EphA2 interactors including Src family proteins, the PTPN3 phosphatase, and PIK3R1, a regulatory subunit of PI3K (**Figure 5.1A**). While many of these hits have been implicated in lung tumorigenesis (272–276), additional studies are required to determine whether these interactors participate in EphA2 signaling during lung tumor progression.

The role of PLCγ1 in tumor cell proliferation is controversial. While PLCγ1 has been implicated in directing cell cycle progression (277,278), other reports suggest that PLCγ1 may negatively regulate cell proliferation (279). These conflicting reports suggest that PLCγ1 regulation of cell proliferation may be context dependent, perhaps varying based on the tumor type or activating growth factor. In this study, we show that loss of PLCG1 reduces cell viability of KRAS-mutant lung cancer cell lines *in vitro* and reduced PCNA staining of KPL lung tumors *in vivo*. Thus, our data suggest in the context of KRAS-mutant lung cancer, PLCγ1 facilitates

tumor cell proliferation. Further, PLCγ has been implicated in AXL-mediated resistance to PI3K inhibition in neck and esophageal squamous cell carcinomas (257). Since EphA2 also plays critical roles in tumor resistance to EGFR kinase inhibitors in lung cancer (18) and B-Raf inhibitors in melanoma (280), it will be interesting to investigate whether PLCγ mediates the EphA2 signaling pathway in drug resistance cells.

In summary, our data reveal that PLCγ1 is a novel interactor of the EphA2 RTK in lung cancer cells, and our data support the idea that targeting this EphA2- PLCγ1 signaling axis could be a promising therapeutic option for treating lung cancer.

Materials and Methods

Cell lines, plasmids, and reagents

293FT, COS-7, and mouse KPL lines were cultured in DMEM supplemented with penicillin/streptomycin and10% FBS. Human lung cancer cell lines (A549, H23, H358, H2030, H2009, and HCC44) and BEAS2B cells were cultured in RPMI 1640 supplemented with penicillin/streptomycin and 10% FBS. Cell lines were either purchased from ATCC or thawed from our lab stocks. Mycoplasma was routinely tested to exclude possible contamination.

For transient knockdown, siRNAs were purchased from Dharmacon (smart pool siEphA2: #L-003116-00-0005; non-targeting pool: #D-001810-10-05; individual siPLCG1 #1-3: # J-003559-05, 07, 08). For stable shRNA knockdown, lentiviral vector pLKO.1 was used (EphA2 shRNA#1 CGGACAGACATATGGGATATT; EphA2 shRNA#2 GCGTATCTTCATTGAGCTCAA; PLCG1 shRNA#1 ATGACAAAGCAATGTGACTGG; PLCG1 shRNA#2 ATGTAAACTTTGTTTCCCTGG; PLCG1 shRNA#3 AATTTCACGAATGTCAATGGC; PLCG1 shRNA#4 ATACCATTCGTGGTTCACAGG; GFP shRNA control GCAAGCTGACCCTGAAGTTCAT). For

Crispr/Cas9 mediated gene knockout, lentiviral vector LentiCRISPR v2 was used human PLCG1 gRNA #1 ATAGCGATCAAAGTCCCGTG; human PLCG1 gRNA #2 GTTCACTTCATCCTCAGATG; LacZ gRNA TGCGAATACGCCCACGCGAT; mouse PLCG1 gRNA #1 GCTAATGGAGGATACACTGC; mouse PLCG1 gRNA #2 CCGCGGCGCGGACAAAATCG). The PLCG1 full length cDNA plasmid was purchased from Sino Biological Inc (#MG50804-G) and PLCG1 was subcloned into pCDH-puro vector with Flag-tag at its C-terminus. The EphA2 full length cDNA plasmid (pCDH-puro EphA2-Myc) and its corresponding mutants (S897A, Y588F, Y594F, Y735F, Y930F, K646M, and D739N) were all from lab stocks. For AAV system, AAV9 and pΔF6 plasmids were purchased form Penn Vector Core at the University of Pennsylvania, and AAV-KPL plasmid was from Addgene (#60224). ALW-II-41-27, was purchased from MedChem Express (Monmouth Junction, NJ).

Building a human protein-protein interactome

To construct a comprehensive and high-quality human protein-protein interaction (PPI) network, we assembled 15 commonly used data sources with five types of experimental evidence: (1) binary PPIs tested by high-throughput yeast-two-hybrid (Y2H) systems; (2) binary, physical PPIs from protein three-dimensional structures; (3) kinase-substrate interactions from literature-derived low-throughput and high-throughput experiments; (4) signaling networks derived from low-throughput experiments; (5) literature-derived identified by affinity purification followed by mass spectrometry (AP-MS) and low-throughput experiments. In total, the updated human interactome consisted of 351,444 PPIs (edges or links) linked to 17,706 unique proteins (nodes). The detailed descriptions of building the human interactome are given in our recent studies(281–283). We then mapped the EPHA2, PLCG1 and PLCG2 into the PPIs network to construct EPHA2-PLCG1/PLCG2 sub-network. Next, we performed Kyoto Encyclopedia of Genes and Genomes (KEGG) enrichment analysis to identify the functional pathway related with PLCG1 and PLCG2.

Cell growth assays

MTT Assay was used to evaluate the short-term proliferation of cells. 2×10^3 cells were plated into 96-well plates with six replicates in growth media. MTT reagent was added and the plates were read using plate reader (Synergy HT, BioTek) on days 1-6. Cell viability was normalized to day one. Colony formation assays were used to evaluate the long-term proliferation of cells. 400 cells were plated into 12-well plates with 3-4 replicates in growth media. For drug treatment experiments, drugs were added the day after cell attachment with an initial plating of 2×10^4 cells. Cell colonies were visualized by crystal violet staining after 2 weeks for human cells or 1 week for mouse KPL cells.

Yeast-two-hybrid screen

Yeast two-hybrid (Y2H) screening was carried out by Hybrigenics Services, (hybrigenics-services.com). The cytoplasmic EphA2 tail (AA 559-976) was cloned as a N-LexA-EPHA2-C fusion to be the bait against a lung cancer cDNA library (mix of A549, H1703, and H460) and 79 positive clones were selected on DO-3 selective medium plates. A confidence score (Predicted Biological Score, PBS) was assigned to each interaction, then scores were stratified into categories based on the degree of confidence.

Proximity Ligation Assay

Cancer cells in culture medium were plated onto coverslips coated with 0.5% Gelatin in DPBS. Cells were washed with DPBS and fixed with 4% PFA after 24hr growth. 5% goat serum plus 0.3% triton X-100 in DPBS was used to permeabilize cells. Anti-PLCG1 rabbit polyclonal antibody (Santa Cruz, #SC-81, 1:200) and anti-EphA2 mouse monoclonal antibody (EMD Millipore, #05-480, 1:400) diluted in blocking buffer were applied to cells and incubated for overnight at 4°C. The DuoLink Proximity Ligation Kit (Sigma-Aldrich, #DUO92102) was used according to manufacturer's instructions.

Immunoblots, immunoprecipitation, and immunohistochemistry

For western blotting, 10 to 30µg of total protein from cell lysates were separated by SDS-PAGE, transferred to a nitrocellulose membrane and probed with indicated antibodies. Primary antibodies used in this study were as follows: rabbit anti-EphA2 (Santa Cruz, #SC-924, 1:1000), mouse anti-EphA2 (EMD Millipore, #05-480, 1:1000), mouse anti-PLCG1 (Santa Cruz, #SC-7290, 1:500), rabbit anti-PLCG2 (Santa Cruz, #SC-407, 1:500), rabbit anti-EphA2 Y588 (Cell Signaling, #12677, 1:500), rabbit anti-PLCG1 Y783 (Cell Signaling, #14008, 1:500), mouse anti-β-Actin (Santa Cruz, #SC-47778, 1:1000). Secondary antibodies used were as follows: anti-rabbit IgG HRP (Promega, #W4011, 1:5000), anti-mouse IgG HRP (Promega, #W4021, 1:5000), anti-rabbit IgG IRDye 800CW (LI-COR, #926-32211), and anti-mouse IgG IRDye 680LT (LI-COR, #926-68020). Antibodies were diluted in PBST/5% nonfat milk. Signal was detected using ECL substrate (West Femto or West Pico, Thermo Fisher Scientific) or by LI-COR Odyssey Infrared Imaging System.

For immunoprecipitation, cells were lysed in IP buffer (10mM Tris-HCl pH=7.5, 150mM NaCl, 2mM EDTA, 1% Triton X-100). 1µg of total protein was incubated with anti-Myc tag or anti-Flag agarose beads overnight at 4°C. Beads were washed with lysis buffer and boiled with 20ul SDS loading buffer. The soluble fraction was loaded for immunoblot analysis.

Lung tumor sections were stained with hematoxylin and eosin by Vanderbilt University Translational Pathology Shared Resource. PCNA staining (Cell signaling, rabbit anti PCNA, #13110) for proliferation or terminal deoxynucleotidyl transferase dUTP nick end labeling (TUNEL) assay (Millipore, ApopTag Red In Situ Apoptosis Detection Kit, #S7165) for apoptosis was performed as described previously(284,285). Tumor area of 20x images was analyzed by ImageJ or CellSens software.

Animal Studies

AAV was produced in 293FT cells, chemically purified and concentrated according to published methods(217). AAV titer was determined using AAVpro Titration Kita (Takara Bio Inc., #6233). A titer of 2×10^{11} viral genome copies in 75ul DPBS was intratracheally injected into 7-8-week-old Rosa26-LSL-Cas9-EGFP mice (stock #: 024858, Jackson Labs). Tumor development was monitored weekly by MRI and by GFP imaging after sacrifice. For orthotopic lung tumor growth, KPL lines were transfected with luciferase expression plasmid and intravenously injected via tail vein. Lung tumor growth was measured once a week by bioluminescence imaging.

All animal experiments were pre-approved by the Vanderbilt Institutional Animal Care and Use Committee and followed all state and federal rules and regulations.

Statistical analysis

Data were presented as Mean ± SD or SEM and statistically analyzed by two-tailed student's t-test or two-way ANOVA. All experiments were performed at least two independent times and $p < 0.05$ was treated as statistically significant. GraphPad Prism 8 was used for statistical analysis.